New insights into the physiology and pathophysiology of the atypical sodium leak channel NALCN

Arnaud Monteil, Nathalie C. Guérineau, Antonio Gil-Nagel, Paloma Parra-Diaz, Philippe Lory, Adriano Senatore

New insights into the physiology and pathophysiology of the atypical sodium leak channel NALCN

Arnaud Monteil[1,2,3,6], Nathalie C. Guérineau[1,2], Antonio Gil-Nagel[5], Paloma Parra-Diaz[5], Philippe Lory[1,2], Adriano Senatore[4]

[1]IGF, Université de Montpellier, CNRS, INSERM, Montpellier, France
[2]LabEx 'Ion Channel Science and Therapeutics', Montpellier, France
[3]Department of Physiology, Faculty of Medicine Siriraj Hospital, Mahidol University, Bangkok, Thailand.
[4]Department of Biology, University of Toronto Mississauga, Mississauga, Ontario, Canada.
[5]Department of Neurology, Epilepsy Program, Hospital Ruber Internacional, Madrid, Spain
[6]Correspondence to Arnaud Monteil: arnaud.monteil@igf.cnrs.fr

Graphical Abstract

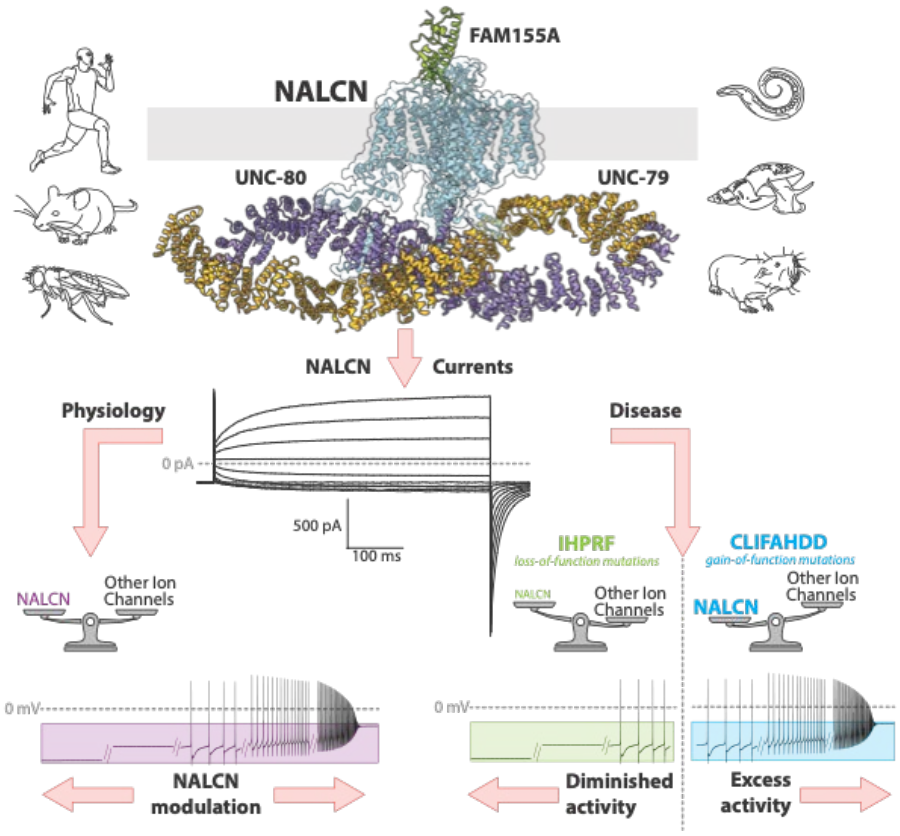

CLINICAL HIGHLITGHTS

This article reviews our current knowledge on the sodium leak channel NALCN, an important player of cell excitability. NALCN is highly conserved across species and is involved in fundamental physiological functions such as respiratory rhythm, circadian rhythm, sleep and locomotion. NALCN dysfunction, especially in patients carrying genetic mutations, results in severe disease states including serious respiratory defects, failure to thrive, hypotonia, developmental and cognitive delay, ataxia, epilepsy and early death. The recent development of animal and cellular models for the study of NALCN-related diseases now provides tools to understand their etiology and pave the way to the identification of novel therapeutic opportunities.

Arnaud Monteil[1,2,3,6], Nathalie C. Guérineau[1,2], Antonio Gil-Nagel[5], Paloma Parra-Diaz[5], Philippe Lory[1,2], Adriano Senatore[4]

[1]IGF, Université de Montpellier, CNRS, INSERM, Montpellier, France
[2]LabEx 'Ion Channel Science and Therapeutics', Montpellier, France
[3]Department of Physiology, Faculty of Medicine Siriraj Hospital, Mahidol University, Bangkok, Thailand.
[4]Department of Biology, University of Toronto Mississauga, Mississauga, Ontario, Canada.
[5]Department of Neurology, Epilepsy Program, Hospital Ruber Internacional, Madrid, Spain
[6]Correspondence to Arnaud Monteil: arnaud.monteil@igf.cnrs.fr

Cell excitability and its modulation by hormones and neurotransmitters involve the concerted action of a large repertoire of membrane proteins, especially ion channels. Unique complements of co-expressed ion channels are exquisitely balanced against each other in different excitable cell types, establishing distinct electrical properties that are tailored for diverse physiological contributions, and dysfunction of any component may induce a disease state. A crucial parameter controlling cell excitability is the resting membrane potential (RMP) set by extra- and intra-cellular concentrations of ions, mainly Na^+, K^+, and Cl^-, and their passive permeation across the cell membrane through leak ion channels. Indeed, dysregulation of RMP causes significant effects on cellular excitability. This review describes the molecular and physiological properties of the Na^+ leak channel NALCN, which associates with its accessory subunits UNC-79, UNC-80, and NLF-1/FAM155 to conduct depolarizing background Na^+ currents in various excitable cell types, especially neurons. Studies of animal models clearly demonstrate that NALCN contributes to fundamental physiological processes in the nervous system including the control of respiratory rhythm, circadian rhythm, sleep and locomotor behavior. Furthermore, dysfunction of NALCN and its subunits is associated with severe pathological states in humans. The critical involvement of NALCN in physiology is now well established, but its study has been hampered by the lack of specific drugs that can block or agonize NALCN currents *in vitro* and *in vivo*. Molecular tools and animal models are now available to accelerate our understanding of how NALCN contributes to key physiological functions, and the development of novel therapies for NALCN channelopathies.

Keywords: Sodium leak channel, NALCN, Resting membrane potential, Cell excitability, Fundamental physiological functions, Human disease, Phylogeny and evolution

Abbreviations

2-APB:	2-aminoethoxydiphenylborane
AAV:	Adeno-Associated Virus
Ach:	Acetylcholine
AD:	Alzheimer disease
AITC:	Allyl isothiocyanate
AP:	Action potential
AS:	Association study
AVP:	Arginine vasopressin
BASIC:	Bile acid-sensitive ion channel
BLAST:	Basic Local Alignment Search Tool
BPAP:	Bilevel positive airway pressure
CaM:	Calmodulin
CaSR:	Calcium-sensing receptor
Ca_V:	Voltage-gated Ca^{2+} channel
CCI:	Chronic constriction injury
CCS:	Case control study
CFA:	Complete Freund's adjuvant
CLIFAHDD:	Contractures of the Limbs and Face, Hypotonia, and Developmental Delay
CNV:	Copy number variation
CP96345:	(2S,3S)-cis-2-(Diphenylmethyl)-N-[(2-methoxyphenyl)methyl]-1 azabicyclo[2.2.2]octan-3-amine
CPAP:	Continuous positive airway pressure
CPG:	Central pattern generator
CRD:	Cysteine-rich domain
Cryo-EM:	Cryo-electron microscopy
CTD:	Carboxyterminal domain
DA:	Dopamine
DD:	Constant darkness
dbcAMP:	dibutyryl cAMP
DMH:	Dorsomedial hypothalamic nucleus
DN:	Dorsal neuron
DNV:	*De novo* variation
Do:	Day-old
DpMe:	Deep mesencephalic nucleus
DRG:	Dorsal root ganglia
E2:	Estrogen
EEG:	Electroencephalogram
eGFP	Enhanced green fluorescent protein
ELISA:	Enzyme-linked immunosorbent assay
EMG:	Electromyogram
ENaC:	Epithelial Na^+ channel
ENU:	Ethylnitrosourea
ER:	Estrogen receptor
ERE:	Estrogen responsive element
E_{rev}:	Reversal potential
FBAT:	Family-based association test
FGF21:	Fibroblast growth factor 21

FFA:	Flufenamic acid
FRET:	Fluorescence resonance energy transfer
GABA:	γ-aminobutyric acid
GDPβ-S:	Guanosine-5'-(β-thio)-diphosphate
GDV:	Gastric dilatation-volvulus
GHK:	Goldman, Hodgkin, Katz
GI:	Gastrointestinal
GPCR:	G proteins-coupled receptor
GTPγS:	Guanosine 5′-[γ-thio]triphosphate
GWAS:	Genome-wide association study
GWM:	Genome-wide methylation
HAM:	Haplotype association mapping
HCN:	Hyperpolarization-activated cation channel
HP:	Holding potential
ICC:	Interstitial cell of Cajal
IA:	Integrative analysis
IHPRF:	Infantile Hypotonia with Psychomotor Retardation and characteristic Facies
I/V:	Intensity/Voltage
K_{2P}:	Two-pore K^+ channel
KI:	Knockin
K_{ir}:	Inward rectifier K^+ channel
K_V:	Voltage-gated K^+ channel
KO:	Knockout
L703606:	(2S,3S)-2-Benzhydryl-N-((2-iodophenyl)methyl)-1 azabicyclo(2.2.2)octan 3-amine
LA:	Linkage analysis
LD:	12 hr Light:12 hr dark conditions
LepRb:	Long form of the leptin receptor
LFP:	Local field potential
LN:	Lateral neuron
lncRNA:	Long non-coding RNA
LPN:	Lateral posterior neuron
M3R:	Muscarinic M3 receptor
Maropitant:	(2*S*,3*S*)-2-Benzhydryl-*N*-(5-*tert*-butyl-2-methoxybenzyl) quinuclidin-3-amine
MCA:	Multiple correlation analysis
MeSa:	Methyl salicylate
Mo:	Month-old
MSMC:	Myometrial smooth muscle cell
mTLE:	mesial temporal lobe epilepsy
mV:	milli Volts
NALCN:	Na^+ leak channel
Na_V:	Voltage-gated Na^+ channel
NK1:	Tachykinin 1
NREM:	Non-rapid-eye-movement sleep
ND:	Not determined
NI:	Not indicated
NP:	Non-pregnant

NT:	Neurotensin
NTS:	Tractus solitary tract
P4:	Progesterone
PB:	Parabrachial
PBA:	Pathways-based analysis
PD:	Parkinson disease
PIP2:	Phosphatidylinositol-4,5-bisphosphate
PLA:	Proximity ligation assays
PP:	Post-partum
PR:	Progesterone receptor
PRE:	Progesterone responsive element
PreBötC:	PreBötzinger complex
PRL:	Prolactin
QTL:	Quantitative trait loci
REM:	Rapid-eye-movement sleep
RPeD1:	Right pedal dorsal 1
RMP:	Resting membrane potential
RTN:	Retrotrapezoid nucleus
rVRG:	Rostral ventral respiratory group
SF:	Selectivity filter
SFK:	Src family kinase
SNP:	Single nucleotide polymorphism
SNr:	Substancia nigra pars reticulata
SP:	Substance P
SPN:	Spino-parabrachial neuron
TRP:	Transient receptor potential
TTX:	Tetrodotoxin
Vm:	Membrane potential
VSD	Voltage-sensor domain
WB:	Western blotting
WES:	Whole exome sequencing
WGS:	Whole genome sequencing
WT:	Wild-type
Yo:	Year-old

I. INTRODUCTION

Since its molecular identification roughly 25 years ago by Perez-Reyes and colleagues (1), the sodium leak channel NALCN has emerged as an important regulator of cellular excitability. NALCN is a four domain Pore-loop channel homologous to voltage-gated sodium and calcium channels which conducts depolarizing Na^+ leak currents in neurons and recombinant systems (2).

The first experimental and quantitative description of a Na^+ leak current was provided by Hodgkin and Katz over 70 years ago (3), when they estimated that the Na^+ permeability (P_{Na}) across the squid giant axon membrane is, at rest, only 4% relative to that of K^+ (*i.e.,* $P_{Na}/P_K = 0.04$). Sub-threshold Na^+ leak currents have since been reported in a multitude of neurons and other cell types from both vertebrates and invertebrates. Physiologically, beyond providing an offset current that counters K^+ leak to establish a more depolarized RMP, Na^+ leak currents serve numerous important functions. First, by varying the baseline expression of Na^+ leak currents, animal cells can establish heterogeneous resting V_m, as in different neurons types as well as other excitable and non-excitable cell types (4, 5). By depolarizing RMP to voltages near action potential (AP) threshold, Na^+ leak currents also contribute to neuronal pacemaking, for example by providing a depolarizing drive between APs that brings V_m to threshold sooner, increasing frequency (6). A schematic representation of the general contribution of the Na^+ leak conductance in excitable cells is shown in **FIGURE 1**. As $G_{Na\text{-}leak}$ amplitude increases, V_m depolarizes and the frequency of AP discharge increases (**FIGURE 1A**). From resting V_m, APs can fire either phasically or tonically, and subtle changes of a few millivolts can orchestrate significant changes in the spiking pattern. One of the most important changes is likely the switch from a regular tonic discharge mode to a rhythmic bursting activity (**Figure 1B**), which can serve to regulate neurological processes such as locomotion, breathing, and hormone secretion.

Like K^+ leak channels (7, 8), dynamic modulation of Na^+ leak currents through cellular signaling allows modulation of RMP and cellular excitability. An example of this is observed in bag cell neurons in the central nervous system of the sea slug *Aplysia californica*, which secrete neuropeptides that initiate egg laying behavior (9). Presynaptic stimulation of these neurons activates a cation leak current that depolarizes the V_m resulting in a prolonged bout of excitation and a burst of APs, triggering exocytosis of the egg laying neuropeptides at neurohemal interfaces (*i.e.,* blood-brain interfaces) (10, 11). Similar depolarizing leak currents subject to neuromodulation have been reported in neurons, endocrine, and neuroendocrine cells of mammals and other vertebrates (12, 13). Another general role for leak channels, especially those that are non-selective, is to contribute to neuronal input resistance, an intrinsic feature that determines how electrical signals propagate through membranous cellular structures like dendrites and axons (14).

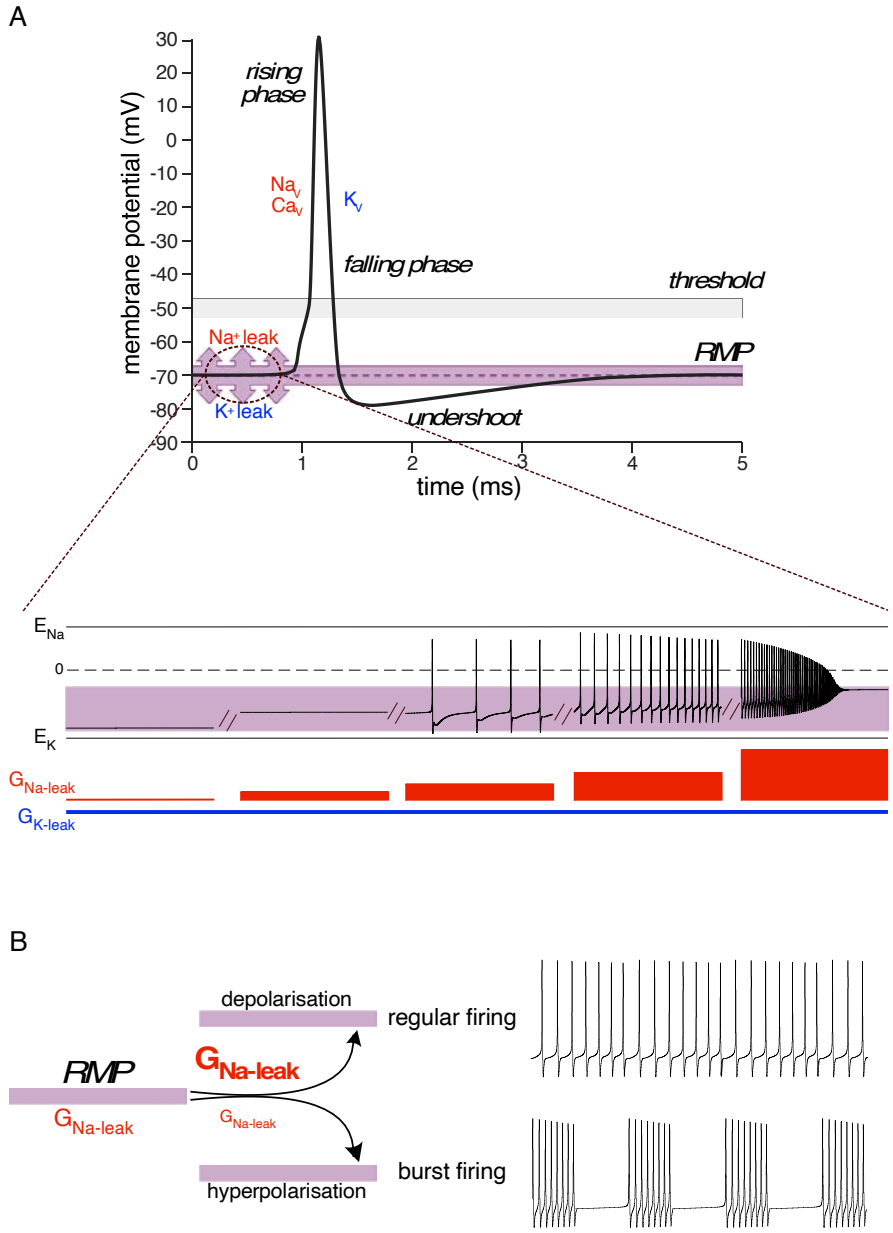

FIGURE 1. Ionic bases for electrical signaling and cellular excitability: contribution of a Na^+ leak conductance. ***(A)*** Contribution of a Na^+ leak conductance in regulating resting V_m (RMP). ***(Upper panel)*** Illustration of the action potential (AP), denoting the RMP, the rising phase driven by Na_V channels with contributions in some cells from voltage-gated Ca^{2+} (Ca_V) channels, and the falling phase or repolarization and subsequent AP undershoot driven by K_V channels. The purple dotted line and arrows delineate contributions of leak Na^+ and K^+ currents to establish and modulate the RMP, providing avenues for regulating membrane excitability by influencing the degree of stimulatory depolarization required to reach AP threshold. Both the RMP and the threshold voltage for generating AP are depicted as ranges, since these do not occur at fixed voltages. ***(Lower panel)*** Illustration of the role of Na^+ leak conductance in setting up the RMP. In a computed model of an excitable cell (12), the leak conductance has been divided into a K^+ ($G_{K\text{-}leak}$) and a Na^+ ($G_{Na\text{-}leak}$) components. The model was played by maintaining $G_{K\text{-}leak}$ amplitude as a constant value during the simulation runs, while $G_{Na\text{-}leak}$ amplitude sequentially increased. As the weight of the Na^+ component over the K^+ one increases, Vm gradually depolarizes from the resting value (set by E_K when $G_{Na\text{-}leak} = 0$) until the threshold for generating spontaneous spikes is reached. By regulating V_m, $G_{Na\text{-}leak}$ appears as a crucial protagonist in cell excitability. ***(B)*** Schematic representation of the contribution of $G_{Na\text{-}leak}$ in regulating the spiking pattern. From RMP and depending on its strength, the $G_{Na\text{-}leak}$ can contribute to either hyperpolarize (modest $G_{Na\text{-}leak}$ weight) or depolarize (robust $G_{Na\text{-}leak}$ weight) the cell, leading thus to distinct spiking patterns. The "hyperpolarized" state favors the burst firing while in a more "depolarized" state, the cell exhibit a regular firing.

Electrophysiological studies have reported a diversity of Na^+ leak conductances in neurons and other excitable cell types, attributable to different ion channel types capable of producing sub-threshold Na^+ leak currents. The molecular counterparts of these Na^+ leak conductances include Na_V channels (through different mechanisms) (15, 16), hyperpolarization-activated cation (HCN) channels (17), Transient Receptor Potential (TRP) channels (12), Epithelial Na^+ Channels (ENaC channels), Bile Acid-Sensitive Ion Channels (BASIC channels) (18), and finally, the Na^+ leak channel NALCN (19).

In this review, we aim to provide a detailed and up-to-date presentation of the current knowledge on NALCN, expanding on previous reviews published over 9 years ago by Ren, 2011 (13), Lu & Feng 2012 (20) and most recently by ourselves (Cochet-Bissuel et *al*, 2014 (19)). Since 2014, numerous important studies have emerged that increase our understanding of NALCN, including its protein structure in complex with its ancillary subunits UNC-79, UNC-80, and FAM155/NLF-1, its unique ion-conducting properties in recombinant expression systems, its modulation by various cell signaling pathways, and its contribution to physiology and various pathologies in humans. Hence, below we seek to highlight these advances, and integrate them into the general understanding of NALCN channel function and dysfunction. Some important milestones from the first identification of the *nalcn* allele (*i.e., narrow abdomen*) in *D. melanogaster* in 1934 to the identification of the cryogenic electron microscopy (Cryo-EM) structure of the NALCN channelosome is shown in Figure 2.

II. THE NALCN CHANNELOSOME

1- Identification and structure of the Na^+ Leak Channel NALCN

After the initial discovery of a subset of ion channel genes and corresponding protein structures (*e.g.,* Na_V and K_V channels), sequencing of various genomes in the late 1990s and early 2000s (21), as well as next-generation mRNA sequencing, ushered in an era of accelerated ion channel discovery. For example, identification of a human expressed sequence tag transcript encoding a portion of a novel voltage-gated calcium (Ca_V) channel led to the discovery that Ca_V3 or T-type channels give rise to neuronal low-voltage activated Ca^{2+} currents (22). Similarly, the discovery that HCN channels give rise to hyperpolarization-activated (*a.k.a.* funny currents or I_f) began with the sequence identification of ion channel genes that resembled K_V channels but had distinct structural features (23, 24). During this era, several other putative ion channel-related genes were identified with unknown functions or known current counterparts in native cells. This was the case for NALCN (for *Na^+ Leak Channel*; formerly named Rb21 or VGCNL1 in mammals), whose gene sequence was first reported in 1999 (1). In this study, the program Basic Local Alignment Search Tool (BLAST) (25) was used to search the NCBI GenBank database, using known ion channel protein sequences as query, to identify 2 novel genes related to Na_V and Ca_V channels present within the *C. elegans* genome. These were referred to as C27f2.2 (acc NP_498054; now referred to as *nca-2*) and C11d2.6 (acc NP_741413; formerly referred to as *unc-77* and now referred to as *nca-1*). A rat homolog cDNA was then cloned from a rat brain complementary DNA (cDNA) library (acc. Q6Q760.1; **FIGURE 3A**) (1). By homology with Na_V and Ca_V channel α_1 subunits (26), the pore-forming subunit of NALCN was similarly composed of four homologous repeat domains, referred to as Domains I to IV, each containing six membrane spanning helices or segments (*i.e.*, segments 1 to 6 or S1 to S6; **FIGURE 3B**). Segments 1 to 4 make of the

voltage-sensor domain (VSD), while segments 5 and 6 make up the pore-domain, with each set projecting a large pore-loop (P-loop) structure into the extracellular environment, shared with all members of the P-loop superfamily of ion channels which includes, Ca_V channels, Na_V channels, K_V channels, HCN channels, and TRP channels (**FIGURE 3B**).

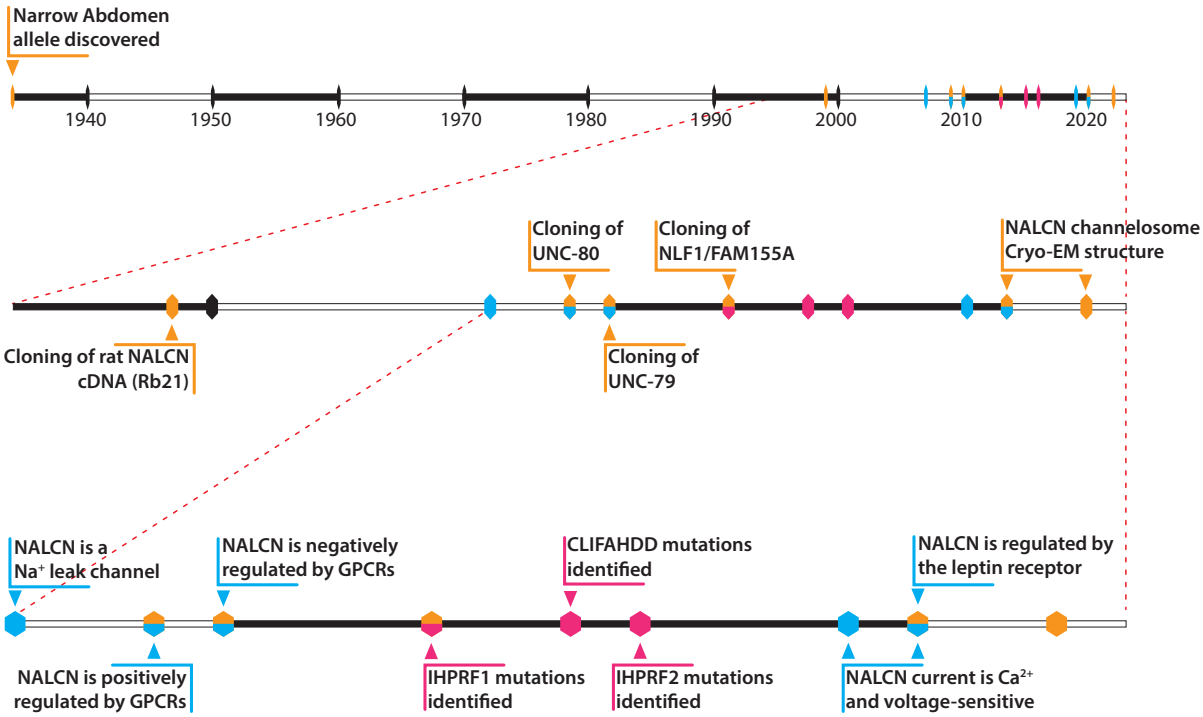

FIGURE 2. A timeline of NALCN research milestones. The major advances in NALCN research includes the first description of its allele in 1934 (upper line), its molecular identification and cloning in 1999, the cloning of its ancillary subunits (UNC-80, UNC-79 and NLF-1/FAM155A) and the elucidation of the 3D structure of the NALCN channelosome by cryogenic-electron microscopy (Cryo-EM) in 2020 and 2022 (orange marks, middle line). Regarding NALCN activity, its functional expression as a Na^+ leak channel and a G-protein-coupled receptor (GPCR)-activated channel was identified in 2007 and 2009 respectively, as well as novel NALCN modulations, including its calcium- and voltage-sensitivity in 2019 and 2020 (blue marks, bottom line). In the meantime (2013 – 2015 years), the first pathogenic variants of NALCN were described in patients with the IHPRF and CLIFAHDD syndromes (red marks, bottom line).

Interestingly, the S4 segments within the VSDs of the NALCN protein contain less positively-charged lysine/arginine amino acids compared to the other channels, especially in Domain IV (**FIGURE 3C**). This is notable because these residues are critical for voltage-sensing. In addition, four key amino acids in the P-loops that form the ion selectivity filter (SF) motif resemble Ca_V channels in having glutamate (E) residues in Domains I, II, and IV, but also Na_V channels in having a lysine (K) in domain III (*i.e.,* NALCN=EEKE; Ca_V=EEEE/EEDD; Na_V=DEKA; **FIGURE 3A**). The 3D cryo-electron microscopy (Cryo-EM) structure of NALCN, in complex with its ancillary subunit NLF-1/FAM155A subunit (*see below*), confirmed an overall similar architecture to Na_V and Ca_V channels despite some unique features (PDB: 6XIW (27); PDB: 7CM3 (28); PDB: 7CU3 (29); **FIGURE 4A,B**). In contrast to Na_V and Ca_V channels, the S4-S5 linkers that surround the S6-bundle give rise to an asymmetrical assembly (27, 29). The Domain I S5-helix extends in the cytoplasm by 3 additional α-helical turns leaving a shorter loop connecting to the Domain I S1-S4 VSD (27, 28). The Domain IV S5-helix is 1 turn shorter than expected

from Na_V and Ca_V channels, displacing the distal end of the Domain IV S4-S5 linker alpha helix towards the extracellular side. These observations suggest key differences in how the VSDs are functionally coupled to the S5-S6 pore module in NALCN compared to Na_V and Ca_V channels. This is supported by functional data indicating that it is mostly the VSDs of DI and DII that contribute to NALCN voltage sensitivity (*see below*)(30). These structural studies also identified 4 disulfide bonds on the extracellular P-loops of NALCN (28), which play important roles in maintaining the structure of the P-loops. Additional possible extracellular post-translational modifications of perceived importance were also identified. This included 3 glycosylation sites (p.N210, p.N216, p.N1064)(28), all with possible implications for NALCN structure and stability. The SF appears slightly narrower and more electronegative than those found in Na_v, but similar to those in Ca_v channels (27, 28). In analogy to Na_V and Ca_V channels, the SF side chains of p.E280, p.E554 and p.K1115 point towards the center of the pore, while p.E1389 exhibits 2 alternative conformations (29). The 3D structure of NALCN was only elucidated in a closed conformation, likely reflecting a low opening probability that was observed experimentally through single channel recordings (27-29, 31). The closed helix bundle crossing of the S6 helices from DI-DIV forms the channel gate (28). Both the DII-III and DIII-IV linkers interact with the carboxyterminal domain (CTD)(27-29), which consists of at least 5 to 6 short helices (C1-C6). Among these, C1-C4 form an EF-hand-like domain that packs below the III-IV linkers (28, 29). GST-pull down experiments further revealed an interaction between a fragment of the DII-DIII linker (aminoacids 751-765) and the CTD of NALCN (aminoacids 1455-1571)(29). Both NALCN structure and sequence suggest the absence of a fast inactivation motif, such as the IFM motif present in Na_V channels (27).

2- NALCN belongs to a protein complex that includes at least 4 subunits

Identification of NALCN ancillary subunits in invertebrates.

Many ion channels from the superfamily of voltage-gated and related cation channels require ancillary subunits to function *in vitro* and *in vivo* (26). This is also the case for NALCN, with first insights coming from studies in *C. elegans* which resulted in the identification of 3 NALCN subunits referred to as UNC-79 (for uncoordinated-79), UNC-80 (uncoordinated-80), and NLF-1/FAM155A (NALCN localization factor)(32-35). Specifically, a genetic screen aimed at identifying proteins that act downstream of Phosphatidylinositol-4,5-bisphosphate (PIP2) during synaptic vesicles endocytosis revealed that three alleles of the *unc-80* gene could suppress locomotor deficits caused by mutation of synaptojanin (*unc-26*), a key regulator of vesicle recycling at the presynaptic terminal (32). *Unc-26* mutant animals exhibited a severe uncoordinated locomotor activity and an increased number of synaptic vesicle number due to a recycling defect. These phenotypes were rescued when *unc-26* mutants were crossed with *unc-80* mutants. In this study, the locomotor behavior defects of *unc-80* mutant animals were similar to *nca-1:nca-2* double mutants (*C. elegans* harbors two gene copies of NALCN, NCA-1 and NCA-2), with further investigation showing reduced expression of NCA-1 (~40%) and NCA-2 (~48%) in axons of *unc-80* animals, but not in the cell bodies of motoneurons and nerve rings compared to control animals. Taken together, these results suggested that UNC-80 is required for NCA-1 and NCA-2 neuronal localization. UNC-80 is a large protein with at least two isoforms and no homologous domains and motifs that could suggest its function. The use of the GFP under the control of the *unc-80* promoter further revealed that *unc-80* is broadly expressed in the nervous system in both acetylcholine and GABA

motoneurons (32). This study also identified another gene referred to as *unc-79* with a suppressor effect in the uncoordinated phenotype of synaptojanin mutants like *unc-80* and *nca-1:nca-2* mutants (32). UNC-79 resembles UNC-80 in being a large protein with no described domains or motifs that could suggest function. Notably, the expression of the NCA-1 protein in *C. elegans*, and its orthologue Narrow Abdomen (NA) *a.k.a* Dmα1U in *D. melanogaster*, was attenuated below detection limits in UNC-79 mutants as determined *via* both Western blotting and immunocytochemistry (33). The NCA-1/NA disappearance did not correlate with the expression of the corresponding mRNAs, altogether indicating that UNC-79 regulates NALCN expression through a post-translational mechanism in both of these invertebrate species (33). Interestingly, the use of reporter constructs with GFP linked to the promoter regions of *unc-79*, *nca-1*, or *nca-2* showed that, although each reporter shows conspicuous (but not exclusive) expression in the nervous system, the pattern of *unc-79* does not coincide with that of *nca-1* or *nca-2* or with their sum (33). Nonetheless, the requirement of UNC-79 and UNC-80 for protein expression and localization of NCA-1 in cells was then confirmed using immunocytochemistry by Yeh et *al*, 2008, who found that UNC-79, UNC-80, and NCA-1 facilitate each other's colocalization along axons (34). Here, NCA-1 staining was eliminated or greatly reduced in multiple *unc-80* mutant strains, and further rescue experiments indicated that UNC-80 is both necessary and sufficient to localize NCA-1 along axons. Conversely, UNC-80 localization along axons depended on the presence of NCA-1 and/or NCA-2 (34). A strongly reduced NCA-1 and UNC-80 signal was also observed in *unc-79* animals while a reduction of UNC-79 expression/localization was observed in both *unc-80* and *nca-1:nca-2* animals (34, 35). This interdependent regulatory relationship between NALCN, UNC-79, and UNC-80 is also apparent in *D. melanogaster* (36). In addition, co-immunoprecipitation experiments from *D. melanogaster* head extracts indicated that NALCN (NA), UNC-79 and UNC-80 belong to the same protein complex (36).

The fourth subunit of the NALCN/NCA-1/NCA-2/NA channelosome to be identified was FAM155A, also in *C. elegans*. It was named *NALCN Localization Factor-1* or *NLF-1* (35). NLF-1 was identified through a genetic suppressor screen for altered locomotor behavior of *nca-1* gain-of-function mutants. In this study, premotor interneurons of *nlf-1* mutants exhibited a drastically reduced Na^+ leak current and a more negative RMP, attributable to a partial loss of NCA-1/NCA-2 function (35, 37). Immunostaining of both endogenous NLF-1 as well as an NLF-1::GFP transgene both indicated that NLF-1 is expressed in most if not all neurons and was first described as an ER resident protein that specifically promotes axon delivery of the NCA channel as well as of UNC-79 and UNC-80 (35, 37). Indeed, the protein expression and axonal localization of NCA-1 and NCA-2 was abolished in *nlf-1* animals similarly to what is observed in *unc-79* and *unc-80* animals (32, 34, 35, 37). The axonal localization of NCA-1 and NCA-2 was restored by acute expression of NLF-1. In addition, endogenous UNC-79 levels were significantly decreased in *nlf-1* mutants (35). Notably, decreased expression of a Na^+ leak conductance concomitant with altered electrical activity has also been observed in *D. melanogaster* neurons upon *nlf-1* knockdown, attributable to dysregulation of NA/Dmα1U activity (38).

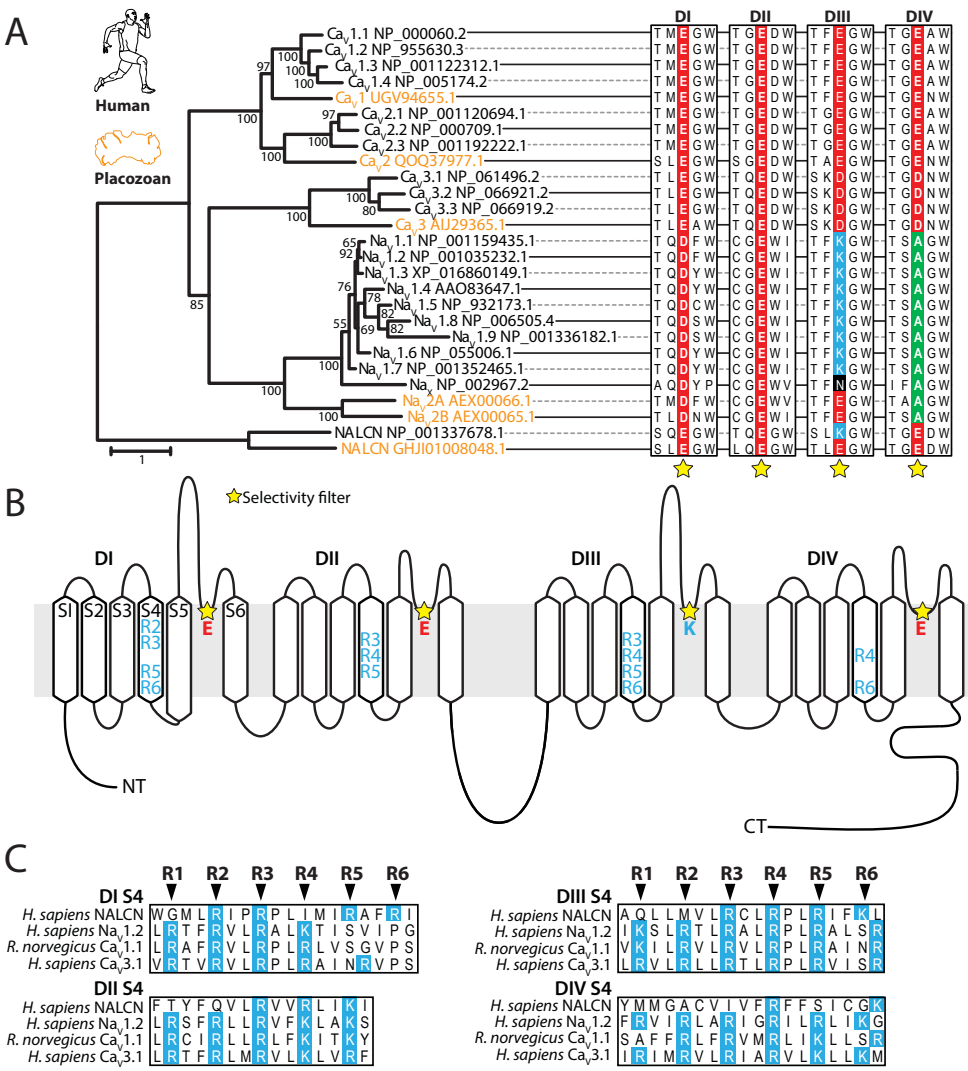

FIGURE 3. NALCN channels represent a fourth class of metazoan four-domain channels that includes Cav and Nav channels. ***(A)*** Maximum likelihood phylogenetic tree of the complete human four-domain ion channel set and homologues from *Trichoplax adhaerens*, the most early-diverging animal to possess a complete set of orthologues (NCBI sequence accession numbers are provided). Evident are four distinct classes of four-domain channels, comprised of Cav1/Cav2 channels, Cav3 channels, Nav channels, and NALCN. The tree was inferred from a protein alignment generated with the program MUSCLE (39) and trimmed with the program trimAl (40) using a gap threshold of 0.6. ModelFinder (41) was used to identify a best-fit model of LG+R5 under the Bayesian Information Criterion, and the program IQTree (version 2)(42) was used to infer the depicted phylogenetic tree. Node support values for 1,000 ultrafast bootstrap replicates are shown, and the scale bar on the lower left indicates the average number of substitutions per site in the trimmed protein alignment. To the right of the tree are sequence alignments of the four pore-loop regions from each domain, harboring the key selectivity filter residues (*black chevrons*) that make up the motifs of EEEE (Cav1 and Cav2 channels), EEDD (Cav3 channels), DEKA, DENA, or DEEA (Nav channels), and EEEE or EEKE (NALCN channels). ***(B)*** Illustration of the general membrane topology of the NALCN channel protein, comprised of four homologous repeat domains, each containing six transmembrane helices or segments (S1-S4). The R1 to R6 positions on the S4 helices denote the number of positively charged lysine (K) and arginine (R) amino acids in the human NALCN channel S4 helices which are a critical for voltage sensing. In addition to the S4 helices, S1 to S3 helices form the voltage sensor modules of each repeat domain. Also depicted are the general positions of the four selectivity filter residues (*yellow stars*), positioned within the extracellular pore-loops of each domain that project into the extracellular environment from the S5 and S6 helices. ***(C)*** Protein alignment of the S4 helices of various four-domain channels reveals a reduced number of repeating cationic K and R residues (at positions R1 to R6 of the S4 helix) compared to Nav and Cav channels, particularly in domain IV. For panels A and C, positively charged residues are back-colored *blue*, negatively charged residues are back-colored *red*.

NALCN ancillary subunits are conserved in mammals.

The relevance of the identified subunits mentioned above was confirmed in mammals via co-immunoprecipitation experiments using protein lysates from both transfected HEK-293T cells and mouse brain tissue (30, 43, 44). Notably, UNC-79 was first described to form a complex with NALCN *via* its interaction with UNC-80 but not NALCN in the mouse brain (44). However, more recent structural studies reveal that both UNC-79 and UNC-80 directly interact with NALCN, although the former with considerably fewer contacts perhaps accounting for its inability to coprecipitate with the channel (31, 45, 46). Contrasting with observations made in *C. elegans* and *D. melanogaster*, the expression levels of NALCN are not appreciably disrupted in mice harboring UNC-79 or UNC-80 knockout mutations while UNC-79 knockout mutations decrease the expression levels of UNC-80 (44, 47, 48). UNC-79 is also detected in brain extracts from *Unc-80* knockout mice (49). This indicates that there are differences between mammals and invertebrates with respect to the noted interdependent nature of subunit expression. Functionally, the Na^+ background conductance is strongly reduced in hippocampal neurons from *Unc-80* knockout mice and restored by overexpression of UNC-80, but not UNC-79, suggesting that UNC-80 is more critical for the proper functional expression of NALCN. Indeed, there is no obvious difference in amplitude of the Na^+ background conductance between wild-type and *Unc-79*$^{-/-}$ hippocampal neurons (44), despite the observation that both UNC-79 and UNC-80 appear to be specific ancillary subunits of NALCN since affinity-depletion of NALCN from mouse brain extracts also fully depletes the UNC-79 and UNC-80 proteins (49). Altogether, although there may be some differences between mammals and invertebrates with respect to the interplay between NALCN subunits, the strong interdependence of NALCN, UNC-80, and UNC-79 appears to be conserved.

Accordingly, UNC-80 promotes NALCN expression at the plasma membrane by approximately threefold when both proteins are co-expressed in HEK-293T cells (49). Co-expression experiments of NALCN along with UNC-80 in HEK-293T cells followed by electrophysiological recordings and co-immunoprecipitation revealed that the N-terminal part of UNC-80 (*i.e.*, amino acids 300 to 1,700) is sufficient for the interaction with the channel, since its deletion abrogates the interaction along with NALCN activity (49). Of note however, a separate study reported that deletion of the 733 first amino-acids of UNC-80 does not impact NALCN currents *in vitro* (30). UNC-80 with deletions of C-terminal residues up until residue 2,554 is fully functional and residues 1,701 to 2,387 are essential for the generation of a NALCN current *in vitro* (49). Similar deletion experiments also delineated an UNC-79-interacting domain (amino acids 2,758 to 2,947) on UNC-80. The binding of UNC-79 to UNC-80 was proposed to relieve a soma-retention of the complex. Indeed, a soma-retention region was identified within residues 2,387 to 2,657 of UNC-80, which presumably becomes masked *via* interactions with UNC-79 at a more C-terminal location.

With respect to NLF-1, two proteins referred to as FAM155A (human acc. NP_001073865.1; 458 amino acids) and FAM155B (human acc. NP_056501.2; 472 amino acids) were identified in mammals for their sequence homology to the invertebrate subunit. Evidence that these are true orthologues comes from observations that the mammalian NLF-1/FAM155A protein is able to functionally substitute for NLF-1 in *C. elegans* neurons, and its knockdown in primary mouse cortical neurons strongly

599 decreases a Na^+ leak conductance (35). In COS7 cells, ectopically-expressed NLF-1 and
600 NLF-1/FAM155A both exhibit ER localization, and both co-immunoprecipitate with
601 NALCN (35). It was therefore suggested that NLF-1 and NLF-1/FAM155A have a
602 conserved function by acting as chaperones to facilitate NALCN folding and delivery to
603 the plasma membrane. Both NLF-1 and NLF-1/FAM155A exhibit a tail-anchored, type I
604 ER membrane topology, and a membrane yeast two-hybrid system showed the
605 interaction between NALCN and NLF-1/FAM155A involves the Domain II S5 to S6 pore
606 module of the channel subunit (35).
607
608 In mammals, NLF-1/FAM155A co-immunoprecipitates with NALCN when co-
609 expressed in HEK-293T cells and can be substituted by NLF-1/FAM155B, a mammalian
610 paralogue of NLF-1/FAM155A, to produce functional NALCN channels (*see below*)(30).
611 However, unlike in *C. elegans* where NLF-1 is thought to be restricted to the ER, FAM155A,
612 along with UNC-79, UNC-80, and NALCN, were shown to traffic to the cell surface when
613 expressed alone in HEK-293T cells *via* cell-surface biotinylation assays. These new
614 findings prompt further investigation to determine the subcellular localization of NLF-1
615 in mammals, where NLF-1/FAM155A (458 amino acids) is predicted to contain at least
616 one transmembrane segment and a conserved cysteine-rich domain (CRD)(35, 50).
617
618 *Structure of the NALCN channelosome in mammals.*
619
620 Recent cryo–electron microscopy (Cryo-EM) structures of NALCN in complex with
621 NLF-1/FAM155A, and subsequently of the entire NALCN channelosome complex (*i.e.*,
622 NALCN, NLF-1/FAM155A, UNC-79 and UNC-80) revealed that UNC-79 and UNC-80 do not
623 impose notable structural changes in the NALCN-NLF-1/FAM155A subcomplex (**FIGURE**
624 **3A**)(31, 45, 46). However, the intracellular linker regions of NALCN show extensive
625 ordering when associated with UNC-79 and UNC-80, which is not apparent in the NALCN-
626 NLF-1/FAM155A subcomplex (31, 45, 46). UNC-79 and UNC-80 form a massive,
627 intertwined, intracellular assembly that hangs beneath the voltage sensor domains
628 (VSDs) from Domains I to III of NALCN. Below the DIV VSD, the C-terminal domain (CTD)
629 of NALCN is embraced by calmodulin (CaM), which itself is docked against UNC-80 near
630 the midpoint of the intracellular assembly. A small portion of the NALCN DI-DII linker
631 contacts a membrane proximal surface of UNC-79, while two discrete regions from the
632 DII-DIII linker form an elaborate clamp-like interaction with UNC-80. Systematic
633 substitution of intracellular regions from $Na_v1.4$ into NALCN revealed an absolute
634 requirement for the DI-DII and DII-DIII linkers for NALCN channelosome activity *in vitro*
635 (31). The identified channelosome structure also provided first structural insights into
636 UNC-79 and UNC-80. These 2 proteins are well-folded intracellular globular proteins that
637 form a head-to-tail super helical assembly, resembling an infinity sign. Both proteins
638 appear to belong to the HEAT repeat superfamily, in bearing tandem repeat structural
639 motifs composed of two α-helices linked by a short loop, although some of the repeats in
640 both UNC-79 and UNC-80 display motifs comprised of 3 α-helices, as observed in the
641 related armadillo repeat proteins. UNC-79 and UNC-80 contain 32 and 31 HEAT repeats
642 respectively. Notably, UNC-79 and UNC-80 are reported to lack significant sequence
643 identity, however both proteins share a similar structural architecture. UNC-80 also
644 exhibits a ubiquitin-like domain (1,983 to 2,076), while both UNC-79 and UNC-80 bear 3
645 tandem importin-α3 motifs. 3 large interacting regions between UNC-79 and UNC-80
646 were identified, referred to as the N_{UNC-79}-C_{UNC-80} interface (N-C), the Crossover Interface,
647 and the C_{UNC-79}-N_{UNC-80} (C-N) interface. The presence of the three extensive and conserved

UNC-79-UNC-80 interaction interfaces suggests that these subunits form a phylogenetically conserved subcomplex. *In vitro* channelosome function tolerates deletion from the C-terminal region of UNC-79 (Δ2,401-2,635) and the N-terminal region of UNC-80 (Δ1-733), indicating that portions the C-N interface are dispensable, at least for functional expression in *Xenopus laevis* oocytes (30).

Cryo-EM studies also showed that NLF-1/FAM155A contains 2 lobes, the N-lobe and the C-lobe, which are stabilized by 6 disulfide bonds (27-29). The N-lobe consists of 3 short β strands and 2 short α helices (H1-H2), while the C-lobe contains 4 α helices (H3-H6). Part of this extracellular domain fold shows similarity to the structure of the frizzled-like cysteine-rich domain (CRD) of the receptor tyrosine kinase MuSK. The C-lobe of NLF-1/FAM155A interacts with NALCN. A sugar moiety linked to p.N1064 in the NALCN domain III P-loop appears to contribute to the interaction by potentially forming a hydrogen bond with residue p.E350 on NLF-1/FAM155A. The globular CRD formed by NLF-1/FAM155A is anchored onto the DIV pore module and forms extensive interactions with P-loops in domains I, III, and IV (28, 29). The interaction between NLF-1/FAM155A and NALCN involves the highly conserved NALCN P-loop residues p.W1085/p.R1062/p.R1094 located in domain III, a p.D1408 residue in domain IV, and p.D1397 and p.E1364 in domain IV. In vertebrates, NLF-1/FAM155A has 2 predicted transmembrane helices that may anchor the CRD in proximity to NALCN, and creates a sealed dome-like structure that walls off most extracellular access pathways to the SF (27-29). As a consequence and in contrast to Na_v and Ca_v, channels, NALCN does not show lateral fenestrations in its pore module that could provide an access route for drugs to enter into the central cavity for block in the closed state (27). One glycosylation site on NLF-1/FAM155A (p.N217) is detected (28), however the functional role of glycosylation on NLF-1/FAM155A is currently unknown and needs to be investigated. The functional relevance of having NLF-1 paralogues in mammals, FAM155A and FAM155B, is also unknown. Of note, while the *NLF-1/FAM155A* mRNA is mainly expressed in various regions of the brain as well as in the pituitary gland, the *NLF-1/FAM155B* mRNA is mainly expressed in heart and thyroid gland in humans (https://www.gtexportal.org).

3- NALCN and its subunits are conserved in most animals

Here, we provide an updated survey of NALCN channel complex homologues present within the genomes and transcriptomes of several species from a range of animal phyla (**Figure 4A**). Consistent with previous reports (51, 52), it appears that humans and other vertebrates (phylum Chordata) possess single-copy genes for NALCN, UNC-79, and UNC-80, and two NLF-1/FAM155 paralogues, NLF-1/FAM155A and NLF-1/FAM155B (**Figure 4B**). The early-diverging chordate *Ciona intestinalis*, an invertebrate tunicate (sea squirt), only possesses a single NLF-1/FAM155 homologue. Generally, protostome and deuterostome invertebrates similarly possess single copy genes for all four NALCN subunits. A well-known exception is the nematode worm *Caenorhabditis elegans*, which appears to have duplicated NALCN to give rise to the paralogues NCA-1 and NCA-2 (33). Given the absence of duplicated NALCN genes in early-diverging nematodes such as the parasitic species *Trichinella pseudospirallis*, this duplication likely occurred within a subclade of the nematode phylum. Similar within-phylum variability is evident for the Platyhelminthes, where the non-parasitic (free-living) flatworm *Macrostomum lignano* duplicated NALCN and NLF-1/FAM155 to give rise to two copies each, while the parasitic species *Schistosoma mansoni* retained single copies of all subunits. The fellow spiralian,

and freshwater rotifer *Rotaria socialis* is unique amongst examined species in duplicating UNC-80, along with NLF-1/FAM155.

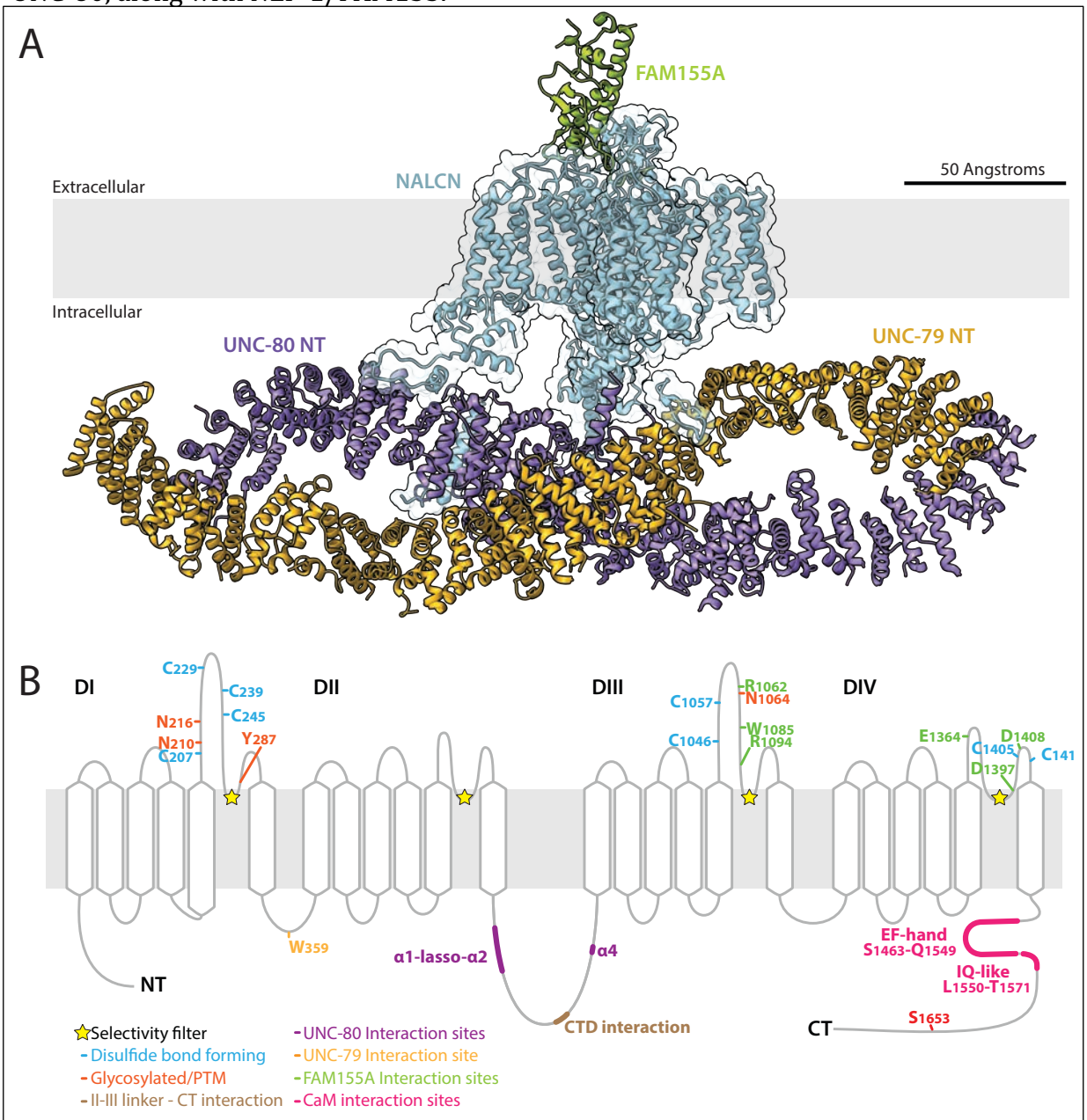

FIGURE 4. Structural features of the NALCN channel complex. ***(A)*** Ribbon diagram representation of the recently resolved core NALCN channel complex (31) consisting of the NALCN pore-forming α_1 subunit (in *blue*), the large cytoplasmic UNC-79 and UNC-80 subunits (yellow and purple, respectively), and the extracellular FAM155A subunit (*green*). The image was prepared using the program UCSF ChimeraX (354), using the published structural PDB file 7SX4. ***(B)*** Illustration of the NALCN α_1 subunit transmembrane structure illustrating locations of various structurally important features as indicated by the legend below. Denoted are the paired extracellular cysteine residues (C) that form important disulfide bonds in the pore-loop regions (cyan), extracellular asparagine (N) and tyrosine (Y) residues that are post-translationally modified through glycosylation (N) and/or sulfation (Y) (*orange*), key amino acids important for interactions with the FAM155A subunit (*green*; arginine/R, tryptophan/W, glutamate/E, aspartate/D), an important tryptophan in the domain I-II linker that interacts with the UNC-79 subunit, and two regions in the domain II-III linker that are required for interactions with UNC-80 (*purple*; *i.e.*, the α1-lasso-α2 motif and the α4 helix). Also represented is the region of the domain II-III linker region shown to interact with the channel C-terminus (*light brown*), and regions in the C-terminus where the Ca^{2+} sensor protein calmodulin (CaM) binds (*pink*).

Previously, the non-bilaterian invertebrate *Nematostella vectensis* (sea anemone, phylum Cnidaria which includes jellyfish and corals), as well as the Great Barrier Reef sponge *Amphimedon queenslandica* (phylum Porifera), were reported to possesses 2 NALCN channel genes (51, 52). However, only a single homologue is evident in the most recent and complete *N. vectensis* genome assembly (53). Instead, the 2 *A. queenslandica* paralogues are significantly different in their sequence, and hence represent *bona fide* paralogues that likely emerged through duplication. That the NALCN subunits duplicated independently in *M. lignano*, *C. elegans*, and *A. queensalidica* is suggested by their respective monophyletic relationships on a protein phylogenetic tree (**Figure 5**). Like *N. vectensis*, the other non-bilaterian species *Trichoplax adhaerens* (phylum Placozoa) also possesses single copy genes for all NALCN subunits. Perhaps most remarkable within the Metazoa is the complete absence of NALCN subunits in the gene data available for ctenophores, including the well-studied species *Mnemiospsi leidyi* (**Figure 5B**). Recent phylogenomic studies strongly support either sponges or ctenophores as the most divergent animal lineage (54, 55), suggesting that either ctenophores lost the channel complex (if sponges are the most divergent), or it evolved after ctenophores diverged in the common ancestor of Porifera, Placozoa, Cnidaria, and Bilateria (**Figure 5A**).

4- Distribution and cellular localization of NALCN

To date, our understanding of the cellular (and subcellular) co-expression of NALCN and its subunits is incomplete and requires further investigation, especially in mammals. In rodent and human, northern and dot blot analysis highlighted that *NALCN* mRNA is expressed in all brain regions, as well the heart, pituitary, and adrenal glands (1, 56). A similar expression pattern was described by RT-qPCR in the pond snail *Lymnea stagnalis* that express *NALCN* mainly in the central nervous system but also in the heart, secretory organs, and the buccal musculature (51). Of note, this latter study also reported localization of *NALCN* mRNA at axons/neurites, suggesting that translation of NALCN could occur outside the cell body through a process referred to as local protein synthesis. In mice, NALCN mRNA is abundantly expressed in neurons (http://www.mousebrain.org)(57), while in humans, the temporal expression of *NALCN* mRNA in different parts of the brain closely parallels the expression of synapse, dendrite, and myelination development genes (http://hbatlas.org/)(58).

In mammals, the development of antibodies that can reliably detect NALCN in tissues has recently paved the way for determining its cellular and subcellular distribution, permitting confirmation that the channel protein is expressed in proximal dendritic compartments of rodent nigral dopaminergic neurons as well as in dorsal root ganglia neurons, dorsal spinal cord neurons and in a human cell line *via* immunocytochemistry (59-63). Furthermore, the NALCN ancillary subunit UNC-80 localizes to dendrites in mouse cultured hippocampal neurons when overexpressed *in vitro* (49), implying that NALCN and its other subunits might also be localized to dendrites. In *C. elegans*, the use of both GFP-tagged endogenous proteins and immunostaining revealed that the two NALCN channel paralogues, NCA-1 and NCA-2, both localize along axons and are enriched at nonsynaptic regions (32, 34). By contrast, the *D. melanogaster* NA/Dmα1U channel protein is mainly concentrated in the neuropil region of the brain which is enriched in synapses, but not areas occupied primarily by cell bodies or axon tracts (64). Another study reported expression of NA/Dmα1U in the cell body and terminals of pacemaker ventral lateral neurons which play a central role in regulating circadian rhythm (65). In *L.*

stagnalis, the NALCN homolog of appears to be enriched in neurites (acc. AGC13754.1)(51).

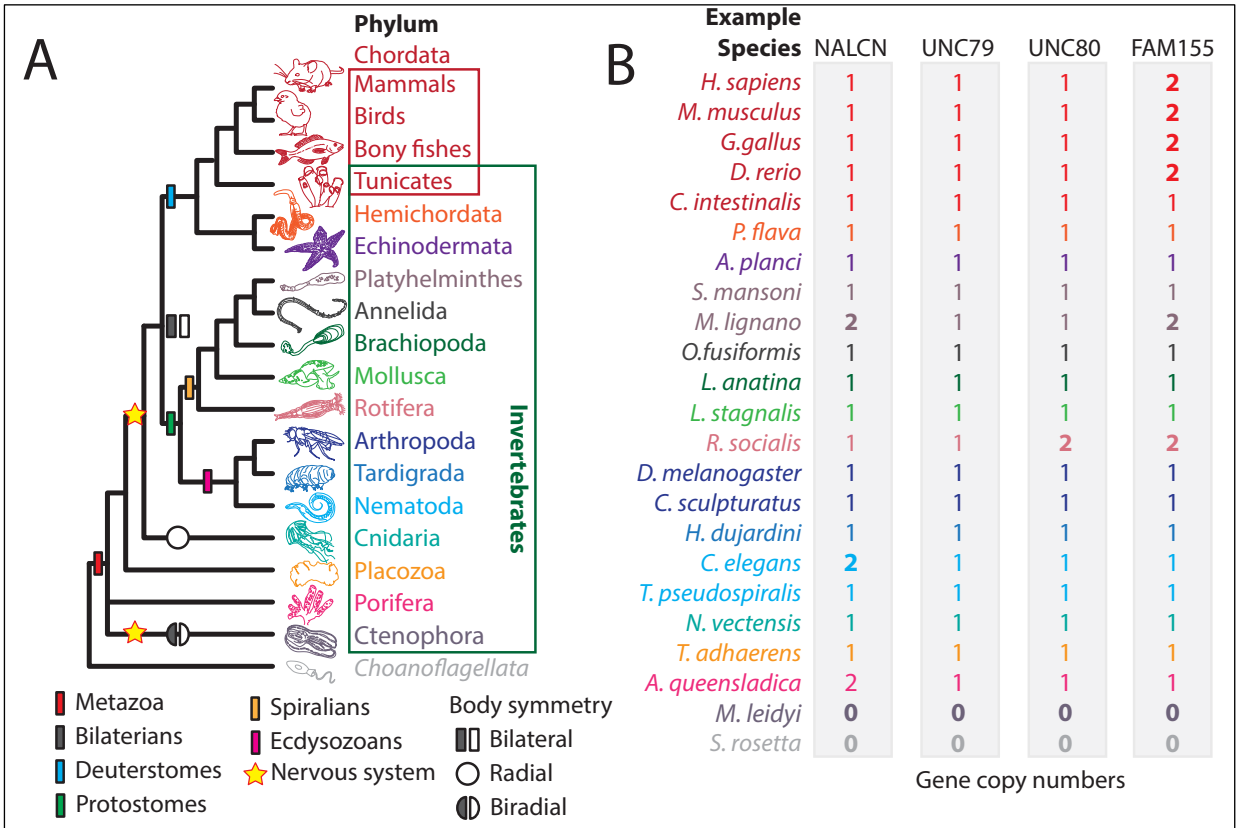

FIGURE 5. NALCN subunits are conserved between animals and fungi. ***(A)*** Cladogram depicting the phylogenetic relationships of representative phyla from the Kingdoms of Metazoa and Fungi. Animal groupings based on body symmetry (*i.e.*, bilateral, radial, biradial, and lacking symmetry), differences in embryonic development (*i.e.*, deuterostomes *vs.* protostomes, ecdysozoans *vs.* spiralians), and presence/absence of a nervous system are depicted by symbols located at the stems of corresponding clades, according to the legend located underneath the cladogram. ***(B)*** Gene counts for the NALCN α_1 subunit, and the accessory subunits UNC-79, UNC-80, and FAM155, identified for various representative species. Species names are color-coded according to the different phyla depicted in panel *A*. Sequences were identified by searching through various genome and transcriptome databases available on NCBI using reciprocal protein BLAST, except for *Ptychodera flava* and *Trichoplax adhaerens* whose sequences were extracted from available databases (66, 67). To confirm that the identified sequences are *bona fide* NALCN subunit homologues, each was subjected to further analysis using NCBI smartBLAST and phylogenetic analysis.

5- NALCN currents in native cells

The first study describing the functional properties of NALCN as a TTX-resistant Na^+ leak channel in neurons was provided by Lu et *al*, in 2007 (2). In this pioneer study, Dejian Ren and colleagues generated a knockout mouse model by removing the first coding exon of the *Nalcn* gene. Primary hippocampal neurons from knockout mice were found to be hyperpolarized with a RMP ~10 mV lower than wild-type neurons. Furthermore, patch-clamp recordings of wild type hippocampal neurons where external Na^+ was replaced with the impermeant large inorganic cation $NMDG^+$, in the presence of TTX and Cs^+ which block Na_v and HCN channels respectively, revealed the disappearance of a pronounced Na^+ background conductance. Instead, this effect was not evident in neurons from knockout mice, strongly suggesting that NALCN is responsible for this leak current.

Furthermore, both the RMP and the Na^+ background conductance were restored by overexpressing NALCN in a knockout background, producing a more depolarized RMP and the re-appearance of a Na^+ background conductance compared to control neurons. The relative contributions of I_{NALCN}, I_h and I_{Nav} to the total background Na^+ current was estimated to be ~70%, ~10%, and ~20% respectively in hippocampal neurons (2). As a consequence of the *Nalcn* knockout, neuronal electrical activity is almost fully abolished as demonstrated by electrophysiological recordings from the C4 nerve root in the spinal cord. That the major contribution of NALCN in regulating the RMP and the firing rate of neurons is by conducting background Na^+ leak currents was also confirmed in suprachiasmatic nucleus neurons (38), GABAergic substantia nigra pars reticulata (SNr) neurons (68), neurons in the deep mesencephalic nucleus (69), CO_2/H^+-sensitive neurons of the retrotrapezoid nucleus (34, 70), glutamatergic pre-Bötzinger Complex neurons (34), spino-parabrachial neurons (71), dopamine neurons from the substantia nigra (72), type-2 neurons in the nucleus of the solitary tract expressing the leptin receptor (73), dorsal root ganglia neurons and dorsal spinal cord neurons (61, 62). In addition, the depolarizing function of NALCN is clearly conserved in neurons from invertebrates such as posterior dorsal neurons 1 (DN1p) neurons from *D. melanogaster* (38), pacemaker RPeD1 neurons from *L. stagnalis* (74), and premotor interneurons from *C. elegans* (35, 75). The contribution of NALCN in regulating the RMP and electrical activity was also extended to an endocrine anterior pituitary cell model (76). **TABLE 1** summarizes studies describing NALCN-related currents from native cells, and **Figure 7** (*see below*) illustrates several of these electrical activity modulations described here in association with the physiological roles of NALCN (*see* 'NALCN & Physiology' section).

TABLE 1: Endogenous NALCN currents in native cells

Species	Cell Type	RMP change	Method	References
M. musculus	Hippocampal neurons	≈ -10 mV NI NI ≈ -5 mV	Knockout Knockdown	Lu et *al*, 2007 (2) Lu et *al*, 2009 (43) Lu et *al*, 2010 (44) Ou et *al*, 2020 (77)
M. musculus	Ventral tegmental area neurons	NI	Knockout	Lu et *al*, 2009 (43)
M. musculus	Pancreatic b-MIN6 cells	NI NI	Knockdown Overexpression	Swayne et *al*, 2009 (56)
M. musculus	Interstitial cells of Cajal	NI	Knockout	Kim et *al*, 2012 (78)
M. musculus	Cortical neurons	NI	Knockdown FAM155A	Xie et *al*, 2013 (35)
M. musculus	SCN pacemaker neurons	≈ -11,4 mV	Knockout	Flourakis et *al*, 2015 (38)
H. Sapiens	Myometrial smooth muscle cells	NI	Knockdown	Reinl et *al*, 2015 (79)
M. musculus	Retrotrapezoid neurons	NI ≈ -9,12 mV NI	Knockdown Knockout Knockdown	Shi et *al*, 2016 (70) Yeh et *al*, 2017 (80) Yang et *al*, 2020 (81)
M. musculus	Deep Mesencephalic neurons	≈ +7,8 mV	Gain-of-function mutation	Funato et *al*, 2016 (69)
M. musculus	Substantia nigra pars reticulata neurons	NI	Knockout	Lutas et *al*, 2016 (68)
M. musculus	Glutamatergic preBötC neurons	≈ -5,34 mV	Knockout	Yeh et *al*, 2017 (80)

M. musculus	Spino-parabrachial neurons	≈ -15,7 mV	Knockout	Ford et *al*, 2018 (71)
M. musculus	Dopamine neurons from the substantia nigra	NI NI	Knockout Pharmacological inhibition L-703,606 (10 µM)	Philippart & Khaliq, 2018 (72) Um et *al*, 2021 (82) Hahn et *al*, 2023 (59)
M. musculus	Granule cells of the dentate gyrus	NI	Pharmacological inhibition L-703,606 (10 µM)	Gonzalez et *al*, 2023 (83)
M. musculus	Type-1 and type-2 leptin receptor-expressing neurons in the nucleus of the solitary tract	NI	Knockout	Do et *al*, 2020 (73)
R. Norvegicus	Pituitary GH3 cells	≈ -5.3 mV ≈ +11.7 mV	Knockdown Overexpression	Impheng et *al*, 2021 (76)
R. Norvegicus	Dorsal spinal cord neurons	NI	Knockdown	Zhang et *al*, 2021 (61) Li et *al*, 2021 (62)
R. Norvegicus	DRG neurons	NI	Knockdown	Zhang et *al*, 2021 (61) Li et *al*, 2021 (62)
Bos Taurus	Chromaffin cells	NI	Pharmacological inhibition CP96345 (20-50 µM)	Yang et *al*, 2022 (84)
L. stagnalis	RPeD1 neurons	NI	Knockdown	Lu & Feng, 2011 (74)
C. elegans	Premotor interneurons	≈ -6 mV	Knockout FAM155A Knockout NALCN	Xie et *al*, 2013 (35) Gao et al, 2015 (75)
D. Melanogaster	DN1p neurons	NI	Knockout	Flourakis et *al*, 2015 (38)

Abbrevations: NI, not indicated

6- Functional expression of NALCN in recombinant systems

A rigorous understanding of NALCN function/dysfunction through the study of its biophysical and pharmacological properties requires the ability to express it as a functional channel complex *in vitro* in cell lines such as HEK-293T (85-87). Several configurations and recombinant systems were used to achieve functional expression of NALCN (**TABLE 2**). In addition to the first demonstration that NALCN encodes a Na^+ background conductance in hippocampal neurons, Lu et *al*, 2007, also reported the first functional expression of NALCN in a recombinant system (2). Transient expression of rat NALCN alone in HEK-293T cells resulted in the expression of a voltage-independent leak current with a linear current-voltage (I/V) relationship within the range of -80 to +80 mV, and a reversal potential (E_{rev}) of 0 mV. No voltage-dependent inactivation was observed (2). In this study, NALCN was permeable to cations with a selectivity sequence of $P_{Na}(1.3) > P_K(1.2) > P_{Cs}(1) > P_{Ca}(0.5)$. Interestingly, a mutation in the selectivity filter to create an EEKA sequence instead of an EEKE sequence in the wild-type NALCN resulted in a selectivity sequence of $P_{Na}(1.3) = P_K(1.3) > P_{Cs}(1) > P_{Ca}(0.1)$, indicating a major role of the fourth glutamate in Ca^{2+} permeability. Instead, no current was detected when the selectivity filter was modified to resemble high voltage-activated Ca_V channels, with an

EEEE configuration. In this study, NALCN currents were blocked by Cd^{2+} (IC_{50} = 0.15 mM), Co^{2+} (IC_{50} = 0.26 mM), Gd^{3+} (IC_{50} = 1.4 µM), but not by Ni^{2+} (1 mM) and La^{3+} (100 µM). NALCN was also found to be insensitive to TTX (10 µM), but completely blocked by 1 mM verapamil, a Ca_v channel blocker. Of interest, the fourth glutamate of the selectivity filter was implicated in the sensitivity of NALCN to Gd^{3+} block. Although an enhanced leak current was also reported by other groups, when NALCN was expressed alone in HEK-293T cells (77, 88, 89), a debate has remained for some time regarding how to achieve functional expression of NALCN in this cell line without co-expressing its subunits NLF-1/FAM155, UNC-79 and UNC-80, as NALCN current measured in the absence of its accessory subunits could not be reproduced in other studies (1, 51, 56, 90, 91).

TABLE 2: Functional expression of NALCN in recombinant system

Cell type	Current type	Method/ Subunits expressed	References
HEK-293T	Leak	NALCN	Lu et *al*, 2007 (2) Lu et *al*, 2009 (43) Egenbrod et *al*, 2019 (88) Hahn et *al*, 2020 (89) Ou et *al*, 2020 (77)
HEK-293T	Substance P-activated	NALCN, UNC-80, TACR1	Lu et *al*, 2009 (43)
HEK-293T	Leak	NALCN, UNC-80, SrcY529F	Lu et *al*, 2009 (43) Lu et *al*, 2010 (44) Funato et *al*, 2016 (69) Lee et *al*, 2019 (92)
HEK-293T	Leak	NALCN, UNC-80, Src activator*	Stray-Pedersen et *al*, 2016 (93) Wie et *al*, 2020 (49)
HEK-293T	Leak	NALCN, UNC-79, UNC-80, NLF-1/FAM155A (or B)	Chua et *al*, 2020 (30) Kschonsak et *al*, 2020 (27) Kang et *al*, 2020 (29) Xie et *al*, 2020 (28) Kschonsak et *al*, 2022 (31) Zhou et *al*, 2022 (46) Kang & Chen, 2022 (45)
HEK-293T	Leak	NALCN, NLF-1/FAM155A	Xie et *al*, 2020 (28)
HEK-293T	Acetylcholine-activated Carbachol-activated	NALCN, M3R	Swayne et *al*, 2009 (56) Hahn et *al*, 2020 (89)
MIN6	Acetylcholine-activated	NALCN**	Swayne et *al*, 2009 (56)
Xenopus Oocyte	Acetylcholine-activated	NALCN, M3R	Swayne et *al*, 2009 (56)
SH-SY5Y	Leak	NALCN	Lu et *al*, 2010 (44)
NG108-15	Leak	NALCN, NLF-1/FAM155A***	Bouasse et *al*, 2019 (94)
GH3	Leak	NALCN****	Impheng et *al*, 2021 (76)
Xenopus Oocyte	Leak	NALCN, UNC-79, UNC-80, NLF-1/FAM155A (or B)	Chua et *al*, 2020 (30) Kschonsak et *al*, 2020 (27) Kschonsak et *al*, 2022 (31)

*** Introduced in the Patch pipette; ** MIN6 cells endogenously express *Unc-79* and *Unc-80* mRNAs (not known for *Nlf-1/Fam155A* and *Nlf-1/Fam155B*)(63); *** NG108-15 cells endogenously express *Unc-79* and *Unc-80* but not *Nlf-1/Fam155A* mRNAs (not known for Nlf-1/*Fam155B*)(92); **** GH3 cells endogenously express *Unc-79*, *Unc-80* and *Nlf-1/Fam155A* mRNAs (not known for *Nlf-1/Fam155B*)(80).**

Another configuration was proposed to achieve the functional expression of NALCN in HEK-293T cells. Here, the functional expression of NALCN in HEK-293T cells required co-expression with UNC-80 and a constitutively active form of the src kinase (*i.e.*, a p.Y529F mutant (43). This kinase is involved in NALCN activation by G-protein-coupled receptors (*see below*)(43, 56). This configuration, which was successfully reproduced in other studies (44, 69, 92), also gave rise to a voltage-independent cationic current with a linear I/V relationship, corroborated by loss of inward currents when external Na^+ and K^+ were replaced with the impermeant cation $NMDG^+$. Furthermore, inclusion of a peptide in the patch pipette that activates src was found to regulate the NALCN-UNC-80 currents *in vitro* (44, 49, 93).

More recently, a study showed that functional expression of NALCN in HEK-293T cells and *Xenopus* oocytes requires co-expression with UNC-79, UNC-80 and either NLF-1/FAM155A or NLF-1/FAM155B (30). This configuration revealed some novel and important functional features of the NALCN channelosome. First, contrasting with previous studies performed in HEK-293T cells, the Na^+ leak current generated by NALCN exhibited some voltage-dependence, as was previously described in a neuronal cell line (*see below*; **FIGURE 6**)(94). This voltage-dependence of NALCN current involves most if not all the basic residues located in the S4 helices of Domains I and II, which are conserved with the voltage-sensor residues of Ca_V and Na_V channels. Second, and contrasting with data from Lu et *al*, 2007, suggesting NALCN conducts Ca^{2+} and is negatively regulated by extracellular Ca^{2+} through the calcium-sensing receptor (2, 44), marked Ca^{2+} block of monovalent cation currents though the pore was revealed by site-directed mutagenesis (30). This block was not specific to Ca^{2+} but generalizable to other divalent cations such as Ba^{2+} and Mg^{2+}. In sum, in the presence of ancillary subunits NALCN is permeable to small monovalent cations and is potently blocked by divalent cations such as Ca^{2+} through a direct pore-blocking mechanism. This latter study determined a permeability sequence for NALCN of $P_{Na} \approx P_{Li} > P_K > P_{Cs}$. This sequence changed to $P_{Na} \approx P_{Li} \approx P_K > P_{Cs}$ when the selectivity filter of the wild-type NALCN EEKE was mutated to DEKA to resemble Na_v channels. Mutation p.E1389A slightly lowered the P_{Na}/P_K and increased the P_{Na}/P_{Cs} ratio, while p.D1390A had no effect on P_{Na}/P_K but markedly increased P_{Na}/P_{Cs} (29). In addition to extracellular Ca^{2+}, NALCN current was also inhibited by Mg^{2+} and Ba^{2+}, but less potently at a concentration of 1 mM (83 ± 10%, 59 ± 11%, and 37 ± 11% inhibition respectively). The substitution of eight charged side chains in the selectivity filter of NALCN with alanine showed that inhibition by divalent cations occurs through an interaction with negatively charged residues within the pore. Indeed, SF residue mutations p.E280A (DI) and p.E554A (DII), as well as an adjacent p.D1390A mutation in DIV, showed drastically reduced Ca^{2+} block; p.D558A, p.E1119A, and p.E1389A showed moderately reduced sensitivity, while p.D561A and p.K1115A showed wild type-like sensitivity. Like the original description of NALCN in the absence of ancillary subunits (2), NALCN channelosome currents are not sensitive to TTX (10 μM). Also similar is the block of NALCN currents by by Gd^{3+} (10 μM) and verapamil (1 mM). However, the src kinase inhibitors PP1 (5 μM) and SU6656 (1 μM) do not have noticeable effects on recorded currents. A lack of inhibition by PP1 of the basal leak current mediated by NALCN was also described in primary dopaminergic neurons, altogether suggesting that the leak activity of NALCN does not depend on basal activity of the src kinase (89). The functional expression of NALCN co-expressed with UNC-79, UNC-80 and NLF-1/FAM155A in HEK-293T cells was subsequently confirmed in numerous other studies (27-29, 31, 45, 46). Notably however, expression of just NALCN with NLF-1/FAM155A is also reported to produce a functional channel, but with more

depolarized activation properties (28). Cell-attached recordings of the complete NALCN channelosome transfected in HEK-293T cells revealed a single-channel conductance of 27.2 ±1.1 pS with a reversal potential of 5.7 ±1.1 mV and a low single-channel open probability (P_0) of roughly 0.04 (31).

The functional expression of NALCN has also permitted a better understanding of its voltage-sensitivity (29). Specifically, wild-type NALCN exhibits responses to voltage pulses from holding potential of 0 mV, but mutation of positive residues in the S4 helix of Domain I (*i.e.,* p.R146Q + p.R152Q, or R3 + R5) abrogates voltage sensitivity. A similar observation was made in Domain II, where mutation of S4 residues R3 (p.R481) together with one of R4 (p.R484) or R5 (p.K487) render NALCN unresponsive to voltage changes. Instead, neutralizing mutations of all gating charges in the Domain III S4 helix (p.R989Q + p.R992Q + p.R995Q), or mutation of one of the two gating charges in the Domain IV S4 helix (*i.e.,* p.R1310), does not have any effect on voltage sensitivity, indicating that only Domains I and II are required for voltage sensitivity (30). With these recent studies, requirement of the complete channelosome (*i.e.,* NALCN, NLF-1/FAM155, UNC-79 and UNC-80 subunits) to achieve functional expression of NALCN channels in HEK-293T is now well supported, revealing the unique electrophysiological properties of NALCN. **FIGURE 6**, presents the inward background current Na^+ current that is recorded in the -80 mV / 0 mV range of the Vm (**FIGURE 6A-C**), and the marked slow deactivation current observed when cells are repolarized (**FIGURE 6A**) or hyperpolarized (**FIGURE 6B**). The current-voltage and conductance-voltage relationships of this NALCN current reveal its voltage-dependence, with a reversal potential (E_{Rev}) near + 10mV (**FIGURE 6C-D**).

Prior to observations of NALCN channelosome currents made in HEK-293T cells and *Xenopus* oocytes, a separate study reported the use of the rodent neuronal cell line NG108-15 to functionally express the channel complex indeed providing first evidence that NALCN currents can be voltage-dependent and blocked by extracellular Ca^{2+} ions (94). NG108-15 cells are a neuroblastoma line that can be differentiated into cholinergic neuron-like cells *via* reduction of serum levels in the culture medium and addition of dibutyryl cAMP (dbcAMP) and dexamethasone for 4 to 5 days (95, 96), allowing the functional expression of ion channels in a neuron-like environment. Bouasse et *al*, 2019, found that differentiated NG108-15 cells express both *Unc-79* and *Unc-80* but not *Nalcn* and *Nlf-1/Fam155a* at the mRNA level as assayed by RT-qPCR (94). Accordingly, transient transfection of NALCN and NLF-1/FAM155A in these cells resulted in a Na^+ background conductance with properties consistent with those later reported in HEK-293T cells and *Xenopus* oocytes, including block of inward currents by replacement of external Na^+ with $NMDG^+$, insensitivity to TTX (10 μM), and sensitivity to Gd^{3+} block (10 μM) (**FIGURE 6E**).

The functional expression of NALCN was also reported in the mouse pancreatic β cell line MIN6, stemming from observations that *Nalcn*, *Unc-79*, and *Unc-80* are endogenously co-expressed in this cell type (56). Through combined knockdown and overexpression experiments, NALCN was shown to conduct an acetylcholine-activated Na^+ current activated by the muscarinic M3 receptor (M3R), lacking a baseline leak current component in the absence of receptor activation. This current was completely abolished by the replacement of extracellular Na^+ by $NMDG^+$, and reduced by ≈50% by replacement of Na^+ with Li^+. Consistent with the studies describe above, the current was also sensitive to Gd^{3+} (10 μM) and resistant to TTX (2 μM). Furthermore, the current had a linear I/V relationship within the -100 mV to -25 mV range, with a reversal potential E_{rev}

of roughly -23 mV. In this study, noise analysis was used to estimate a single-channel conductance of ~27 pS, which notably is similar to the one reported for the Na^+ leak current recorded in HEK-293T cells (27). This acetylcholine-activated current could be recapitulated by co-expressing NALCN and M3R in both HEK-293T cells and *Xenopus* oocytes (56, 89). Functional expression of NALCN was also successful in another endocrine cell line: the rat pituitary somatotroph GH3 cell line that endogenously expresses *Nalcn*, *Unc-79*, *Unc-80* and *Nlf-1/Fam155a* at the mRNA level (76). In this cell type, a combination of knockdown and overexpression approaches showed that NALCN generates a Ca^{2+}- sensitive Na^+ leak conductance with a linear I/V relationship within the -110 mv to -30 mV range, and notably, *Nalcn* knockdown significantly reduced prolactin secretion. Lastly, NALCN was also described as a leptin-activated current in type-1 neurons in the nucleus of the solitary tract expressing the leptin receptor (73).

Overall, various *in vitro* studies using different subunits and cell lines (*i.e.*, HEK-293T, *Xenopus* oocytes, NG108-15, MIN6, and GH3) have revealed a core set of functional features of the NALCN current, but also some notable differences. Altogether, most studies agree that NALCN conducts a cation (mainly Na^+) current that is TTX-resistant and Gd^{3+}-sensitive. Given that some laboratories have recorded NALCN currents in HEK-293T cells by expressing it without its ancillary subunits (2, 43, 77, 88, 89), while others have not (1, 51, 56, 90, 91), questions remain about the requirement of these subunits for NALCN function *in vitro*. Perhaps, some of this discrepancy is attributable to variation in the repertoire of expressed genes affected by culture conditions, passage number, and sub-clone types (87). For example, Swayne et *al*, 2009, were unable to detect endogenous expression of *NALCN* in HEK-293T cells, whereas Hahn et *al*, 2020, reported its expression (56, 89). Indeed, we cannot exclude that HEK-293T cells cultured in some laboratories endogenously express genes required for NALCN functional expression not occurring in HEK-293T cells from other laboratories.

7- Pharmacology

To date, no pharmacological compound has been discovered that selectively and specifically modulate NALCN activity *in vitro* or *in vivo*. Future discovery of such compounds is of interest not only in basic research, but also in human therapy where the ability to modulate NALCN activity appears clinically relevant (*e.g.*, pain, cancer, CLIFAHDD syndrome). NALCN's insensitivity to TTX is attributed to the absence of key residues present in Na_V channels that are associated with TTX binding (28). NALCN is also mildly sensitive to the Na_V channel blocker Lamotrigine (300 μM), as well as the Ca_V channel blockers Nifedipine (100 μM), Diltiazem (1 mM), Verapamil (1 mM), D-600 (1 mM), and mibefradil (100 μM) (2, 27, 97-99). No effects however are observed for several other known Ca_V and Na_V channel blockers, toxins, and other selected compounds at relevant concentrations (27). There is evidence that NALCN current is inhibited by 2-aminoethoxydiphenylborane (2-APB, 100 μM)(27, 68, 100) and flufenamic acid (FFA, 100 μM)(68), but not by the TRPC inhibitor SKF-96365 (100 μM)(68). However, 2-APB is pharmacologically promiscuous in that it also positively modulates K_{ir} and K_{2P} K^+ channels, and negatively modulates store-operated channels and TRP channels (100). Indeed, 10 μM 2-APB has only a marginal effect on substance P (SP)-mediated depolarization of Interstitial cells of Cajal attributed to NALCN (78). Similarly, FFA modulates the activity of a large panel of ion channels (101).

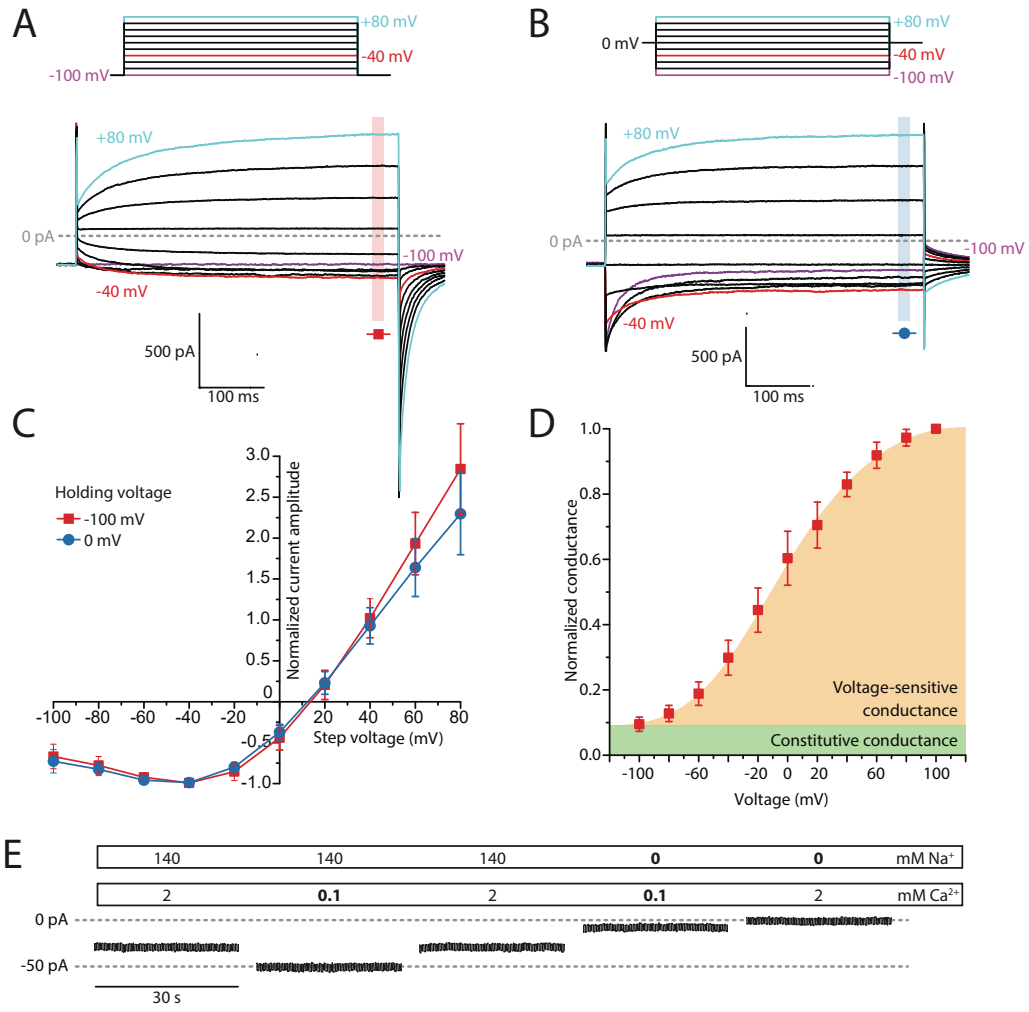

FIGURE 6. Electrophysiological properties of the human NALCN channelosome (*i.e.,* NALCN, UNC-79, UNC-80 and NLF-1/FAM155A) expressed in human embryonic kidney-293T (Panels A-D) and NG108-15 (Panel E) cells. ***(A)*** Representative current traces recorded from the human NALCN channelosome, elicited by depolarizing voltage steps from a holding potential (HP) of -100 mV (voltage clamp protocol illustrated above), using an external solution containing 150 mM Na^+ and 2 mM Ca^{2+}, and an internal solution containing 140 mM Cs^+. ***(B)*** Similar recordings as in (A) but using HP = 0 mV. The voltage-clamp steps and corresponding currents to -100, -40, and +80 mV are colored in *purple*, *red*, and *cyan*, respectively. Evident is the non-inactivating (*i.e.*, constitutive) inward Na^+ leak current at -100 mV that increases upon membrane depolarization to -40 mV, consistent with voltage-dependent activation, with recordings in *(B)* revealing the deactivation component of this current. The legend at the bottom indicates time in milliseconds along the abscissa, and current amplitude in picoamperes along the ordinate. ***(C)*** A plot of average maximal current amplitude normalized for current density at – 40 mV (± standard deviation, n=5) for NALCN currents as a function of depolarizing voltage (*i.e.*, I-V plot), reveals a characteristic U-shaped curve that is consistent with voltage-sensitivity, with (blue circle) corresponding to the steady-state inward current from *(A)* and with (red square) corresponding to the steady-state inward current from *(B)*. Note that the maximum NALCN inward current is obtained at Vm ~ -40 mV. ***(D)*** Conversion of the current amplitude values in panel (*C*) to conductance values using Ohm's law, which permits visualization of NALCN channel activation as a function of depolarization. It reveals a bimodal conductance comprised of a small constitutive component that is active even at hyperpolarized potentials: the inward current at HP-100 mV, and a voltage-sensitive component that increases in amplitude upon membrane depolarization: revealed by the tail current (blue arrow in *(A)*). ***(E)*** Representative traces of the constitutive NALCN current recorded in a NG108-15 cell maintained at V_m=-40 mV and perfused with external recording solutions with varying concentrations of external Na^+ and Ca^{2+}, as indicated above the current traces (*see* (94) for detailed recording conditions).

A recent study reported that N-benzhydryl quinuclidine compounds originally developed as tackykinin receptor-1 antagonists are potent inhibitors of NALCN in a src kinase-independent manner (89). These compounds, referred to as L703606, CP96345 and Maropitant, inhibit NALCN currents in both HEK-293T cells and acutely isolated mouse nigral dopaminergic neurons with IC_{50} values in the 16 to 20 μM range. In contrast, no effect is observed for recombinant TRPC channels, and concentrations of L703606 below 10 μM do not exert effects on $Na_V1.5$, $Ca_V1.2$ and $Ca_V2.1$ currents. Notably, this particular compound (10 μM) was recently used to implicate NALCN in electrical activity of mouse SNc dopaminergic neurons and granule cells of the dentate gyrus (59, 82, 83), and in cell proliferation and migration of lung cancer A549 cells (102). However, this latter observation is confounded by the fact that this cell line also expresses the tachykinin receptor-1 which as noted is sensitive to L703606 (103). Lastly, CP96345 (20 μM & 50 μM) was used to implicate NALCN in the Na^+ background conductance observed in myometrial smooth muscle cells and bovine chromaffin cells respectively (84, 104).

8- Regulation of NALCN by GPCRs

The regulation of NALCN activity through activation of G protein-coupled receptors (GPCRs) has emerged as an important pathway used for hormones and neurotransmitters to modulate cell excitability. Indeed, several studies have revealed that NALCN function is both positively and negatively regulated by GPCRs (**FIGURE 7**).

Positive modulation of NALCN by GPCRs:

Almost simultaneously, Swayne et *al*, 2009, and Lu et *al*, 2009, found that NALCN is positively modulated by the GPCR ligands acetylcholine, substance P, and neurotensin in MIN6 pancreatic β cells and hippocampal and VTA neurons (43, 56). This positive modulation involves the muscarinic M3 receptor (M3R) for acetylcholine and the Tachykinin 1 (NK1) receptor for substance P, while the specific identity of the neurotensin receptor subtype remains to be determined. Interestingly, the positive modulation of NALCN by GPCRs occurred through a G protein-independent but src kinase-dependent pathway (43, 56). Here, application of src inhibitors such as PP1 and SU6656 inhibited the positive modulation, while inclusion of GDP-β-S and GTP-γ-S in the patch pipette, which lock G proteins in an active and inactive state respectively, had no effect. Of note, the involvement of src in the full activation of NALCN by M3R following acetylcholine application was recently challenged in HEK-293T cells transfected with both NALCN and M3R, where the acetylcholine-activated NALCN current was only partially inhibited by PP1 (89). Nonetheless, co-immunoprecipitation experiments from transfected HEK-293T cells revealed that M3R and NALCN belonged to the same protein complex involving the intracellular I-II loop of NALCN and the intracellular I3 loop and carboxyterminal region of the M3R (56). Since the I-II loop of NALCN forms key contacts with the UNC-79-UNC-80 dimer (31, 46), it is unclear whether this interaction is direct, or mediated by the UNC subunits acting as scaffolding proteins. Nonetheless, this interaction seems to be required for the positive modulation of NALCN by acetylcholine, since overexpression of these intracellular fragments fused to enhanced green fluorescent protein (eGFP) in MIN6 cells inhibits acetylcholine-evoked NALCN currents. Consistent with the notion that the UNC proteins might act to scaffold NALCN with other proteins, co-immunoprecipitation experiments revealed that UNC-80 can recruit the src kinase into the NALCN channelosome, presumably to facilitate phosphorylation of both NALCN and UNC-80 (43,

105). However, the src kinase phosphorylation sites on NALCN and UNC-80 remain to be identified. The positive regulation of NALCN by acetylcholine and substance P was also described in interstitial cells of Cajal, substantia nigra pars reticulata neurons, and spino-parabrachial neurons (68, 71, 78). One may hypothesize that positive regulation of NALCN by these and other GPCRs might occur in other neurons and cell types as well. For example, G protein-independent activation of a cationic conductance by glutamate and acetylcholine through GPCRs is observed in CA3 pyramidal neurons and ventricular myocytes respectively (106, 107), where perhaps NALCN is viable molecular counterpart of this cationic conductance.

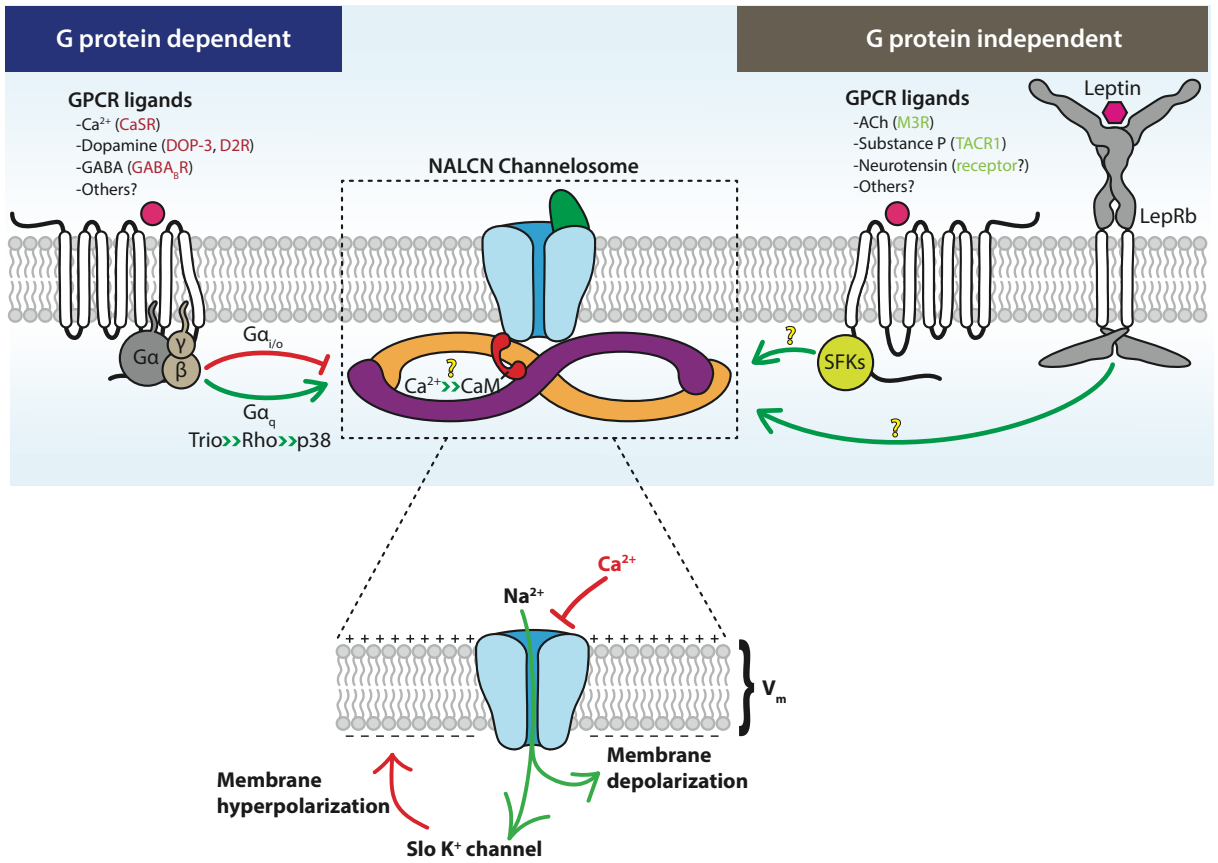

FIGURE 7. Modulation of the NALCN channelosome by various signaling ligands and receptors. ***(Upper panel)*** NALCN was described as negatively and positively regulated by several GPCRs as well as the leptin receptor. Negative regulation was found for extracellular Ca^{2+} (44), dopamine (72, 108), and GABA (72) shown to bind corresponding G protein-coupled receptors (GPCRs; names are in *red* font) to inhibit NALCN channel activity possibly though a $G\alpha_{i/o}$-dependent pathway although $G\alpha_q$ could also be involved (44). Also illustrated is the positive regulation of NALCN by a $G\alpha_q$-dependent pathway elucidated downstream of GPCR activation in *C. elegans*, which exerts its effects on the channel complex though a Trio-, Rho-, p38-dependent pathway (37, 109). NALCN is also positively regulated by acetylcholine (ACh)(56) and the neuropeptides substance P and neurotensin (43), which bind to GPCRs leading to activation of NALCN activity in a G protein-independent, Src family kinase (SFK)-dependent manner. A positive regulation of NALCN activity by the peptide hormone leptin was reported and could involve its receptor, the leptin receptor long isoform (LepRb), through an unknown intracellular signaling pathway (73). The calcium sensor calmodulin (CaM) was found to be part of the NALCN channelosome suggesting NALCN activity could be regulated by intracellular Ca^{2+} (31, 46). ***(Lower panel)*** NALCN activity was also showed to be regulated by extracellular Ca^{2+} through a direct blockade of the pore (30). NALCN was also reported to exhibit a hyperpolarizing effect on V_m through the activation of the Na^+-activated Slo2.1 K^+ channel (104).

Positive G-protein-dependent modulation (**FIGURE 7**) of NALCN homologs NCA-1 and NCA-2 has also been reported in *C. elegans* (37, 109). This modulation is mediated by the Gαq protein via a downstream phospholipase C (PLC)-independent signaling cascade that sequentially involves UNC-73, RHO-1, and SEK-1 in cholinergic neurons. These 3 proteins are the respective homologues of the mammalian RhoGEF Trio protein, the RHO proteins, and the MAPKK protein of the p38 MAP kinase pathway. Indeed, a forward genetic screen identified both NCA-1 and NCA-2 as downstream targets of the Gαq-Rho pathway. Ethylnitrosourea (ENU) mutagenesis to screen for suppressors of the hyperactive locomotion and looping posture of a constitutively activated Gαq mutant led to the identification of 10 recessive mutants: 6 for *unc-80*, 3 for *unc-79* and 1 for *nlf-1/fam155a*. Indeed, the loopy waveform locomotion of Gαq mutant animals was abolished in these 10 recessive mutants. This aberrant behavior was also suppressed by crossing the constitutively activated Gαq mutant with a *nca-1*:*nca-2* double mutant, thus confirming the requirement of the complete NALCN channelosome. Of note, a *nca-1* mutant on its own partially suppressed the locomotor phenotype of the constitutively activated Gαq mutant whereas a *nca-2* mutant did not. This suggests that although *nca-1* and *nca-2* redundantly contribute to normal worm locomotion, channels containing the NCA-1 pore-forming subunit have a larger role in transducing Gαq signals than NCA-2 channels. The loopy waveform behavior of a constitutively activated mutant of Rho that acts downstream of Gαq was also either fully suppressed in *unc-79*, *unc-80*, *nca-1*:*nca-2* mutants, or partially suppressed in *nlf-1* mutants (37). The forward genetic screen mentioned above also identified the kinase SEK-1 as a suppressor of the locomotor phenotype of the constitutively activated Gαq mutant (109). Since SEK-1 is part of the p38 MAP kinase pathway, this result was extended to mutants of other members of this pathway: the adaptor protein TIR-1, the MAPKKK NSY-1, and the MAPKs PMK-1 and PMK-2. However, this was not the case for the transcription factor ATF-7. Mutations in the SEK-1 p38 MAPK pathway also suppressed some aspects of the locomotor defects in *nca-1* gain-of-function mutant animals. One may hypothesize the activation of this pathway would result in NCA-1 channelosome phosphorylation, serving to modulate NALCN activity, cell localization, and/or protein expression. However, the relevance of this regulation on NCA-1 and NCA-2 currents remains to be determined, and whether a similar process occurs in mammals also remains to be explored, but is not without precedent since direct phosphorylation of the $Na_v1.6$ and $Na_v1.8$ by p38 is known to regulate the properties of these particular channels (110, 111).

Negative modulation of NALCN by GPCRs:

In addition to positive modulation of NALCN by some GPCRs, negative regulation by other GPCRs is also described (**FIGURE 7**). The first report of negative regulation involved the Ca^{2+}-sensing receptor CaSR (44). A decrease in external [Ca^{2+}] usually excites neurons and also activates depolarizing, nonselective cation currents in cell bodies and nerve terminals (112-119). Such regulation of neuronal excitability by diminished external [Ca^{2+}] is apparent in primary hippocampal neurons from wild-type mice but not from *Nalcn* knockout mice (44). This response was partially restored by transfecting NALCN cDNA back into neurons of *Nalcn* knockout mice. Furthermore, the current amplitude of NALCN was dependent on external [Ca^{2+}] in both hippocampal neurons and transfected SH-SY5Y cells. Deletion mutants indicated that NALCN modulation by external Ca^{2+} ions required molecular determinants located in the last residues of the carboxy terminus of NALCN. This modulation required the UNC-79 subunit given that it was absent in *UNC79*-

$^{/-}$ hippocampal neurons. Following cell dialysis with a pipette solution containing GTPγS, lowering external [Ca^{2+}] no longer increased the background Na^+ current, suggesting that activation of G proteins by GTP-γ-S suppresses the low Ca^{2+} activation of NALCN. Conversely, cell dialysis with GDP-β-S increased a holding current which was not impacted by external [Ca^{2+}], a process which did not occur in neurons from *Nalcn* knockout mice. In addition, transfection of wild-type hippocampal neurons with an active form of the Gαq protein (*i.e.*, p.Q209L) disrupted the regulation of the Na^+ background conductance by external [Ca^{2+}]. This positive regulation of NALCN by decreased external [Ca^{2+}] can be recapitulated in HEK-293T cells by co-expressing NALCN, UNC-80, a constitutively active form of the src kinase (*i.e.*, SRC-p.Y529F), and CaSR. A more recent study confirmed the negative regulation of NALCN by CaSR and further showed that CaSR-mediated NALCN inhibition involves phosphorylation of NALCN by PKC at residue p.S1652 (92), requiring pre-methylation of residue p.R1653 by the methyltransferase PRMT7. The negative regulation of NALCN by external [Ca^{2+}] was also confirmed in D2 dopamine neurons (72), NG108-15 cells (94), GH3 cells (76), and HEK-293T cells (30), as well as in RPeD1 neurons from *L. stagnalis* (74). However, the CaSR-mediated regulation of NALCN by low external [Ca^{2+}] was recently challenged (30), as noted above. Specifically, external [Ca^{2+}] will directly block the NALCN pore when co-expressed with UNC-79; UNC-80 and NLF-1/FAM155A in HEK-293T cells in the absence of co-expressed CaSR.

In addition to CaSR, negative modulation of NALCN by the D2 dopamine receptor and the $GABA_B$ receptor through a G protein-dependent pathway was described in dopamine neurons (72). Whether this regulation similarly involves phosphorylation of NALCN by PKC is not known. A constitutively active inhibitory G-protein signaling pathway that suppresses intrinsic excitability of granule cells of the dentate gyrus, attributed to the combined activation GIRK channels and suppression of NALCN channels is also reported (83). Lastly, negative regulation of NALCN by the $GABA_B$ receptor may be cell type-dependent since there is no effect on the holding current of spino-parabrachial neurons that express NALCN when the $GABA_B$ receptor agonist R-baclofen (100 mM) is applied in presence of Cs^+ (71).

Negative regulation of NALCN by GPCRs is also apparent in invertebrates. In *C. elegans*, dopamine and the D2-like dopamine receptor DOP-3 negatively modulate NCA-1 and NCA-2 in premotor interneurons (108). This negative modulation involves activation of GOA-1, a Gαo protein. However, inhibition of NCA-1 and NCA-2 is not direct but rather *via* the inhibition of the Gαq-dependent activation of NALCN described above.

9- Other regulations

Metabolic regulation of NALCN:

Several studies have reported links between metabolism and NALCN function. GABAergic neurons from the substantia nigra pars reticulata (SNr) exhibit spontaneous firing at a relatively high frequency (~30 spikes per second)(120-123). In order to explore a role for NALCN in this spontaneous activity, Lutas et *al*, 2016, generated conditional knockout mice where *Nalcn* expression could be disrupted by injection of a viral vector (*i.e.*, AAV9), which drives Cre recombinase expression selectively in neurons *via* the human syntaxin promoter. This study revealed that NALCN deficient neurons have impaired spontaneous electrical activity, and additionally, impaired modulation of firing by glycolytic inhibition

and muscarinic receptor activation. Indeed, in wild-type SNr neurons, inhibition of glycolysis with iodoacetic acid (1 mM) in the presence of the mitochondrial fuel beta-hydroxybutyrate (bHB) slowed the firing rate. In contrast, *Nalcn* knockout neurons showed only a modest change in firing rate after inhibition of glycolysis. Altogether, it is apparent that NALCN activity is regulated by glycolysis and cholinergic signaling in SNr neurons, the latter resembling modulation of NALCN in MIN6 cells by muscarinic acetylcholine receptors (56).

In addition to a modulation of NALCN by glycolysis, leptin, an adipocytokine that regulates neural circuits in the brain that regulate appetite, positively regulates NALCN current in type-1 neurons in the nucleus of the solitary tract *via* the leptin receptor (73). This receptor is a cytokine-related receptor which when activated by leptin binding activates various signaling pathways including Janus tyrosine kinase 2 (JAK2)/STAT3, src homology-2-containing protein tyrosine phosphatase 2 (SHP2)/growth factor receptor-bound protein 2 (Grb2)/mitogen-activated protein kinase (MAPK), forkhead box protein O1 (FoxO1), 5′ adenosine monophosphate-activated protein kinase (AMPK), and others (124). Whether leptin activates NALCN through activation of the leptin receptor and the exact molecular pathway(s) involved remain to be determined.

Potential regulation of NALCN by PIP2

In *C. elegans*, mutations eliminating both NCA-1 and NCA-2 (*i.e.*, *nca-1:nca-2* double mutant) or their ancillary subunits (*unc-79* or *unc-80*) suppress the phenotypes of mutant animals bearing a lesion in the PIP2 phosphatase synaptojanin gene (*unc-26*), as well as phenotypes caused by overexpression of the Type 1 PIP kinase gene *ppk-1* (32). Since the abnormal phenotypes caused by excess PIP2 are exasperated in the presence of NALCN, and genetic disruption of NALCN counters this effect, it seems possible that this signaling lipid directly regulates NALCN activity in a positive manner, and that this contributes to the observed phenotypes. Of note, the Cryo-EM structure of the channel revealed that the pore region in domain II has a binding site for lipids, presumably phospholipids, suggesting a capacity for fine-tuning NALCN activity by lipids (28). However, since PIP2 is known to modulate the activity of numerous other ion channels and transporters (125) the observed phenotypic interaction between NALCN and PIP2 signaling could be at the level of electrophysiology. That is, overexpression of PIP2 might tip the balance of excitation by modulating ion channels and/or transporters that work in parallel with NALCN, such that loss of NALCN activity restores this imbalance.

Potential regulation of NALCN by cytoplasmic Ca^{2+}

In addition to its regulation by extracellular Ca^{2+}, two recent studies highlighted the possibility that NALCN is also regulated by intracellular Ca^{2+} (31, 46). Indeed, the recent elucidation of the Cryo-EM structure of the NALCN channelosome revealed that the Ca^{2+} sensor protein calmodulin (CaM) binds to the NALCN carboxy-terminus. This raises the possibility intracellular Ca^{2+} and CaM can modulate NALCN, as described for several other ion channels including Ca_V and Na_V channels (126). However, the physiological relevance of this elucidated interaction remains to be determined.

III. NALCN & PHYSIOLOGY

The expression of NALCN in a wide range of tissues and organs and in a variety of species suggests the channel contributes to many physiological functions, both in mammals and non-mammals. The early forward genetic screen studies that identified the NALCN channelosome in *C. elegans*, as well as *D. melanogaster* (**TABLE 3**)(19), also provided first insights into the physiological roles of NALCN and its subunits long before NALCN was identified as a channel that generates a Na^+ leak current that contributes to the regulation of cellular excitability. During the last decade, the continued development of animal models to study NALCN physiology, especially mice, was instrumental to uncover physiological roles of NALCN (**TABLE 3**). Indeed, the combined studies of NALCN function in mammals and invertebrates point to a conserved function for the channel in regulating the excitability of various cell types, especially neurons. For example, in mammals, changes in NALCN expression result in substantial changes in neuronal spiking, as illustrated in **FIGURE 8** for regions in the central nervous system, as well as non-neuronal excitable cells in peripheral organs. In this section, we summarized the current knowledge of how the NALCN channelosome contributes to the physiology of living organisms, from invertebrates to mammals (**FIGURE 9**).

1- Locomotor behavior

Several studies from *C. elegans* showed that locomotor alteration is induced by NALCN channelosome dysfunction in a rhythmic network of neurons known as a central pattern generator (CPG), which includes motor neurons and premotor interneurons located in the ventral nerve cord (127, 128). Indeed, null mutations of both *NALCN* orthologs *nca-1* and *nca-2* (*i.e.*, *nca-1:nca-2*), as well as ancillary subunits *unc-79*, *unc-80* and *nlf-1*, cause a "fainter" phenotype (*i.e.*, frequent halting in locomotion)(32-34, 129-131). Mutant animals fail to sustain sinusoidal locomotion and succumb to long periods of halting. A similar phenotype was observed in *D. melanogaster*, referred to as "hesitant walking", caused by null mutations of *na/Dmα1U* (132, 133). Conversely, in *C. elegans* semi-dominant gain-of-function mutations of *nca-1* impose a "coiler" phenotype, characterized by uncoordinated and exaggerated body bends during both spontaneous and stimulated locomotion (34). This phenotype is also apparent in *C. elegans* strains in which CLIFAHDD gain-of-function mutations are emulated in NCA-1 (134)(*see the NALCN & human diseases* section). As noted previously, NCA-1/2 as well at UNC-80 are axonally localized and expressed in both excitatory cholinergic and inhibitory GABAergic motor neurons, as well as premotor interneurons (32, 34). Functional studies revealed that loss of NCA-1 and NCA-2 activity leads to a more negative RMP and reduced synaptic transmission at GABAergic, cholinergic, and serotonergic neuromuscular junctions (34, 35, 135). Conversely, animals carrying gain-of-function mutations of *nca-1* have aberrant synaptic activity (34). *In vivo* Ca^{2+} imaging experiments further indicated that while Ca^{2+} influx in the cell bodies of egg- laying motoneurons is unaffected by altered NCA-1/2 activity, synaptic Ca^{2+} transients are significantly reduced in *nca-1:nca-2* loss-of-function mutants and increased in *nca-1* gain-of-function mutants (34). In addition, rescue experiments suggest that reduced premotor interneuron network activity, instead of motoneuron dysfunction, is the primary cause of the frequent halting exhibited by fainters (35, 75). Taken together, these results suggest that NCA-1 and NCA-2 are required for the persistent motor circuit activity that sustains locomotion, mainly through premotor interneurons. Whether NALCN function in locomotory CPGs is conserved in vertebrate

species remains to be investigated, with a potential link in the locomotory deficits found in patients with the NALCN channelopathies IHPRF1 and CLIFAHDD (*see the NALCN & human diseases* section). A role for NALCN in the *C. elegans* reversal behavior has also been observed in the avoidance response to methyl salicylate (MeSa) (131). Here, a forward genetic screen to identify mutants with defective response to MeSa led to the identification of defective alleles for *unc-79* and *unc-80*. This result was extended to *nca-1:nca-2* and *nlf-1* mutants. Of note, all these mutants exhibit wild type-like responses to repelling odorants 1-octanol and 2-nonanone, and attractive odorants diacetyl and benzaldehyde, suggesting these mutants have normal odorant responses. Neuron-specific transgene rescue experiments of UNC-80 in *unc-80* mutants, combined with neuron-specific knockdown of *unc-80* in wild-type animals, revealed that NALCN's role in regulating reversal behavior induced by MeSa is specific to the command interneurons AVA and AVE, as well as the guidepost neuron AVG (131).

In mammals, a mouse strain carrying a heterozygous loss-of-function mutation of *Unc-79* exhibits moderate hyperactivity in the form of increased locomotor behavior (47). This mouse strain was identified in a forward genetic screen using ENU to mutate and identify loci that influence locomotor behavior in a quantitative manner (136). This led to the identification of a c.G5469T mutation in the coding sequence of UNC-79 (reference sequence NM_001081017.2) which results in a p.E1292X conversion (47). This allele is referred to as *Lightweight*. No UNC-79 protein is detectable via Western blotting in homozygous animals, and Northern blot analysis reveals a decrease in mRNA expression suggesting the occurrence of nonsense-mediated decay. Like homozygous knockout animals of *Nalcn*, *Unc-79* and *Unc-80*, homozygous *Lightweight* mice die shortly after birth (2, 49, 136, 137). Thus, the hyperactivity phenotype noted above has not been assessed in adult, homozygous null mutants of NALCN or its subunits. However, the recent development of mice strains bearing conditional knockout alleles for *Nalcn*, as well as adeno-associated virus-mediated knockdown approaches, will undoubtedly circumvent the observed premature death for null alleles (38, 61, 62, 70, 72, 73, 77, 80, 81).

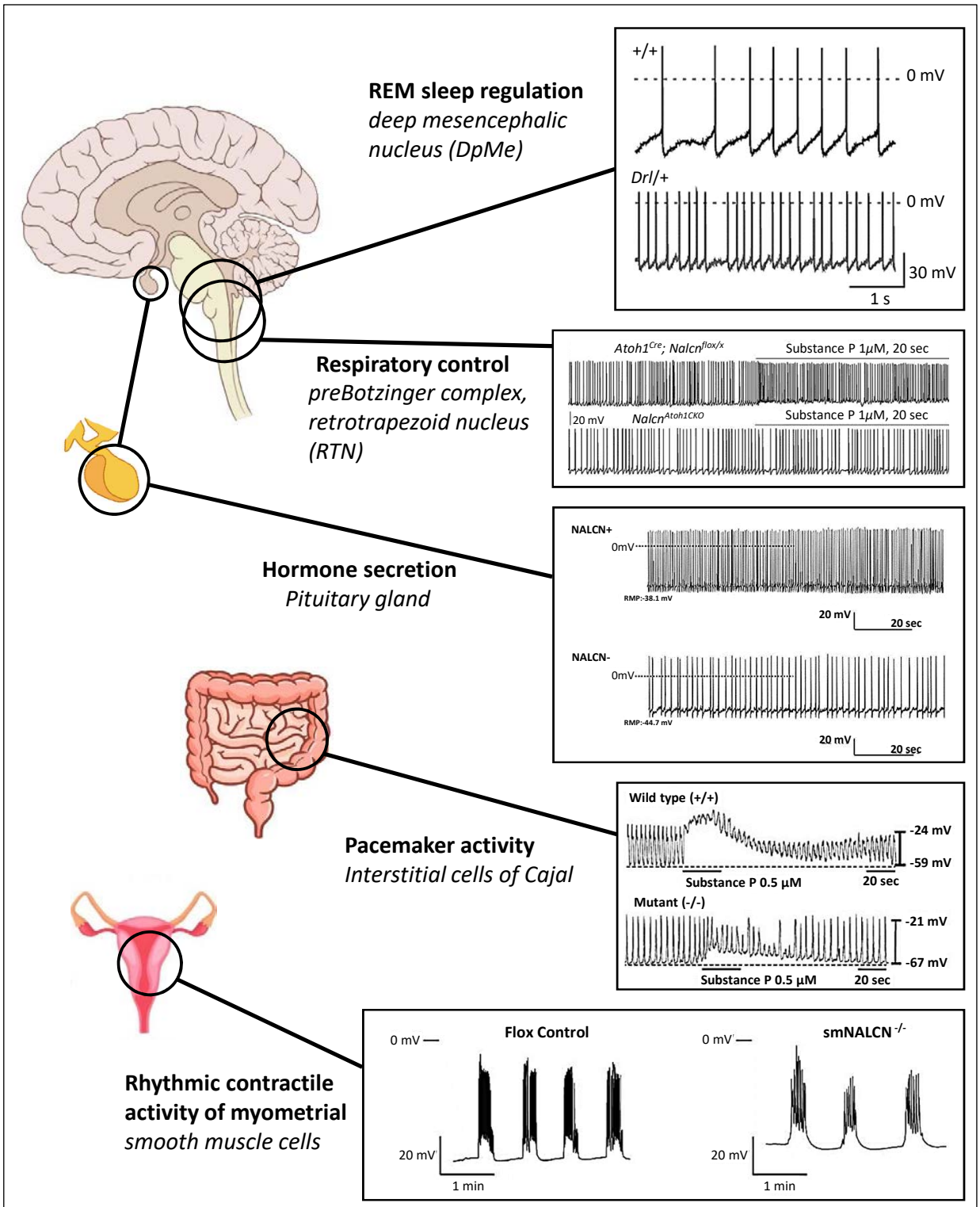

FIGURE 8. Examples of NALCN contribution in tissue function: link with the modulation of RMP and pacemaker activities. (*Upper panel*) Change in cell excitability in deep mesencephalic nucleus (DpMe) in the *dreamless* mouse model carrying a gain-of-function mutation in *Nalcn*. Note the DpMe neuron depolarization and the ensuing increased spiking discharges (from (69), Figure 5 panel f). (***Mid-upper panel*)** NALCN expression in the brainstem neurons of the preBotzinger complex and retrotrapezoid nucleus (RTN) regulates rhythmic activity, RMP and response to substance P in RTN neurons (from (80), Figure 2 panel E). (***Middle panel*)** NALCN modulates the RMP and AP firing frequency in the GH3 cell line, which models pituitary endocrine cells (from (76), Figure 2 panel A). (***Mid-lower panel*)** NALCN in the interstitial cells of Cajal (ICCs) is involved in the electrophysiological response to substance P, by modulating the pacemaking activity. This effect is lost in *Nalcn* knockout (from (78), Figure 7 panel B).

1355 **TABLE 3: The NALCN channelosome in Physiology**

Physiological function	Subunit	Species	Reference
Locomotor behavior	*unc-79*	*C. elegans*	Sedensky & Meneely, 1987 (129) Jospin et *al*, 2007 (32) Humphrey et *al*, 2007 (33) Yeh et *al*, 2008 (34) Pierce-Shimomura et *al*, 2008 (130) Zhou et *al*, 2020 (131)
	unc-80	*C. elegans*	Sedensky & Meneely, 1987 (129) Jospin et *al*, 2007 (32) Yeh et *al*, 2008 (34) Pierce-Shimomura et *al*, 2008 (130) Zhou et *al*, 2020 (131)
	nca-1/nca-2 (NALCN orthologues)	*C. elegans*	Jospin et *al*, 2007 (32) Humphrey et *al*, 2007 (33) Yeh et *al*, 2008 (34) Pierce-Shimomura et *al*, 2008 (130) Bouhours et *al*, 2011 (135) Xie et *al*, 2013 (35) Gao et *al*, 2015 (75) Zhou et *al*, 2020 (131)
	nlf-1 (FAM155A/B orthologue)	*C. elegans*	Xie et *al*, 2013 (35) Gao et *al*, 2015 (75) Zhou et *al*, 2020 (131)
	na (NALCN orthologue)	*D. melanogaster*	Krishnan & Nash, 1990 (132) Mir et *al*, 1997 (139) Guan et *al*, 2000 (133) Humphrey et *al*, 2007 (33)
	unc-79	*D. melanogaster*	Humphrey et *al*, 2007 (33)
	Unc-79	*M. musculus*	Speca et *al*, 2010 (47)
Respiratory rhythm	*Nalcn*	*M. musculus*	Lu et *al*, 2007 (2) Shi et *al*, 2016 (70) Yeh et *al*, 2017 (80) Yang et *al*, 2020 (81) Do et *al*, 2020 (73)
	Unc-80	*M. musculus*	Wie et *al*, 2020 (49)
	U-type (NALCN orthologue)	*L. stagnalis*	Lu & Feng, 2011 (74) Lu et *al*, 2016 (140)
Circadian Rhythm/Photic control of locomotion	*na (NALCN orthologue)*	*D. melanogaster*	Nash et *al*, 2002 (64) Lear et *al*, 2005 (65) Lear et *al*, 2013 (36) Ghezzi et *al*, 2014 (141) Flourakis et *al*, 2015 (38)

	unc-79	*D. melanogaster*	Lear et *al*, 2013 (36) Murakami et *al*, 2021 (142)
	unc-80	*D. melanogaster*	Lear et *al*, 2013 (36)
	nlf-1 (FAM155A/B orthologue)	*D. melanogaster*	Ghezzi et *al*, 2014 (141) Flourakis et *al*, 2015 (38)
	*Nalcn?**	*M. musculus*	Flourakis et *al*, 2015 (38)
Sleep/Rest activity behavior	*Nalcn*	*M. musculus*	Funato et *al*, 2016 (69)
	na (NALCN orthologue)	*D. melanogaster*	Joiner et *al*, 2013 (143)
	unc-79	*D. melanogaster*	Murakami et *al*, 2021 (142)
	nca-1 (NALCN orthologues)	*C. elegans*	Huang et *al*, 2018 (144)
	unc-79	*C. elegans*	Huang et *al*, 2018 (144)
Myometrial activity during labor	*Nalcn*	*M. musculus*	Reinl et *al*, 2015 (79) Reinl et *al*, 2018 (138) Amazu et *al*, 2020 (60) Ferreira et al, 2021 (104)
	na (NALCN orthologue)	*D. melanogaster*	Krishnan & Nash, 1990 (132)
Gastrointestinal motility	*Nalcn*	*M. musculus*	Kim et *al*, 2012 (78)
Morphology	*na (NALCN orthologue)*	*D. melanogaster*	Krishnan & Nash, 1990 (132) Mir et al, 1997 (139) Nash et *al*, 2002 (64) Humphrey et *al*, 2007 (33)
	unc-79	*D. melanogaster*	Humphrey et *al*, 2007 (33)
Pain			
Neuropathic pain	*Nalcn*	*M. musculus & R. norvergicus*	Zhang et *al*, 2021 (61)
Inflammatory pain	*Nalcn*	*R. norvergicus*	Li et *al*, 2021 (62)
Chemical nociception	*Nalcn*	*C. h. pretoriae*	Eigenbrod et *al*, 2019 (88)
Thermonociception	*nca-1/nca-2 (NALCN orthologues)*	*C. elegans*	Saro et *al*, 2020 (145)
Osmoregulation	*Nalcn*	*M. musculus*	Sinke et *al*, 2011 (146)
Sensitivity to ethanol and volatile anesthetics			
Volatile anesthetics	*Unc-79*	*M. musculus*	Speca et *al*, 2010 (47)
	Nalcn	*M. musculus*	Ou et *al*, 2020 (77) Yang et *al*, 2020 (81)
	unc-79	*C. elegans*	Morgan & Cascorbi, 1985 (147) Sedensky & Meneely, 1987 (129) Morgan et *al*, 1988 (148) Morgan et *al*, 1990 (149)

			Morgan & Sedensky, 1995 (150) Humphrey et *al*, 2007 (33)
	nca-1/nca-2 (NALCN orthologues)	*C. elegans*	Humphrey et *al*, 2007 (33)
	unc-80	*C. elegans*	Sedensky & Meneely, 1987 (129) Morgan et *al*, 1988 (148) Morgan et *al*, 1990 (149)
	na (NALCN orthologue)	*D. melanogaster*	Krishnan & Nash, 1990 (132) Nash et *al*, 1991 (151) Campbell & Nash, 1994 (152) Leibovitch et *al*, 1995 (153) Mir et *al*, 1997 (139) Nishikawa & Kidoroko, 1999 (154) Guan et al, 2000 (133) van Swinderen, 2006 (155) Humphrey et *al*, 2007 (33)
	unc-79	*D. melanogaster*	Humphrey et *al*, 2007 (33)
	Unc-79	*M. musculus*	Speca et *al*, 2010 (47)
	Nalcn	*M. musculus*	Wu et *al*, 2021 (156)
Ethanol	*unc-79*	*C. elegans*	Morgan & Sedensky, 1995 (150) Speca et *al*, 2010 (47)
	unc-80	*C. elegans*	Speca et *al*, 2010 (47)
	nca-1/nca-2 (NALCN orthologues)	*C. elegans*	Speca et *al*, 2010 (47) Davies et *al*, 2012 (157)
Metabolism	*Unc-79*	*M. musculus*	Speca et *al*, 2010 (47)
Social clustering	*na (NALCN orthologue)*	*D. melanogaster*	Burg et *al*, 2013 (158) Ghezzi et *al*, 2014 (141)
	nlf-1 (FAM155A/B orthologue)	*D. melanogaster*	Ghezzi et *al*, 2014 (141)
Others			
Swallowing	*Nalcn, Unc-80*	*R. Norvergicus*	Li et *al*, 2021 (159)
Cell proliferation	*Fam155A*	*H. sapiens*	Lu et *al*, 2019 (160)
Adaptation to environment	*Nalcn*	*G. gallus*	Gu et *al*, 2020 (161)
Breeding intensification	*Nalcn*	*S. s. domesticus*	Kolosov et *al*, 2022 (162)
Male reproduction	*Nacn*	*Anas platyrhynchos domesticus* × *Cairina*	Yang et *al*, 2022 (163)

		moschata domestica	

*** The Nalcn current was found to exhibit a circadian-dependent expression in neurons from the suprachiasmatic nucleus in mouse but a role in the circadian-dependent locomotor activity remains to be demonstrated.**

2- Respiratory rhythm

Mice bearing genetic lesions of the *Nalcn* gene die within 24 hours after birth from respiratory defects. These mutant animals exhibit a severely disrupted respiratory rhythm characterized by a regular rhythm interrupted by periods of apnea (2). Breathing by NALCN null mice is characterized by apnea for ~5 seconds followed by a burst of breathing for ~5 seconds at a rate of ~5 bouts of apnea per minute. The cause of this, at least in part, is attributable to a complete loss of electrical activity from the fourth cervical nerve root (C4) that innervates the diaphragm and discharges rhythmic electrical signals that regulate breathing. However, since *Nalcn* is widely expressed in the nervous system, a global reduction of excitability in mutant animals may lead to the disruption in respiration. Indeed, both the rhythm and neuromodulatory responses of breathing are controlled by brainstem neurons in the preBötzinger complex (preBötC) and the retrotrapezoid nucleus (RTN)(164-166). Neurons in the preBötC show characteristics of a CPG that generates inspiratory movements through a glutamatergic subpopulation of neurons which are functionally coupled with glutamatergic chemosensory neurons such as the RTN neurons. Here, targeted knockdown of *Nalcn* in the CO_2/H^+-sensitive neurons of the mouse RTN (70) demonstrated that *Nalcn* contributes to a background Na^+ current in these neurons, and is required for their activation by the neuropeptide substance P but not serotonin. Further, RTN-specific depletion of *Nalcn in vivo* constrained CO_2-induced activation of RTN neurons as inferred from activity-dependent c-fos expression after exposure to 8% CO_2, and also blunted the stimulation of the respiratory responses to CO_2 (70, 81). In another study, specific depletion of *Nalcn* in mouse glutamatergic, GABAergic, cholinergic, serotonergic, and glycinergic neurons was performed using a Cre/lox approach (80). In glutamatergic and GABAergic neuron knockout mice, this resulted in full lethality (*i.e.*, 100%) and partial lethality (*i.e.*, 13.2%) within 24h after birth, respectively. Furthermore, while specific depletion of *Nalcn* in glutamatergic RTN neurons did not result in lethality, it did so (partially) in glutamatergic neurons of the preBötC with 32.6% neonatal lethality attributed to respiratory defects. 28.6% of the knockout newborns exhibited a significantly greater frequency of apnea than other newborns. Of note, it was hypothesized that the surviving knockout newborns might receive compensatory respiratory activity from other glutamatergic neurons (80). Patch-clamp recordings on glutamatergic RTN and preBötC neurons revealed a hyperpolarized RMP, a lower firing frequency, and a loss of excitatory modulation by substance P. Taken together, these data demonstrate an important involvement of NALCN in respiratory rhythm generation and its modulation by substance P. Of note, contrasting with results from Shi et *al*, 2016 (70) and Yang et *al*, 2020 (81) mentioned above, the stimulation of the *in vivo* respiratory responses to an increase in CO_2 is not impacted in mice bearing a *Nalcn* knockout in RTN neurons (80), a discrepancy that remains to be explained. In RTN neurons, NALCN is also required for the ventilatory response to CO_2 during anesthesia (81). Interestingly, like *Nalcn*, both *Unc-80* and *Unc-79* knock-out mice die shortly after birth (49, 137). Whereas *Unc-80* knockout animals also suffer from respiratory defects, the origin of mortality observed for *Unc-79* knockout mice is currently unknown.

Strengthening the role of NALCN in breathing function is the finding that NALCN channels can be activated by leptin. Leptin is a pleiotropic hormone produced by adipocytes. It is a master regulator of metabolism and, interestingly, of many other biological functions including breathing (167). A recent study identified NALCN as a major player in the leptin-mediated link between breathing and metabolism (73). In mice, leptin activates NALCN to depolarize a subgroup of LepRb (*i.e.*, long form of the leptin receptor)-expressing neurons of the tractus solitary tract (NTS), distinguished by their expression of the glutamate transporter vGluT2 and the neuropeptide galanin. Selective knockout of *Nalcn* in mouse LepRb neurons causes an increase in spontaneous apneas and breathing irregularity as well as a decrease in CO_2 chemosensitivity (73). In addition, while wild-type mice fed with a high-fat diet for 3 weeks maintain constant minute ventilation, LepRb-selective *Nalcn* knockout mice show a marked depression in ventilation. LepRb NTS neurons are classified into two electrophysiologically distinct populations according to their somatic size referred to as type-1 (smaller neurons) and type-2 (larger neurons). Single-cell transcriptomics revealed a different molecular profile between these two populations of neurons. Leptin is able to depolarize type-1 NTS neurons (which uniquely express vGluT2 and galanin) but not type-2. Leptin-mediated depolarization is lost in LepRb-selective *Nalcn* knockout mice. Interestingly, type-2 neurons from these knockout mice have hyperpolarized resting potentials and increased membrane resistance consistent with depleted leak channels at the cell membrane. These results demonstrated that NALCN is tightly regulated by leptin in type-1 neurons while it conducts a Na^+ background conductance that facilitates spontaneous firing in type-2 neurons. The molecular underpinnings for this observed difference in NALCN function remain to be elucidated.

The importance of NALCN in regulating the respiratory rhythm appears to be conserved across species, as demonstrated by two studies using the pond snail *L. stagnalis* as an animal model (74, 140). The aerial respiration of *L. stagnalis* is controlled by a simple well-described respiratory CPG network consisting of three large identified neurons, including one intrinsic pacemaker neuron, the right pedal dorsal 1 (RPeD1), that initiates rCPG rhythmic activity, as well as the VD4 and IP3I neurons (168). The pacemaker neuron RPeD1 exhibits rhythmic activity characterized by intermittent action potential bursts. This rhythmic activity is fully inhibited upon RNA knockdown of NALCN (referred to as the U-type channel) (74). A computational model of RPeD1 activity based on recording measurements of the various conductances expressed in these neurons illustrated the high sensitivity of this neuron to changes in the Na^+ leak current (140). Lastly, *in vivo*, RNA knockdown of NALCN resulted in a reduced opening of the pneumostome (*i.e.*, breathing pore) reflecting reduced breathing activity (74).

3- Photic control of locomotion

In addition to rhythmic locomotor activity and respiration, NALCN is also involved in the photic control of locomotion in *D. melanogaster* (36, 38, 64, 65). Hypomorphic mutants of NALCN in *D. melanogaster* referred to as $Dm\alpha1U^{na}$, $Dm\alpha1U^{har38}$ and $Dm\alpha1U^{har85}$, exhibit most of their activity at night in contrast to wild-type animals that exhibit most of their activity during the daytime (64). A strong decrease in the rhythmic amplitude of behavior is also observed in $Dm\alpha1U^{na}$ mutant animals compared to wild-type animals when flies were put in a constant darkness (*i.e.*, DD). Western-blotting experiments of brain extracts obtained at different times within a 24-hour period did not reveal alterations in

NA/Dmα1U protein levels suggesting that expression of the channel protein is not under circadian control, a finding which was confirmed at the mRNA level (169). Since there was no difference in activity between wild-type and mutant animals maintained in DD, it seems as though aberrant motor responses to photic input, despite normal clock function, is a feature of NA/Dmα1U mutants (64). In agreement, another study reported that neural *na/Dmα1U* RNAi knockdown induces a robust mutant phenotype characterized by a significant reduction of morning activity as well as reduced anticipation of the "lights-off" transition compared to control animals (141). Notably, an inverted day/night behavioral pattern does not occur in knocked down flies, but significant reductions in activity are observed during both "lights-on" and "lights-off" transitions. These observations are phenocopied by *nlf-1* knockdown (141). There are several populations of pacemaker and clock-expressing neurons identified in *D. melanogaster*: the lateral neurons (LN_d, l-LN_v, s-LN_v), the Dorsal Neurons (DN_1, DN_2, DN_3), and the three cells in the posterior lateral brain (lateral posterior neurons; LPN)(170). Notably, *na*/*Dmα1U* is expressed in a subset of these neurons (65). During a 12 hr light:12 hr dark conditions (*i.e.*, LD), $Dm\alpha1U^{na}$ mutants exhibit an altered evening anticipation, timing of morning anticipation, and response to lights on. Further genetic rescue experiments showed that *na*/*Dmα1U* expression in all lateral neuron groups and a subset of dorsal neurons is sufficient to promote evening anticipation but fails to fully rescue the morning anticipation phenotype, indicating that additional dorsal neuron expression may be required for wild-type morning behavior. It was concluded that *na*/*Dmα1U* expression within lateral neurons and a broad group of dorsal neurons is required for complete wild-type behavior in LD conditions. As noted above, *na*/*Dmα1U* likely acts outside of the core molecular clock since the circadian expression of the PERIOD protein is not different in a $Dm\alpha1U^{na}$ background compared to wild-type animals.

Loss-of-function mutants for the *unc-79* and *unc-80* subunits also displayed severe defects in circadian locomotor rhythmicity in both LD and DD conditions which are indistinguishable from $Dm\alpha1U^{na}$ mutant phenotypes (36). Like *na/Dmα1U*, these defects can be rescued by expression of the subunits in pacemaker neurons. Also similar, neither *unc-79* nor *unc-80* display rhythmic expression at least in DN1p pacemaker neurons (38). Nonetheless, patch-clamp recordings revealed that both DN1p and large-LNv neurons from $Dm\alpha1U^{na}$ mutants have hyperpolarized membrane potentials and are electrophysiologically silent compared to wild-type DN1p neurons (38). Furthermore, these neurons no longer exhibit circadian regulation of membrane excitability and RMP, associated with *na/Dmα1U* function. A possible mechanism for altered NALCN activity, without changes in channel protein expression could involve regulation by the NFL-1 subunit. Specifically, expression of *nlf-1/fam155* was found to be under circadian control, and the CLOCK protein, a core component of the circadian transcriptional feedback loop, binds the genetic locus of *nlf-1* in a rhythmic manner (171). *In vivo* knockdown of *nlf-1/fam155* phenocopies cell excitability defects of DN1p neurons observed in $Dm\alpha1U^{na}$ mutants. Indeed, Flourakis et *al*, 2015, found dramatic reductions in rhythmic strength in DD and reduced anticipation of "lights-on" and "lights-off" transitions under LD conditions (38). Conversely, *nlf-1/fam155* overexpression depolarized the membrane, elevated the firing rate and cellular excitability, and resulted in increased NA/Dmα1U current density. It was concluded that *nlf-1/fam155* is rhythmic and mediates the rhythmic activity of *na/Dmα1U*, with the following model proposed: during the morning/day, the Na^+ leak current mediated by NA/Dmα1U is elevated while resting K^+ currents are reduced, depolarizing cells and promoting sustained firing rates. During the

evening/night, the Na^+ leak current is low and resting K^+ currents are elevated, thus hyperpolarizing the cell to decrease firing rate. The clock-controlled transcript *nlf-1/Fam155a* drives the rhythm of the NA/Dmα1U current, linking the core clock to ion channel activity. Notably, one study has shown contrasting results to the ones described above. Ghezzi *et al*, 2014, who used RNA extracted from whole *Drosophila* heads, failed to observe changes in the mRNA expression of *nlf-1* according to the circadian rhythm (141). Perhaps, this inconsistency is attributable to differences in cell/tissue sampling, where circadian expression of *nlf-1* is restricted to a specific subset of neurons. Nonetheless, this same study reported only weak effects on circadian (evening) behavior after knockdown of *nlf-1/fam155* knockdown on evening behavior (141).

Not yet determined is the mechanism by which the differentially expressed NLF-1/FAM155 subunit regulates NA/Dmα1U channel activity. Indeed, in *D. melanogaster*, the temperature-inducible knockdown of *na/Dmα1U*, *nlf-1/fam155* and *unc-79* showed that proteins produced during the development are stable and functional at least 5-7 days at the adult stage (172). The half-life of NA/Dmα1U is estimated at ~29 days. This pool of proteins is sufficient for rhythmic behavior in adults. This suggests that the complex is highly stable and it is tempting to speculate that the NALCN channelosome cycles between endocytic compartments and the plasma membrane through a NLF-1/FAM155-dependent mechanism during circadian cycles. However, it is difficult to reconcile the observed rhythmic expression of *Nlf-1/Fam155a* (38), with the noted observation that the NALCN channelosome, including the NLF-1/FAM155A subunit, is expressed early during development and endures well into adulthood to regulate circadian function.

A role for Nalcn in circadian rhythm-dependent locomotor activity in mammals has not been thoroughly established. However, as discussed below, NALCN contributes to sleep behavior in mice with implications for circadian behavior. Furthermore, electrophysiological recordings from organotypic slices from wild-type and CaMKIIα-Cre;$NALCN^{fx/fx}$ mice demonstrated that the NALCN current is under control of the circadian clock in suprachiasmatic pacemaker neurons (SCN) in the hypothalamus (38). However, this finding was recently challenged. Indeed, Yang et *al*, recently described that Na^+ leak current amplitudes are similar in daytime and nighttime SCN neurons and proposed a mechanism by which Nalcn modulates daily rhythms in the rates of spontaneous action potential firing of SCN neurons as a consequence of rhythmic changes in subthreshold K^+ currents (173). In this context, whether oscillations in NALCN activity regulated by the NLF-1/FAM155 subunit occurred in mammals as documented in *D. melanogaster*, is not clear. Whether Nalcn also contributes to circadian locomotory behavior, remains to be determined.

4- Sleep/Rest-activity behavior

In mammals, Nalcn mRNA is highly expressed in several brainstem nuclei involved in REM sleep regulation, such as the ventrolateral periaqueductal grey, deep mesencephalic nucleus and sublateral dorsal nucleus, and its function has been implicated in sleep (69). Mammalian sleep is a swiftly reversible state of decreased metabolism, responsiveness and, motor activity, which is broadly categorized into two states: a non-rapid-eye-movement sleep (NREM sleep also referred to as deep sleep) and rapid-eye-movement sleep (REM sleep also known as paradoxical sleep or dream sleep)(174, 175). Both states are defined by characteristic activity of electroencephalogram (EEG) and electromyogram

(EMG). A large forward-genetic screen in mice (*i.e.,* >8000 animals) aiming to identify genes involved in sleep was carried out using ENU to introduce random point mutations. This approach led to the identification of two groups of mice with variations in sleep patterns (69). One of these, dubbed *Dreamless*, showed a reduction in the total time spent in REM sleep (~44%), and in the duration of REM bouts. Subsequent genome sequencing revealed that the mutation in *Dreamless* mice affected *Nalcn* by inducing a missense mutation of p.N315K, within the 6th transmembrane segment of Domain I of NALCN. Functional expression of p.N315K NALCN in HEK-293T cells showed a gain-of-function effect, while deep mesencephalic nucleus (DpMe) neurons, which are REM-inhibiting neurons, exhibited a depolarized RMP and an increased action potential firing frequency (**FIGURE 8**)(69). *Dreamless* mice have normal circadian period lengths but exhibit a greatly reduced amplitude of behavioral circadian rhythms under DD. A marked reduction in the REM sleep time of *Dreamless* mice is also apparent under DD. Spectral analysis of EEG data showed a decrease in the theta-range power during both NREM sleep and REM sleep and an increase in low-frequency power during the wake state and REM sleep in *Dreamless* mice, suggesting that NALCN may regulate various oscillations in the brain.

A role for NALCN in regulating rest-activity behavior is also documented in invertebrates (**FIGURE 9**). In *D. melanogaster*, both *Dmα1U*^{na} and *unc-79* mutants exhibit highly fragmented bouts of waking and rest-activity behavior (143). A more recent study in this species identified a wake-promoting role for *unc-79* (142). Here, a genetic screen to identify genetic regulators of both rest-activity behavior and metabolic function delineated several candidate genes including *unc-79.* Flies with ubiquitous knockdown or knockout of *unc-79* exhibit significantly more rest-activity than control flies and resistance to rest suppression induced by starvation, suggesting that *unc-79* is required for metabolic regulation of rest behavior. These phenotypes do not likely depend on NALCN function in circadian activity as *unc-79* knockdown in circadian neurons does not affect sleep and starvation resistance. By contrast, a specific knockdown in the mushroom body, a brain region associated with sleep regulation as well as olfactory learning and memory, largely phenocopies ubiquitous knockdown or knockout of *unc-79*. Interestingly, knockdown of *na*/*Dmα1U* or *unc-80* throughout the mushroom body does not increase rest-activity behavior duration or disrupt starvation-induced rest suppression, and has little effect on starvation resistance. Together, these findings raise the possibility that *unc-79* functions independently of its canonical complex with *unc-80* and *na*/*Dmα1U* to regulate rest-activity behavior and starvation resistances.

Another study reported a role for NCA-1 in regulating rest-activity behavior in *C. elegans* (144). Rest bouts during L4-to-Adult (L4/A) lethargus are almost fully abolished in animals carrying a gain-of-function *nca-1* mutation. However, animals carrying loss-of-function mutations for both *nca-1* and *nca-2* spend normal amounts of time in rest bouts during L4/A lethargus compared to wild-type animals, and rest/motion bout timing and duration are also normal. *Unc-79* loss-of-function animals exhibit a small increase in total rest time while *unc-80* loss-of-function animals do not. However, loss-of-function alleles of *nca-1/nca-2*, *unc-79* and *unc-80* cause increased latency to respond to an arousing blue light stimulus during bouts of rest. Instead, no changes are evident in L4/A lethargus rest quantity, or arousal thresholds for rest or motion bouts in *nlf-1* loss-of-functions animals.

5- Myometrial activity during labor

Beyond roles in neurons, the NALCN channelosome is also described as an important player in the rhythmic contraction of the uterus during labor (60, 79, 104, 138). This rhythmic activity is under the control of myometrial smooth muscle cells (MSMCs). Before the labor, MSCMs exhibit a RMP of -75 mV and this potential becomes depolarized to -50 mV during labor (176). In this context, MSMCs exhibit a phasic and regenerative depolarization and repolarization of the membrane resulting in rhythmic spontaneous contractions (177). RNA sequencing and specific non-quantitative RT-PCR data from human myometrial tissues revealed the expression of the NALCN channelosome suggesting it could play a role in the rhythmic contraction of the uterus (79, 178). In mouse, the *Nalcn* mRNA is detected in the uterus of non-pregnant animals and all pregnant stages without any significant differences in expression levels (138). However, Western blotting revealed that NALCN levels in the uterus decrease in mid-pregnancy (P14, P18, P19) compared to early pregnancy (P7, P10), and then increase during labor and remain high in the early postpartum period (138). It is not clear why there is no difference in RNA level between P7 to P19 while the protein expression level decreases, perhaps involving post-translational regulation of NALCN expression. *Nalcn* expression at the transcriptional level is be modulated by both progesterone (P4), a proquiescent hormone and estrogen (E2), a procontractile hormone (60, 179). Indeed, using the human myometrial HM6ERMS2 cell line as a cell model, quantitative RT-PCR revealed a 2.3-fold decrease in *NALCN* mRNA expression when cells were treated with E2 while a 5.6-fold increase was observed in cells treated with P4+E2 (60). The use of specific estrogen receptor (ER) and progesterone receptor (PR) antagonists showed these receptors are involved in the transcriptional regulation of *NALCN* induced by the E2 and P4 hormones, respectively. At the protein level, Western blotting experiments confirmed the negative regulation of NALCN expression by E2. However, there was no significant upregulation of NALCN in cells exposed to both P4+E2 compared to control cells, although the negative regulation of E2 was lost. The positive regulation of *NALCN* mRNA transcription by progesterone was found to involve three progesterone responsive elements (PRE) identified in the NALCN promoter. Notably however, negative regulation of *NALCN* mRNA expression does not involve an identified estrogen responsive element (ERE) in the NALCN promoter since mutations of this element did not impact the inhibition of *NALCN* transcription by E4. This suggests that E2 and ERα work through a separate mechanism to modulate *NALCN* transcription. Of note, the identified ERE sequence overlaps with one of the PRE sequences. For an unknown reason, all these data contrast with Western blotting experiments of mouse uterus at different stages, which instead suggest that NALCN protein levels are downregulated by P4 and upregulated by E2 (138). A temporal analysis of NALCN expression and hormone concentrations would be of interest to explain the species-specific differences in hormonal regulation of NALCN expression.

At the functional level, a Na^+ leak current with sensitivity to Gd^{3+} in the micromolar range is reported in MCSCs from pregnant rats, the human myometrial HM6ERMS2 cell line, as well as freshly isolated and cultured MCSCs from pregnant women (60, 79, 180). Knockdown of *NALCN* in human MCSCs indicated the leak Na^+ current is, at least in part (~50%), attributable to NALCN (79). Acetylcholine and substance P, which are known to positively modulate NALCN, also increase uterine contractility (181, 182). The relevance of NALCN being involved in parturition was explored in a mouse model in which *Nalcn* expression was specifically deleted in smooth muscle cells using the Cre/lox system

(smMHC$^{Cre\text{-}eGFP}$ x NALCN$^{fx/fx}$)(138). SmNALCN$^{-/-}$ and smNALCN$^{+/-}$ mice experience a higher rate of abnormal labor (*i.e.*, prolongated labor, delayed labor, dysfunctional parturition) of ~40 and ~60%, respectively compared to control animals with only ~20%. In addition, these mice produce smaller litter sizes and their labor has a longer duration. Further, smNALCN$^{-/-}$ mice have larger pups than control animals. An examination of myometrial electrical activity at P19 revealed no difference neither in burst interval or spike density but a significant decrease in burst duration and the number of spikes/burst in smNALCN$^{-/-}$ mice. It was concluded that NALCN is important for sustaining burst duration in the myometrium and is necessary for successful delivery (138). The involvement of NALCN in reproduction appears to be of importance also in *D. melanogaster,* as loss-of-function Dmα1U^{har38} and Dmα1U^{85} animals produce considerably fewer offspring than wild-type flies (132).

A more recent study identified a functional coupling between the Na^+-activated K^+ channel SLO2.1 and NALCN for the regulation of human MSMCs membrane potential, excitability and uterine contractility (104). Indeed, the use of two non-specific inhibitors of NALCN (*i.e.*, 10 µM Gd^{3+} and 50 µM CP96345,) uncovered that Na^+ influx into the cytoplasm of myometrial smooth muscle cells, working as a cytoplasmic messenger, activates SLO2.1 to induce K^+ efflux resulting in hyperpolarization of the membrane. Conversely, a decrease in this SLO2.1/NALCN functional coupling induces a membrane depolarization which triggers Ca^{2+} through Ca_V channels to promote contractions. The functional coupling between the SLO2.1 and NALCN likely involves the co-inclusion of the two channels in the same protein complex, as revealed by proximity ligation assays (PLA) in both human MSMCs and the related cell line hTERT. However, the existence of a physical complex remains to be confirmed with other approaches such as co-immunoprecipitation and FRET/BRET studies. Notably, SLO2.1 is also known to form a functional complex with Na_V channels in neurons (183, 184). In sum, the proposed model for the role of NALCN in MSMC contractility is the following: rather than acting to depolarize RMP, NALCN causes hyperpolarization of myometrial smooth muscle cells through its functional interaction with SLO2.1. Consistent with this idea, NALCN conducts about 50% of the Na^+ leak current at the membrane potential in human MSMCs (79). If NALCN was involved in setting pacemaker activity, cells lacking NALCN should have a disrupted inter-burst action potential frequency. Instead, MSMCs from NALCN knockout mice (at day 19 of pregnancy) only show a significant reduction in burst duration, but no significant effect on inter-burst frequency, indicating the channel does not contribute to pacemaking in these cells (**FIGURE 8**)(138). Clearly, an interesting prospect that should be investigated is whether SLO2.1 and NALCN are also functionally coupled in the nervous system. Taken together, these data suggest that during quiescence, progesterone serves to induce NALCN expression and activity. As a result, Na^+ current through NALCN activates SLO2.1, leading to membrane hyperpolarization (**FIGURE 7**). In these conditions, L-type voltage-gated Ca^{2+} channels are closed and uterine contractions do not occur. Instead, in the contractile state, NALCN expression is inhibited by estrogen leading to a decrease in SLO2.1 activity, depolarizing the membrane resulting in activation of L-type Ca_V channels that drive uterine contractility.

6- Pacemaker activity in the intestine

NALCN is involved in regulating the pacemaking activity of Interstitial cells of Cajal (ICCs). ICCs are pacemaking cells in gastrointestinal (GI) muscles that generate rhythmic

oscillations of the RMP known as slow waves (185). In mice, the pacemaker activity of ICCs is modulated by substance P (SP) through the activation of a non-specific cation channel (78, 186, 187). Here, SP induces a concentration-dependent depolarization of the membrane that is prevented by application of SP receptor antagonists (78), one of which, notably, is also a potent blocker of NALCN (*i.e.*, L703706; *see section above on NALCN pharmacology*) (89). In this study, NALCN expression was detected at both the RNA and protein levels in ICCs (78). The SP-dependent depolarization was prevented by application of external Gd^{3+} or by decreasing extracellular Na^{+}. Application of the constitutive G-protein antagonist GDP-β-S and the agonist GTP-γ-S did not affect SP-induced depolarizations, while bath application of the phosphotyrosine kinase inhibitor genistein or PP1 inhibited them. Conversely, intracellular dialysis of a Src Family Kinase (SFK) was found to mimic the SP-induced depolarization, as did activation of the neurotensin (NT) receptor (**FIGURE 7**)(78). Taken together, these data strongly suggest that NALCN is involved in the SP- and NT-induced depolarization in ICCs. ICCs of *Nalcn* knockout mice exhibit attenuated SP-induced depolarization (~75%), and an almost fully abolished inward current at -60 mV. The remaining contribution to the SP-induced depolarization (~25%) is attributed to TRPC channels. The physiological relevance of these findings remains to be confirmed in animal models in which NALCN expression can be selectively manipulated in ICCs, for example by crossing the available $Nalcn^{fx/fx}$ allele with a c-$Kit^{CreERT2}$ knock-in allele to specifically target ICCs (188).

In light of the implication that the NALCN channelosome contributes to digestive system physiology, a genome wide association study (GWAS) was done in dogs, combined with whole genome sequencing (WGS) of a subset of individuals, identifying a possible association between *NALCN* and canine gastric dilatation-volvulus (GDV)(189). GDV is characterized by rotation of the stomach around its axis, trapping air within the gastric lumen and increasing intragastric pressure. Dogs with GDV exhibits abnormalities in both gastrointestinal and gastric motilities (190).

7- Pain

Several studies have identified a role for NALCN in pain signaling and sensory processing in both mammals and invertebrates (61, 62, 71, 88, 145, 191).

Ascending pain signaling

A large-scale screen to search for genes that enriched in the dorsal spinal cord compared to the ventral cord in rat using DNA microarray analysis revealed that *Nalcn* mRNA is 6.9-fold more expressed in the dorsal spinal cord (191). This result was confirmed by quantitative RT-PCR, although the fold increase was lower than observed in the DNA microarray analysis. Accordingly, NALCN is described as an important player in the excitability of spino-parabrachial neurons (SPN)(71), which convey nociceptive signals from the dorsal horn to multiple brain regions. This includes the parabrachial (PB) nucleus, a cell grouping that surrounds the superior cerebellar peduncles in the dorsolateral pons acting as a sensory hub for pain signaling (192). The firing of SPNs is strongly controlled by neuromodulators released from primary afferent C fibers, including SP. SPN neurons express a Gd^{3+}-sensitive Na^{+} leak current with biophysical properties consistent with those of NALCN (71). Furthermore, application of Gd^{3+} significantly hyperpolarizes their membrane, decreasing their firing frequency, and

increasing the threshold for excitation. NALCN function in this cell type was confirmed by disrupting its expression in the PB nucleus of the mouse brain. Additionally, application of the selective NK1R antagonist SR140333 blocked SP-evoked transient inward current in SPN cells, which like NALCN, was sensitive to block by Gd^{3+} but insensitive to GDP-β-S. However, this current was inhibited by the src kinase inhibitor PP2, whereas NALCN is insensitive to the similar compound PP1 *in vitro* (*see section above on NALCN pharmacology*). Nonetheless, SP significantly depolarizes the membrane of SPNs and increases the firing frequency in wild type mice, but has no significant effect on the membrane potential of SPNs from NALCN knockout animals (71). Altogether, NALCN seems to be a crucial player in regulating the excitability of SPNs, implicating the channel in ascending pain signaling to the brain.

Neuropathic pain

A recent study found a significant increase in *Nalcn* mRNA, potentially through a cAMP-PKA-dependent pathway, after chronic constriction injury of the hind limb (CCI) in adult rats, both in dorsal root ganglia (DRG) neurons and the spinal cord (61). Immunocytochemistry revealed that the NALCN protein is widely expressed in nearly all DRG neurons. Specifically, NALCN is expressed in DRG neurons that co-labeled with neurofilament (NF200, A-fibers), transient receptor potential cation channel subfamily V member 1 (TRPV1, noxious receptor), isolectin B4 (IB4, non-peptidergic neurons), and peptidergic SP neurons. The percentage of DRG neurons that co-express NALCN and SP is greater after CCI. Broad NALCN protein expression is also evident in the spinal cord. An increase in a Gd^{3+}-sensitive and Na^{+}-dependent background conductance following CCI is documented in both DRG and spinal cord neurons. This current is potentiated by application of SP. A knockdown approach demonstrated that: (i) this current is mediated by NALCN, (ii) increased expression of NALCN contributes to the hyperactivity of both DRG and spinal cords neurons after CCI in rats, and (iii) *Nalcn* knockdown alleviates the mechanical allodynia and thermal hyperalgesia after CCI. *Nalcn* knockdown also reduces SP-induced pain behaviors in adult rats. Notably, the involvement of NALCN in the CCI-induced mechanical allodynia and thermal hyperalgesia appears to be conserved at least among rodents, being also observed in mice. Indeed, conditional knockout of *Nalcn* completely prevents mechanical allodynia and thermal hyperalgesia in adult mice. These results strongly suggest that NALCN contributes to the initiation and maintenance of neuronal sensitization in neuropathic pain. Thus, NALCN could represent a viable therapeutic target for the treatment neuropathic pain. This is especially relevant since effective treatment for neuropathic pain is currently unavailable because of an imprecise understanding of its etiology (193, 194). Indeed, general sensory functions of rats and mice are not altered by *Nalcn* knockdown/knockout, suggesting that targeting NALCN could be valuable to treat neuropathic pain without altering normal sensation. Lastly, transcriptomic data from Sun et *al*, 2002, showed that *Nalcn* mRNA is not upregulated in the dorsal horn of a chronic neuropathic pain model, suggesting that in this case, NALCN is not playing an active role in pain development (191).

Inflammatory pain

In addition to neuropathic pain, the same laboratory identified a role for NALCN in inflammatory pain (62). Specifically, the same *Nalcn* knockdown approach mentioned above was applied to a rat model of inflammatory pain induced by complete Freund's

adjuvant (CFA) injection in the left footpad. A significant increase in *Nalcn* mRNA expression, as well as SP, was detected in both DRG neurons and the spinal cord 2 hours following CFA injection, lasting up to 8 hours (DRG) or 3 days (spinal cord). A significant increase of NALCN protein was also observed, concurrent with an increase in the current density of a Gd^{3+}-sensitive, Na^{+}-dependent background conductance in small- and medium-sized DRG neurons from adult and neonatal animals. In contrast, increased current density was not observed upon downregulation of *Nalcn* expression. As expected, small- and medium-sized DRG neurons in both adult and neonatal CFA-animals exhibit a hyperactive electrical activity (*i.e.*, a depolarized RMP, an increased excitation threshold, and an increased action potential frequency), which is absent in siRNA-treated animals. As expected, knockdown of *Nalcn* in the DRG neurons and the spinal cord reduces both SP- and CFA-induced pain behaviors. Like neuropathic pain, this study suggests that NALCN could be a therapeutic target to treat inflammatory pain.

Chemical nociception

In addition to neuropathic and inflammatory pain, NALCN is also proposed to be involved in chemical nociception in the highveld mole-rat (88). This study aimed at characterizing algogen/algesiogenic-driven behaviors in several African rodent species using a combination of techniques including next-generation RNA sequencing and *de novo* transcriptome assembly, gene expression analysis, and functional experiments. One species, the highveld mole-rat (*Cryptomys hottentotus pretoriae*) is completely insensitive to allyl isothiocyanate (AITC). When comparing gene expression levels of this species to others, only the *Nalcn* mRNA was found to be significantly up-regulated, specifically in the spinal cord with levels more than six-fold higher than all other species. It was thus postulated that the overexpression of NALCN in sensory neurons could contribute to AITC insensitivity. In this context, the presence of increased numbers of NALCN channels at nociceptor terminals would induce a depolarized membrane, preventing initiation of action potential firing by TRPA1 by promoting the inactivation of Na_V channels (**FIGURE 9**). Consistent with this idea, pain behaviors of verapamil-treated highveld mole-rats were increased to resemble those of all other rodents. However, since verapamil is not a NALCN specific blocker, the use of specific inhibitors, when available, as well as molecular techniques such as *in vivo*-mediated knockdown in sensory neurons, will be required to definitively prove that NALCN is involved in chemical nociception in this species, as well as other rodents and humans.

Thermal nociception

In addition to the role of NALCN in ascending nociceptive transmission highlighted by Ford et *al*, 2018 (71), a role for NALCN in primary nociceptors has also been described. In *C. elegans* FLP neurons, the NALCN orthologues NCA-1/NCA-2 were shown to contribute to thermonociception (**FIGURE 9**)(145). FLP neurons are polymodal nociceptors capable of detecting high temperatures and harsh touch (195). They exhibit an arborized morphology like peripheral polymodal sensory neurons in vertebrates (196). Using null mutants of ion channels, the authors of this study discovered that TRPV channels (OSM-9 and OCR-2), the Ca_V channels L- , N-, but not T-type (*i.e.*, EGL-19, UNC-2), as well as NCA-1 and NCA-2, play a role in FLP activation. In addition, data suggested that NCA-1 controls FLP thermal sensitivity, whereas NCA-2 plays a role in thermal sensitivity, sensory gain maintenance, and signal kinetics during thermal stimuli termination (145). Of interest,

nca-2 animals who display slow kinetics of cytoplasmic [Ca^{2+}] decrease in FLP upon stimulus cessation also present a delayed decrease in reversal rate in the post-stimulus period. The mechanism involved in the NCA-1- and NCA-2-mediated FLP activation remains to be investigated. It is also of importance to determine whether this mechanism is conserved in mammals.

8- Other functions

a) Metabolism/Weight/Hormone secretion

Male and female *Lightweight* (Lwt)/+ and heterozygous *Unc-79* mice weigh less and are smaller than their wild-type littermates (47, 48). Monitoring food and water consumption for 19 days starting at post-natal day 80 (P80), followed by body composition analysis, revealed that Lwt/+ mice consume similar amounts of food and water, yet accumulate less fat than wild-type animals. Mutant specimens with similar weights as wild-type mice consumed significantly more food on a gram per kilogram basis, and on average the body of Lwt/+ animals consistent of a higher proportion of lean mass and less body fat. These results suggest a higher metabolic rate, an increase in protein turnover, and/or a difference in energy usage compared to wild-type animals. Interestingly, a few *Unc-79* knockout pups can survive beyond 24 hours after birth, sometimes until P7. Although these pups are active soon after birth, after half a day, they appear weak and their movements decrease gradually presumably due to an observed inability to nurse and consume milk (137).

Supporting a role of the NALCN channelosome in metabolism, a genome-wide association study in human found an association between FAM155A and circulating fibroblast growth factor 21 (FGF21)(197). FGF21 is an evolutionarily conserved factor that plays important roles in metabolic homeostasis (198).

In the same vein, the expression of NALCN (either at the RNA and/or protein level) in endocrine/neuroendocrine tissues suggests that NALCN could contribute to hormone secretion (56, 76, 84, 199). At rest, a Na^+ leak conductance which shares common biophysical properties with the NALCN current is present in endocrine cells of the anterior pituitary, pancreatic beta cells, and adrenomedullary chromaffin cells (12). Interestingly, this conductance mainly operates at resting membrane potential and thus contributes to regulate RMP and action potential discharges, which in turn trigger increases in cytosolic Ca^{2+} and exocytosis. It therefore seems reasonable to suggest that NALCN contributes to hormone secretion, a question that remains open for future investigation.

b) Osmoregulation

A role of NALCN in osmoregulation is also described (146). Haplotype association mapping (HAM) on aging groups of mice from 27 different strains was carried out to identify novel genes involved in the regulation of water homeostasis. Although this HAM analysis did not identify any peaks above the stringent significance threshold of $\alpha = 0.05$, several peaks above the suggestive threshold were identified, with the strongest mapping to a genetic locus containing the distal part of the NALCN channel coding sequence. The involvement of NALCN in regulating levels of Na^+ in blood serum was then confirmed in

mice harboring a heterozygous *Nalcn* knockout allele (since homozygous *Nalcn* knockout mice die within 24 h after birth). At 12 weeks of age, heterozygous mice were found to display small but significantly higher serum Na^+ concentrations compared to wild-type mice (146). Supporting a role of NALCN in osmoregulation, a study aiming to investigate genomic regions associated with Na^+ intake, K^+ intake, and Na^+ -to- K^+ ratio measured from 24-h or half-day urine samples revealed a possible association between NALCN and potassium excretion in humans (200). How NALCN impacts serum Na^+ levels, as well as K^+ excretion, remains to be determined. A better understanding of the cell types that express *Nalcn*, combined with the recent development of conditional knockout mouse models will be useful in this context (38, 71-73, 80). This will allow the determination of whether NALCN plays a role in physiological processes that are known to influence ionic homeostasis. This includes, for example, the potential role of NALCN in regulating heart rhythm, in the neuronal arginine vasopressin (AVP) release and thirst sensation, and in adrenocortical aldosterone release.

c) Sensitivity to ethanol and volatile anesthetics

A large set of studies reported the involvement of NALCN in the sensitivity to volatile anesthetics in both *C. elegans* and *D. melanogaster* (33, 129, 132, 133, 139, 147-155)(**TABLE 3**; **FIGURE 8**). General anesthetics are known to depress fast excitatory and enhance fast inhibitory synaptic transmission mediated primarily by glutamate and GABA, respectively (201, 202). Several ion channels are proposed to contribute to the anesthetized state by inhaled anesthetics. This includes several types of K^+ channels (*e.g.*, K_v, K_{2P}), HCN, Na_v, GABA-A, NMDA, nicotinic acetylcholine receptors and glycine receptors (201, 203-206). Stemming from combined observations that the NALCN channelosome is a crucial regulator of neuronal excitability, and is involved in anesthesia by inhaled anesthetics in *C. elegans* and *D. melanogaster* (*see below*), researchers sought to examine whether NALCN could also be involved in inhaled anesthetics responses in mammals (77). This work revealed that isoflurane enhances NALCN conductance at sub-anesthetic concentration and *Nalcn* knockdown reduces behavioral hyperactivity after isoflurane induction. In mouse CA3 hippocampal neurons that express NALCN, isoflurane at sub-anesthetic concentrations increases the firing rate and depolarizes the membrane while isoflurane at anesthetic concentrations decreases the firing rate and hyperpolarizes the neurons. Within both concentration ranges, a Na^+ leak current is increased at -60 mV. *In vivo* knockdown of *Nalcn* revealed that isoflurane-induced hyperactivity during anesthesia induction is reduced in NALCN knockdown animals compared to wild-type counterparts. Because isoflurane inhibits Na_V channels at anesthetic concentration, but not at sub-anesthetic concentrations, it was concluded that isoflurane bidirectionally modulates the excitability of hippocampal CA3 pyramidal neurons, by either enhancing NALCN current to induce hyperexcitability, or by inhibiting Na_V channels to induce hypoexcitability. The same laboratory that reported these findings also identified a NALCN-mediated increase in neuronal activity by isoflurane, as well as sevoflurane but not propofol in retrotrapezoid nucleus neurons (81). However, contrasting with CA3 hippocampal neurons, isoflurane at anesthetic concentrations does not decrease the firing rate of RTN neurons (81). Importantly, isoflurane has no effect on NALCN current when expressed in HEK-293T cells (77), likely because these cells lack other factors involved in NALCN sensitivity to isoflurane. Indeed, it is possible that the configuration used for NALCN expression in these experiments (in HEK-293T cells without accessory subunits) may not have been suitable for detecting isoflurane effects on NALCN currents.

Overall, this study suggested that NALCN is not involved in promoting the anesthetic state. This contrasts with published data showing that *Lightweight* heterozygous mice (Lwt/+) with decreased level of *Unc-79* are resistant to anesthesia with isoflurane (47). Indeed, there is no apparent alteration in minimal alveolar concentration in response to halothane, cyclopropane, or sevoflurane in Lwt/+ mice. However, there *is* a significant resistance to isoflurane-induced anesthesia relative to wild-type animals. Consistent with NALCN contributing to the response to volatile anesthetics, an identified patient with a *de novo* gain-of-function mutation on the *NALCN* gene (p.A319V) was found to exhibit high sensitivity to sevoflurane anesthesia at usual dosage with severe respiratory depression culminating in cardio-respiratory arrest (27, 207). Further work is now needed to clarify the role of the NALCN channelosome in volatile anesthetic-mediated effects on neurons in mammals.

Previous studies performed In *C. elegans* showed *unc-79* and *unc-80* mutants are either moderately resistant to ethanol-induced immobility, or to exhibit a wild-type sensitivity in liquid media (150). These results contrast with other studies showing a pronounced hypersensitivity to ethanol in *unc-79*, *unc-80*, *nca-1, nca-2* and *nca-1:nca-2* double mutants when compared to wild-type N2 animals (47, 157). In mammals, a highly significant increase in the sensitivity to the acute sedative effects of ethanol is apparent for Lwt/+ mice as measured using righting reflex tests (47), despite blood ethanol levels remaining similar to wild-type littermates. Unlike wild-type animals that exhibit significant locomotor activation following ethanol injection, no such activation is observed in Lwt/+ mice. Also, Lwt/+ mice exhibit a higher preference for ethanol relative to wild-type mice, but no alteration in taste sensitivity for either consumption or preference for saccharin- and quinin-containing solutions over water (47). Taken together, these data showed that Lwt/+ mice have acute hypersensitivity to and increased voluntary consumption of ethanol. The mechanisms involved in alcohol hypersensitivity and preference by loss-of-function UNC-79 mutations (and possibly other NALCN subunits) remain to be established. Interestingly, ethanol induces dopamine release in rat nucleus accumbens (Nac) and dopamine is known to negatively modulate the NALCN channelosome through the D2 dopaminergic receptor (D2R)(72, 208). One may postulate that ethanol decreases the electrical activity of D2R-expressing neurons, an effect which would be partly attenuated if NALCN is rendered unfunctional or diminished in its activity.

Since many studies have highlighted the importance of the Nac in regulating the process of drug-induced locomotor sensitization, such as methamphetamine and ethanol (209-212), a recent study examined the hypothesis that NALCN in NAc may contribute to the ethanol-induced acute stimulant responses and locomotor sensitization in mouse (156). In the NAc, *Nalcn* mRNA (as well as *Unc-79* but not *Unc-80* mRNA) and NALCN protein levels increase after ethanol-induced locomotor sensitization. *In vivo* knockdown of *Nalcn* demonstrated that decreased NALCN expression alleviates both ethanol-induced acute stimulant responses and locomotor sensitization. The mechanisms involved remain to be elucidated and are likely complex since the acute effect is probably due to a direct or indirect functional effects on the NALCN channelosome, while the effect on the locomotor sensitization is likely due to effects on *Nalcn* gene expression.

d) Social clustering

In *D. melanogaster*, mutation of *na/Dmα1U* impacts several complex behaviors including social clustering (*i.e.*, the distance maintained between individuals) (158). $Dm\alpha1U^{har38}$ hypomorphic mutants exhibit a significantly reduced social space index in several behavioral tests, and effect that can be either fully or partially restored by expressing *na/Dmα1U* in cholinergic neurons and glutamatergic neurons, respectively. Reduced social clustering is also observed when *na/Dmα1U* and *nlf-1* are knocked down (141).

e) Development and morphology

Adult *D. melanogaster* specimens with the genotypes $Dm\alpha1U^{na}$, $Dm\alpha1U^{har38}$, and $Dm\alpha1U^{85}$ have subtle morphological phenotypes: they are noticeably smaller and their abdomens are slenderer and more elongated compared to wild-type flies (*i.e.*, hence the name narrow abdomen), implicating NALCN in development (64, 132). Yet to be determined is whether the NALCN channelosome contributes to development and morphology in mammals. Since mouse pups harboring *Nalcn*, *Unc-79* and *Unc-80* knockout lesions appear physically normal at birth but die shortly afterwards, assessment of abnormal morphology has not been possible during postnatal development (2, 47, 49, 137). However, it is notable that patients with pathogenic variants of *NALCN*/*UNC-80* exhibit numerous morphological alterations *(see below*). To date, no morphological alterations associated with NALCN disruption have been reported for *C. elegans*.

f) Miscellaneous

Western blotting of protein lysates from the brainstem nucleus tractus solitarius of a rat model of dysphagia after stroke revealed increased expression of NALCN and UNC-80 proteins (159), suggesting NALCN could be involved in swallowing.

A comparative transcriptomic study between human supernumerary teeth derived stem cells (SNTSCs) and normal dental pulp stem cells (DPSCs) highlighted a total of 12,861 differentially expressed genes, including *NLF-1/FAM155A* which was found to be more highly expressed in SNTSCs compared to DPSCs (160). Here, the proliferative capacity of SNTSCs was found to be inhibited by *FAM155A* knockdown, while cell migration was promoted. Thus, *NLF-1/FAM155A* might contribute to cell proliferation and migration.

A study investigating putative genome regions associated with adaptation to harsh and arid environments in native chickens revealed a putative involvement of *Nalcn* (161). Here, whole-genome sequencing of different chicken breeds living in different environmental conditions across China led to the identification of 161,322 SNPs located within coding regions of the chicken genome, including 46,063 non-synonymous SNPs, 355 stop gain, 89 stop loss and 114,815 synonymous SNPs. SNP analysis highlighted the association of several genes in adaptation to harsh and arid environments including *NALCN*.

Another study investigating the genetic architecture of pigs subjected to breeding intensification (162) identified *Nalcn* as a possible locus involved in changes associated with the intensification of the selection process in pigs.

More recently, a comparative transcriptome study aimed at identifying genes related to sexual differentiation and sterility of the sterile Mule duck compared to Jinding and Muscovi ducks revealed that *Nalcn* is part of a group of 8 genes involved in male sterility (163).

FIGURE 9. Schematic tile grid representation of the physiological roles linked to NALCN in various model species. Most studies have been performed in the mouse species *Mus musculus* (knockout *vs* wild type) disclosing a role of NALCN in circadian rhythm and sleep, sensitivity to external chemical such as anesthetics, locomotion, respiratory rhythm, pain, parturition and gastrointestinal motility. The non-vertebrates fly and worm model species *Drosophila melanogaster* and *Caenorhabditis elegans*, respectively, have also been exploited to establish further the role of NALCN in the photic control of locomotion, sensitivity to anesthetics and locomotion. Other animal models, such as the snail *Lymnaea stagnalis* and the mole rat *Cryptomis hottentotus* have been used to support a role of NALCN in respiratory rhythm and pain, respectively.

To close this chapter on the various physiological functions of the NALCN channelosome, we provide a graphical abstract (**FIGURE 9**) that summarizes the main take home messages, namely that: i) NALCN is involved in many cell and body functions; ii) NALCN functions in several species, including mammals and non-mammals, point to conserved functions but also differences in contributions to physiology; and iii) there are still many gaps in our understanding of NALCN physiology in mammals and non-mammals especially, and additional roles will likely be discovered as new research tools are developed and implemented.

IV- THE NALCN CHANNELOSOME IN HUMAN DISEASE

In this section, we describe the studies linking NALCN and its subunits to various human diseases.

General genomic features of NALCN subunit genes in humans.

The five genes encoding NALCN subunits in humans are located on chromosomes 13q32.3-q33.1 (*NALCN*), 14q32.12 (*UNC-79*), 2q34 (*UNC-80*), 13q33.3 (*FAM155A*), and Xq13.1 (*FAM155B*) (**TABLE 4**). Interestingly, an intronic and probably non-coding transcript referred to as *FAM155A-IT1* is predicted within the *FAM155A* gene, arranged in the same orientation as *FAM155A*. Similarly, a long non-coding RNA (lncRNA) referred to as *NALCN-AS1* that partially overlaps with *NALCN* in an inverted orientation is also predicted. Exons #6 and #8 of *NALCN-AS1* overlap with exons #43 and #44 of *NALCN*, respectively, raising the possibility *NALCN-AS1* regulates *NALCN* mRNA expression. Of note, both *FAM155A-IT1* and *NALCN-AS1* appear to be unique to humans. A search in the GTex portal (https://www.gtexportal.org) indicates that *FAM155A-IT1* is mainly expressed in testis and at low levels in the pituitary gland and brain tissues. *NALCN-AS1* is mainly expressed in brain tissues, pituitary gland, bladder, and arteries. Since non-coding RNAs are important regulators of cell physiology and function, the relevance of both *FAM155A-IT1* and *NALCN-AS1* in regulating *FAM155A* and *NALCN* expression/function remains to be investigated (213). A search in the NCBI database (https://www.ncbi.nlm.nih.gov) also suggests the existence of alternative splicing events for *NALCN*, *UNC-79* and *UNC-80* (*not shown*). Many studies have described pathogenic variants of the NALCN channelosome in rare genetic diseases as well as possible association with many other diseases such as psychiatric diseases and cancer (**TABLES 5-11**).

TABLE 4: Chromosomal location of the human NALCN channelosome-encoding genes

Gene	Chromosomal location	Reference sequence*	Coordinates	Size	Number of identified exons (Reference sequence)
NALCN *Canlon* *BA430M15.1* *VGCNL1* *Rb21*	13q32.3-q33.1	NC_000013.11	chr13:101,053,774-101,417,206	363,433 bases	44 (NM_052867.4)
NALCN-AS1	13q32.3	NC_000013.11	chr13:100,708,312-101,066,090	357,779 bases	6 (NR_047687.1)
UNC-79 *KIAA1409*	14q32.12	NC_000014.9	chr14:93,333,182-93,710,473	377,292 bases	50 (NM_020818.5)
UNC-80 *KIAA1843* *C2orf21*	2q34	NC_000002.12	chr2:209,771,832-209,999,300	227,469 bases	66 (NM_001371986)
NLF-1/FAM155B *NALF1*	13q33.3	NC_000013.11	chr13:107,163,510-107,867,496	703,987 bases	3 (NM_001080396.3)
FAM155A-IT1 *NALF1-IT1*	13q33.3	NC_000013.11	chr13:107,787,360-107,835,458	48,098 bases	2 (NR_046848.1)
NLF-1/FAM155B *NALF2*	Xq13.1	NC_000023.11	chrX:69,504,326-69,532,508	28,183 bases	3 (NM_015686.3)

TMEM28					

***Genome assembly GRCh38/hg38**

1- Infantile Hypotonia with Psychomotor Retardation and characteristic Facies 1 and 2 (IHPRF1 and 2)

In both humans and mice, individuals heterozygous for *UNC-80*, *UNC-79* and *NALCN* null mutations develop normally, are fertile, and do not have obvious abnormalities such as lethality and severe intellectual disability, suggesting that a reduction in gene dosage is phylogenetically tolerable. However, homozygous deleterious mutations of *NALCN* and *UNC-80* are described in patients with the IHPRF1 (OMIM #615419) and IHPRF2 (OMIM #616801) syndromes respectively (*see below*). Previous studies reported that patients with interstitial deletions of the long arm of chromosome 13 (referred to as the 13q syndrome) where *NALCN*, *NALCN-AS1* and *FAM155A* localize, have widely varying phenotypes (214-217), including severe malformations in the brain, heart, kidneys, lungs, other organ systems, and digits. Instead, other individuals are only mildly affected with minor dysmorphic features, developmental delay, and growth failure (218).

Microdeletions in a region of chromosome 2, where *UNC-80* resides along with several other genes, are associated with brain anomalies, mental retardation and dysmorphic features (219, 220). Since these regions underlie several genes, it is not possible to correlate NALCN function with these phenotypic defects. However, symptoms described below for *NALCN* and *UNC-80* loss-of-function pathogenic variants clearly suggest an involvement, since the observed defects in patients with deletions in chromosomes 13q and 2q highly resemble these NALCN channelopathies.

NALCN subunit mutations, IHPRF1 (OMIM #615419):

A first study described 2 siblings from a co-sanguineous family suffering from a severe developmental disorder (221)(*also see* (222) for previous descriptions of siblings). These siblings carried a recessive homozygous truncating mutation p.Q642X on NALCN. The disease was first referred to as an atypical form of Infantile Neuroaxonal Dystrophy and later renamed IHPRF1. Following this first report, several patients carrying mainly homozygous nonsense, but also missense mutations (*i.e.*, p.W1287L; p.P908L; p.R1094Q; p.F1427L; pV1528I; pV1400F; pG1303D), were described with no specific hot spots regarding their location on the protein sequence (**TABLE 5**; **FIGURE 10**)(223-236). Nonsense mutations are predicted to result either in a mRNA decay process or the expression of a truncated and non-functional protein. The missense pathogenic variant p.W1287L was found to be loss-of-function when expressed both in the neuronal NG108-15 cell line and *Xenopus* oocytes (27, 94). The recessive mutation p.R1094Q occurs at the interface between NALCN and FAM155A and is also predicted to be loss-of-function (29). More than 43 IHPRF1 patients from 29 families are described to date. Unsurprisingly, patients exhibit a large panel of symptoms of variable severity (**TABLE 7**).

UNC-80 subunit mutations, IHPRF2 (OMIM #616801):

Autosomal recessive mutations in the *UNC-80* gene are also reported (39 patients from 25 families; **TABLE 6**)(93, 229, 237-246). Like *NALCN*, both nonsense and missense mutations are described. Imposing the p.P1700S mutation on the mouse UNC-80 cDNA causes a loss-of-function property to recorded currents when expressed in HEK-293T

cells (93). Interestingly, the truncated p.L2586X mutant is functional when overexpressed both in HEK-293T cells and mouse hippocampal neurons (49). However, while the wild-type UNC-80 localizes to both soma and neuronal processes, the mouse UNC-80 variant truncated at p.L2654X (*i.e.*, the analogous truncation of the human p.L2586X truncation in mouse) is retained in the soma without detectable expression in axons and dendrites. Consistent with findings for other *UNC-80* nonsense mutations, three nonsense mutations predicted to be detrimental to UNC-80 folding or channelosome assembly (p.R51X, p.R174X, and p.R2706X) also fail to evoke currents when co-expressed with NALCN, FAM155A and UNC-79 in *Xenopus* oocytes. Three biallelic *UNC-80* missense mutations (p.P1700S, p.V189M and p.R2536T) show wild-type-like function in *Xenopus* oocytes but potentially impact UNC-79/UNC-80 subcomplex stability in neurons (31). A patient appeared to have a similar but milder phenotype than those found in the individuals with *UNC-80* null mutations (49). This patient exhibited a biallelic variations in the *UNC-80* gene. In one allele, he inherited variations of c.1020G > T and c.1021C > T (p.Q340_P341delinsHS) from his mother. In the other, he inherited c.3883G > C (p.E1295Q) from his father. The three mutated residues (p.Q340, p.P341, and p.E1295) in this individual are highly conserved among deuterostome animals, from sea urchins to fishes to humans. Rescue experiments in hippocampal neurons from *Unc-80* knockout mice revealed that while the p.Q341H;P342S mutant (*i.e.*, the mouse homologue mutation of the human p.Q340_P341delinsHS mutation) generates little or no Na^+ leak current, the p.E1296Q mutant (*i.e.*, the mouse homologue mutation of the human p.E1295Q mutation) partially restores it. Indeed, *in vitro* NALCN channelosome current amplitudes are < 50% compared to those of the wild-type complex. In addition, co-transfecting equal amounts of both UNC-80 mutant cDNA constructs into *UNC-80* knockout neurons generates a Na^+ leak current with amplitudes of only ~25% compared to wild-type UNC-80. This led Wie et *al*, 2020, to conclude that while a reduction of 50% in *UNC-80* gene dosage is tolerated, further reduction of UNC-80 function below 25% likely leads to severe phenotypes. This finding unlikely reflects a difference in the stability of the protein since the wild-type UNC-80 and the 2 mutants express at similar protein levels in HEK-293T cells. As for recessive mutations of *NALCN*, patients with recessive *UNC-80* mutations exhibit a large panel of symptoms of variable severity (**TABLE 7**).

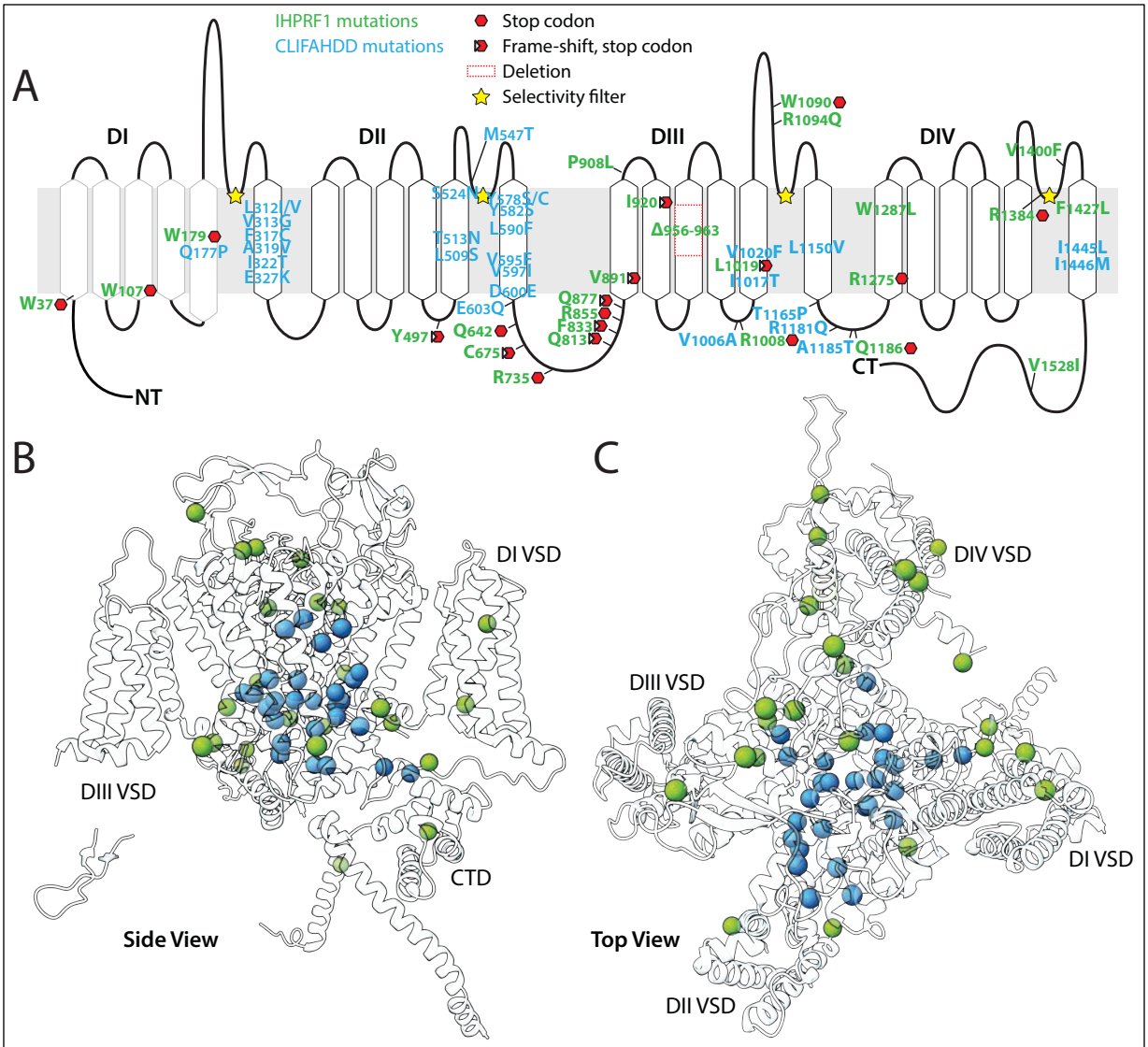

FIGURE 10. Locations of various disease-causing mutations in the human NALCN α_1 subunit. ***(A)*** Illustration of the general locations of the IHPRF1 and CLIFAHDD mutations listed in **TABLES 5** and **8**, respectively. Notable is that most CLIFAHDD mutations (*blue* font) involve missense mutations that are concentrated within the pore-forming S5 and S6 helices, while IHPRF1 mutations (*green* font) are more broadly distributed and most of these produce truncated protein products either though nonsense mutation, frameshift, or deletion (as indicated by the legend above the illustration). ***(B)*** Side view depiction of the location of IHPRF1 mutations (*green* circles) and CLIFAHDD mutations (*blue* circles) within the three-dimensional structure of the NALCN channel. ***(C)*** Top-down view depiction of these same mutations revealing the concentration of CLIFAHDD missense mutations within the ion permeation pathway. For panels *B* and *C*, positions where mutations occur were rendered by displaying the β-carbon of the corresponding residue within the wild type channel structure (PDB structure 7SX4) using ChimeraX.

TABLE 5: Genetics of the IHPRF1 syndrome

Mutation	Location	Patients	Gender (Older Age Reported)	Reference
c.1924C>T p.Q642X	DII-DIII loop	2 siblings	Female (21 yo) Male 18 (18 yo)	Koroglu et *al*, 2013 (221)
c.1489delT p.Y497Tfs*21	Domain I	2 siblings 1 cousin	Male (7.1 yo) Male (4.4 yo) Male (7.3 yo)	Al-Sayed et *al*, 2013 (223)

c.3860G>T p.W1287L	Domain IV	3 siblings	Female (17.6 yo) Female (16 yo) Female (9.4 yo)	Al-Sayed et *al*, 2013 (223)
c.4197+1G>A (Parent 1) c.2392C>T (Parent 2) p.R735X Note: Patient also carries a mutation of ANO3 associated with Dystonia 24	Domain IV DII-DIII loop	1	NI	Farwell et *al*, 2016 (224)
c.G3390A (IVS29-1G > A) p.W1090X	Domain III	3 siblings	Female (8 yo) Female (death at 5 yo) Male (death at 20 mo)	Gal et *al*, 2016 (225)
c.1267-2A>G	nonsynonymous mutation at a splice-acceptor site in intron 11	1	Female (3.8 yo)	Takenouchi et *al*, 2018 (226)
c.2022_2023delAT p. C675Lfs*23	DII-DIII loop (spliced exon 17)	1	Female (11 mo)	Takenouchi et *al*, 2018 (226)
c.3823C>T (Mother) p.R1275X c.2495_2496insTCATA (Father) p.F833Hfs*40 Note : mutations in TRAPPC9	Domain IV DII-DIII loop	2 siblings	Male (22 yo) Female (20 yo)	Angius et *al*, 2018 (227)
c.110G>A (Mother) p.W37X c.2723C>T (Father) p.P908L Note: mutations in ALMS1	N-terminus Domain III	2 siblings	Female (7 yo) Male (8 yo)	Campbell et *al*, 2018 (236)
c.3281G>A (Mother) p.R1094Q c.2563C>T (Father) p.R855X	Domain III Domain III	1	Female (10 yo)	Campbell et *al*, 2018 (236)
c.3823C>T p.R1275X Note: referred to as c.3910C>T, p.R1304X in the original article	Domain IV	1	Male (9 yo)	Bourque et *al*, 2018 (228)
c.3022C>T (Mother) p.R1008X c.2629delC (Father)	Domain III DII-DIII loop	1	Female (11.7 yo)	Bramswig et *al*, 2018 (229)

p.Q877N*fs**16				
c.3022C>T p.R1008X	Domain III	1	NI	Abul-Husn et *al*, 2023 (235)
c.3056dupT, p.L1019F*fs**30	Domain III	2 siblings	Male (7 yo) Female (3.10 yo)	Bramswig et *al*, 2018 (229)
c.4281C > A (Mother) p.F1427L c.4103 + 2T > C (Father) splice donor variant	Domain IV Domain IV	2 siblings	Male (4.6 yo) Male (3 yo)	Bramswig et *al*, 2018 (229)
c.3556C > T p.Q1186X	DIII-DIV loop	1	Female (7 yo)	Bramswig et *al*, 2018 (229)
c.2435dupA p.E813G*fs**23	DII-DIII loop	1	Female (*18.5* yo) Note: One sibling died at the age of 6 years with the same clinical features but undiagnosed	Bramswig et *al*, 2018 (229)
c.2889 + 3_6delAAGT (IVS25 + 3_6) p.V956_L- 963del	Domain III	1	Female (6.10 yo)	Bramswig et *al*, 2018 (229)
c.4150C > T p.R1384X	Domain IV	1	Male (5 yo)	Bramswig et *al*, 2018 (229)
c.321G > A p.W107X	Domain I	2 siblings	Female (4 yo) Male (NI)	Bramswig et *al*, 2018 (229)
c.2758delA p.I920L*fs**7	Domain III	1	Female (3 yo)	Bramswig et *al*, 2018 (229)
c.2671delG, p.V891S*fs**2	Domain III	2 siblings	Male (death at 5 yo) Female (2.9 yo)	Bramswig et *al*, 2018 (229)
c.2671delG p.Val891S*fs**2	Domain III	1	Male (Death at 5.5 yo)	Bramswig et *al*, 2018 (229)
c.537delG p.W179X	Domain I	1	Female (3 yo)	Bramswig et *al*, 2018 (229)
rs767980482 (C>T) pV1528I rs771656968 (C>A) pV1400F Note: Patient also heterozygote for loss of function variants in *VPS13B,* associated with Cohen syndrome	C-terminus Domain IV	1	Female (5 yo)	Carneiro et *al*, 2018 (230)
c.2203C>T p.R735X	DII-DIII loop	2 siblings	Female (4 mo) Male (Death before the 3 yo)	Ope et *al*, 2020 (231)
c.2563C>T p.R855X	DII-DIII loop	1	Female (9 yo) Note: an older male sibling with similar abnormalities who has died undiagnosed at the age of 3.5 months.	Karimi et *al*, 2020 (232)

c.3908C>T p.G1303D	Domain IV	1	Male (10 yo)	Khan et *al*, 2022 (233)
c.1267-924_1434 + 2024del (Mother) c.3022C>T (Father)	Deletion en-compassing exon 12 NI	1	Male (3.2 yo)	Maselli et *al*, 2022 (234)

Abbreviation: NI, not indicated

2- Congenital contractures of the Limbs and Face, Hypotonia and Developmental Delay (CLIFAHDD; OMIM #616226)

The description of CLIFAHDD, the severe developmental syndrome linked to *de novo* dominant mutations of *NALCN*, arose from the study by Chong et *al* 2015, of large series of children with congenital contractures of the limbs and face, hypotonia, and global developmental delay (247). Up to 40 patients with CLIFAHDD syndrome are now reported (**TABLE 8**)(134, 207, 248-261). Like the IHPRF1 and 2 patients, CLIFAHDD patients exhibit a large panel of symptoms of variable severity (**TABLE 9**). Most, but not all, of these mutations are located in the pore-forming region of NALCN (*i.e.*, transmembrane helices 5 and 6 of Domains I to IV) (**FIGURE 9**), suggesting they might exert their pathological functions by modulating NALCN gating directly.

A first study described the impact of the *de novo* pathogenic variant p.R1181Q found in a patient on the locomotor activity in *C. elegans* (256). Indeed, the pan-neuronal expression of *nca-1* carrying the corresponding mutation (*i.e.,* p.R1230Q) in a null nca1/2 background (*i.e., nca-1(gk9);nca-2(gk5)*) induced a coiling locomotion identical to that of the gain-of-function *nca-1(hp102)* or *nca-1(e625)* mutants. By contrast, the pan-neuronal expression of wild-type *nca-1* in the same background restored normal locomotor activity. It was concluded the p.R1230Q mutation of *nca-1* in *C. elegans* and by extrapolation, the p.R1181Q mutation in NALCN are gain-of-function ones. At the functional level, a study then reported that 2 mutations found in CLIFAHDD patients, p.L509S and p.Y578S, cause an increased current density compared to wild-type channels when transiently expressed in the neuronal cell line NG108-15 (94). These results were the first demonstration that pathogenic variants found in the CLIFAHDD syndrome are gain-of-function ones. The gain-of-function property of the p.L509S and p.Y578S variants were then confirmed following transient expression in HEK-293T cells (89). These findings were thereafter extended to a large panel of mutations found in patients following functional expression in *Xenopus* oocyte (27). Functional expression of the NALCN p.Y578S mutation in HEK-293T cells and single channel recordings revealed prolonged channel openings and an increase in open probability (P_0), with no change in the unitary conductance (31). Structural mapping of 25 mutations reveals clusters of local interaction networks, both intra and interdomains (27). Indeed, the p.R1181Q variant identifies the DIII-DIV linker as a hotspot with a potential role in channel gating. Two mutations on the DIII-DIV linker, p.T1165P and p.R1181Q, may lead to changes in channel gating by affecting the local interactions of the III-IV linker with adjacent Domain IS6, the DII-DIII linker, Domain IVS6, and the CTD (28). p.R1181 of the DIII-DIV linker interacts with the main-chain carboxyl group of p.S1451, p.L1452 and p.Y1454 (29).

2236

TABLE 6: Genetics of the IHPRF2 syndrome

Mutation	Patients	Gender (Older Age Reported)	Reference
c.151C>T p.R51X	2 related families *Family 1* 2 siblings + 1 cousin *Family 2* 4 siblings	aged between 9 months and 12 years Female (5 yo) Female (NI) Male (NI) Male (NI) Male (NI) Male (NI) Male (NI)	Perez et *al*, 2016 (237)
c.5098C>T p.P1700S	1	Female (4 yo)	Stray-Pedersen et *al*, 2016 (93)
c.6495G > A p.W2165X	1	Male (6 yo)	Kelesoglu et *al*, 2023 (246)
c.7607G>C p.R2536T Note : Predicted to give rise aberrant alternative splicing	1	Female (4 yo)	Stray-Pedersen et *al*, 2016 (93)
c.7757T>A p.L2586X c .2033delA p.N678Tfs*15	2 siblings	Female (15 yo) Female (9 yo)	Stray-Pedersen et *al*, 2016 (93)
c.3793C>T p.R1265X	1	Male (6.5 yo) Note: Two siblings with similar abnormalities died undiagnosed at the age of 4 yo and 6 yo respectively.	Shamseldin et *al*, 2016 (238)
c.3793C>T p.R1265X	1	Male (2 yo) Note: has older sister with similar abnormalities who died undiagnosed at 16 yo	Shamseldin et *al*, 2016 (238)
c.1078C>T p.R360X	1	Female (7 yo) Note: has younger brother (13 mo) with similar abnormalities	Shamseldin et *al*, 2016 (238)
c.565G>A p.V189M	2 siblings	Female (4 yo) Female (8 yo)	Shamseldin et *al*, 2016 (238)
c.2431C>T (Mother) p.R811X c.3983-3_3994delinsA (Father) p.S1328Rfs*19	2 siblings	Female (13 yo) Female (Death at 7 yo)	Valkanas et *al*, 2016 (239)

c.8525G>A p.R2842Q	1	Female (13 yo)	Obeid et *al*, 2018 (240)
c.8116C>T p.R2706X	1	Male (1 yo)	Bramswig et *al*, 2018 (229)
c.520C>T p.R174X	2 siblings	Male (3 yo) Female (1 yo) Note: had 2 older siblings with similar abnormalities who died undiagnosed at 16 yo	Bramswig et *al*, 2018 (229)
c.520C>T p.R174X	2 siblings	Female (NI) Female (NI)	Bramswig et *al*, 2018 (229)
c.520C>T (Mother) p.R174X c.2399delT (Father) p.L800W*fs**19	1	Male (4 yo)	Bramswig et *al*, 2018 (229)
c.1681_1682delAC p.T561Rfs*33	2 siblings	Male (10 yo.) Male (Death at 4 yo)	Bramswig et *al*, 2018 (229)
c.5671C>T p.R1891X	1	Female (Death at 2.7 yo) Note: a similarly affected paternal cousin passed away at the age of 3 years	Bramswig et *al*, 2018 (229)
c.8058+2T>G p.L2660Rfs*20	1	Male (4 yo)	Bramswig et *al*, 2018 (229)
c.601-1G>A p.R174Qfs*58	2 siblings	Male (Death at 10 yo.) Male (Death at 9.6 yo) Note: had another sibling with similar abnormalities who died undiagnosed at 1.6 yo	Bramswig et *al*, 2018 (229)
c.3719G>A p.W1240X c.4926_4937del p.Q1643_L1646del	2 siblings	Female (5.9 yo) Note: had another sibling (Male) with similar abnormalities who died undiagnosed at 1 yo	He et *al*, 2018 (241)
c.4963C>T p.R1655C c.8385C>G p.Y2795X	1	Male (*9.5* yo)	He et *al*, 2018 (241)
Mutation not indicated	1	Male (8 yo)	Hong et *al*, 2018 (242)
c.3226C > T p.R1076X c.3205C > T p.R1069X	1	Female (Death at 3 yo)	Kuptanon et *al*, 2019 (243)
Mutation not indicated	1	Male (3 yo)	Stenehjem et *al*, 2019 (244)

c.5609-4G>A Note: Predicted to give rise aberrant alternative splicing	1	Male (8 yo)	Tao et *al*, 2021 (245)

Abbreviation: NI, not indicated

3- Symptomatology of the IHPRF and CLIFAHDD syndromes

Mutations in *NALCN* and *UNC-80* are associated with IHPRF1, IHPRF2 and CLIFAHDD syndromes (*see* above). To the best of our knowledge, since the first publications in 2013 (221, 223), there are more than 100 cases of *NALCN*/*UNC-80*-related disorders reported in the literature (*see* **TABLES 5, 6 and 8)**. However, despite the growing number of articles, the lack of homogeneity in the clinical data provided is a major obstacle towards establishing a complete clinical picture. *NALCN* is universally expressed in the brain, especially in neurons, but also in a variety of other organs/cell types (*e.g.*, heart, endocrine cells, intestine interstitial cells of Cajal, myometrial smooth muscle cells) and takes part in numerous physiological functions (**TABLE 3**). Therefore, diseases can lead to a broad spectrum of clinical manifestations. In general, *NALCN*/*UNC-80*-related disorders can be described as a static encephalopathy usually detected since the first months of life, leading to a severe global developmental delay and intellectual disability, in association with hypotonia, failure to thrive, dysmorphic facial features, and distal arthrogryposis in CLIFAHDD syndrome, as the main clinical characteristics. Also, there are several other prominent manifestations reported in the literature, including central apneas and periodic breathing, epilepsy, hyperkinetic movement disorders, ataxia, sleep disturbances and constipation. All clinical manifestations are summarized in **TABLE 7** and **TABLE 9**.

TABLE 7: Symptoms in patients with the IHPRF1 & 2 syndromes

System reviewed	Clinical description	Reference
Perinatal problems	- Intra-uterine growth retardation - Oligohydramnios - Need for hospitalization at birth	Al-Sayed et *al*, 2013 (223) Pérez et *al*, 2016 (237) Valkanas et *al*, 2016 (239) Takenouchi et *al*, 2018 (226) Bramswig et *al*, 2018 (229) Bourque et *al*, 2018 (228) Campbell et *al*, 2018 (236) Ope et *al*, 2020 (231)
Growth, feeding difficulties and gastrointestinal disturbances	- Poor sucking after birth - Feeding difficulties (not characterized) - Severe failure to thrive - Need for feeding tube - Severe constipation	All authors reported feeding difficulties or failure to thrive. See tables 5 and 6 for the complete list of references.
Dysmorphic facial features	- Frontal bossing - Secondary microcephaly - Triangular face - Convergent strabismus - Large, low set, posteriorly rotated ears - Mouth persistently opened, wide mouth - Thin and/or tented upper lip - Short and/or smooth philtrum - Hypotonic facies, only mild dysmorphism	All authors reported some dysmorphic facial features. See tables 5 and 6 for the complete list of references.

Musculoskeletal features	- Long thin fingers - Tapering of distal phalanx - Scoliosis - Small hands and/or feet - Joint hypermobility/lax joints - Joint contractures, developing progressively	Koroglu et *al*, 2013 (221) Pérez et *al*, 2016 (237) Stray-Pedersen et *al*, 2016 (93) Valkanas et *al*, 2016 (239) Takenouchi et *al*, 2018 (226) Bramswig et *al*, 2018 (229) Campbell et *al*, 2018 (236) Obeid et *al*, 2018 (240) Karimi et *al*, 2020 (232)
Developmental milestones, cognitive functioning, psychiatric disturbances	- Absence of speech development - Severe persistent hypotonia after birth: most cannot sit or walk - Severe intellectual disability - Autistic features - Irritability/self-injury behaviors - Sociable, happy disposition	All authors reported developmental delay. See tables 5 and 6 for the complete list of references.
Other neurological disturbances	- Seizures, usually non-refractory when reported (interpret with caution) - Dystonic posture of limbs - Dyskinesias, mainly in upper limbs - Choreoathetoid movements - Stereotypic movements	Al-Sayed et *al*, 2013 (223) Koroglu et *al*, 2013 (221) Pérez et *al*, 2016 (237) Stray-Pedersen et *al*, 2016 (93) Valkanas et *al*, 2016 (239) Gal et *al*, 2016 (225) Bramswig et *al*, 2018 (229) Obeid et *al*, 2018 (240) Angius et *al*, 2018 (227) Bourque et *al*, 2018 (228) Hong et *al*, 2018 (242) Kuptanon et *al*, 2019 (243) Khan et *al*, 2022 (233) Maselli et *al*, 2022 (234) Kelesoglu et *al*, 2023 (246)
Respiratory disturbances	- Central sleep apneas - Periodic breathing with frequent central apneas	Stray-Pedersen et *al*, 2016 (93) Gal et *al*, 2016 (225) Bramswig et *al*, 2018 (229) Campbell et *al*, 2018 (236) Bourque et *al*, 2018 (228) Hong et *al*, 2018 (242) Karimi et *al*, 2020 (232) Maselli et *al*, 2022 (234)
Sleep disturbances	- Light sleep - Complete reversion of sleep-wake cycle - Periodic limb movements during sleep - Sleep disturbances not characterized	Stray-Pedersen et *al*, 2016 (93) Takenouchi et *al*, 2018 (226) Campbell et *al*, 2018 (236) Bramswig et *al*, 2018 (229) Kuptanon et *al*, 2019 (243) Maselli et *al*, 2022 (234)
Other	- Increased tendency to infections - Small atrial defect in echocardiography - Recurrent increases of TSH - Hypothyroidism	Stray-Pedersen et *al*, 2016 (93) Shamseldin et *al*, 2016 (238) Takenouchi et *al*, 2018 (226) Bramswig et *al*, 2018 (229) Stenehjen et *al*, 2019 (244) Karimi et *al*, 2020 (232)

Patient characteristics are summarized in **TABLES 5**, **6** and **8**. Sex distribution seems to be very similar among the three syndromes, while the age at last evaluation is highly variable. Early death is reported in 5 cases of IHPRF1 and in 6 cases of CLIFAHDD, with the causes attributed to respiratory failure after pneumonia or sepsis in three cases (one

associated with a status epilepticus), and withdrawal of life supporting measures in one severe case of CLIFAHDD. Byrne et *al*, 2023 also found a heterozygous variant in *NALCN* in a case of fetal/newborn death (259).

Most patients are born full term after an uneventful pregnancy. Oligohydramnios, polyhydramnios, and intrauterine growth retardation are reported in IHPRF1, IHPRF2 and CLIFAHDD patients, respectively. Birth weight, height, and head circumference are within the norm in almost all cases. The need for a prolonged hospital stay after birth is not consistently reported, but some cases required hospitalization and respiratory support, usually after an emergency C-section for fetal distress (134, 207, 223, 228, 229, 231, 236, 249, 252).

Failure to thrive

Failure to thrive is one of the most striking features in IHPRF1 and 2 syndromes, even despite adequate caloric intake provided by gastrostomy (225). This particular study suggested a role for *NALCN* in metabolic pathways involved in the pathogenesis of cachexia, as this is a common manifestation of pancreatic tumors, where mutations in *NALCN* are found (**TABLE 10**)(262). Feeding difficulties and poor sucking after birth are also very commonly reported, which mirrors observations made in *Unc-79* knockout mice (137). In some cases (5 patients with IHPRF1, 7 patients with IHPRF2 and 5 patients with CLIFAHDD), a feeding tube was necessary for adequate nutrition. The origin of these feeding difficulties remains unknown, and while endocrine function is described as normal in some cases, exocrine function has not been documented in the majority of patients with *NALCN*/*UNC-80*-related disorders, leaving a possible explanation to date unexplored.

TABLE 8: Genetics of the CLIFAHDD syndrome

Mutation	Location	Gender (Older Age Reported)	Reference
c.191A>G p.Y64C	Domain IS1	NI	Pergande et *al*, 2020 (260)
c.530A>C p.Q177P*	Domain IS5	Death at 6 months	Chong et *al*, 2015 (247)
c.934C>A p.L312I*	Domain IS6	NI	Chong et *al*, 2015 (247)
c.934C>G p.L312V*	Domain IS6	Female (4.6 yo)	Fukai et *al*, 2016 (248)
c.938T>G p.V313G*	Domain IS6	Death at 6 years	Chong et *al*, 2015 (247)
c.950T>G p.F317C*	Domain IS6	Female (Death at 9 mo)	Karakaya et *al*, 2016 (249) Pergande et *al*, 2020 (260)
c.956C>T p.A319V*	Domain IS6	Female (3 yo)	Lozic et *al*, 2016 (207)
C.965T>C p.I322T	Domain IS6	Male (3 yo)	Sivaraman et *al*, 2016 (250)
c.979G>A p.E327K*	Domain IS6	NI	Chong et *al*, 2015 (247)
c.985A>G p.R329G	DI-DII loop	NI	Stark et *al*, 2016 (261)

c.1526T>C p.L509S*	Domain IIS5	NI	Chong et *al*, 2015 (247)
c.1534T>G p.F512V*	Domain IIS5	NI	Chong et *al*, 2015 (247)
c.1538C>A p.T513N*	Domain IIS5	NI	Chong et *al*, 2015 (247)
c.1571G>A p.S524N*	Domain IIS5	Male (Death at 10 mo)	Angius et *al*, 2019 (251)
c.1640T>C p.M547T	Domain II P loop	Male (3 yo)	Kumaki et *al*, 2022 (252)
c.1733A>C p.Y578S*	Domain IIS6	NI	Chong et *al*, 2015 (247)
c.1733A >G p.Y578C*	Domain IIS6	Male (17 yo) Female (33 mo)	Vivero et *al*, 2017 (253) Vivero et *al*, 2017 (253)
c.1745A>C p.Y582S*	Domain IIS6	Male (9 mo)	Vivero et *al*, 2017 (253)
c.1768C>T p.L590F*	Domain IIS6	Death at 4 months Female (NI)	Chong et *al*, 2015 (247) Bend et *al*, 2016 (134)
c.1783G>T p.V595F*	Domain IIS6	Female (Death at 3 mo)	Karakaya et *al*, 2016 (249) Pergande et *al*, 2020 (260)
c.1789G > A p.V597I*	Domain IIS6	Female (33 yo)	Wang et *al*, 2016 (254)
c.1800C>A p.D600E*	Domain IIS6	Female (Death at 3.5 mo)	Angius et *al*, 2019 (251)
c.1870G > C p.E603Q	Domain IIS6	Male (2 yo)	Winczewska-Wiktor et *al*, 2022 (255)
c.3017T>C p.V1006A*	Domain III ECL 4-5	NI	Chong et *al*, 2015 (247)
c.3050T>C p.I1017T*	Domain IIIS5	NI	Chong et *al*, 2015 (247)
c.3058G4T p.V1020F*	Domain IIIS5	Female (15 mo)	Fukai et *al*, 2016 (248)
c.3448C >G p.L1150V	Domain IIIS6	Female (13 yo)	Vivero et *al*, 2017 (253)
c.3493A>C p.T1165P*	DIII-DIV loop	NI	Chong et *al*, 2015 (247)
c.3542G>A p.R1181Q*	DIII-DIV loop	NI Female (7.5 yo) Female (5 yo)	Chong et *al*, 2015 (247) Aoyagi et *al*, 2015 (256) Fukai et *al*, 2016 (248)
c.3553G>A p.A1185T	DIII-DIV loop	NI	Vissers et *al*, 2017 (257)
c.4205C>T p.L1324F	Domain IVS4	fetal or newborn death	Byrne et *al*, 2023 (259)
c.4300A>G p.I1434V	Domain IVS6	Male (3 yo)	Liao et *al*, 2022 (258)
c.4333A>T p.I1445L	Domain IVS6	Male (Death at 4 mo)	Bramswig et *al*, 2018 (229)
c.4338T>G* p.I1446M	Domain IVS6	NI	Chong et *al*, 2015 (247)

2294 *** Functionally expressed in recombinant system, gain-of-function. Abbreviation: NI, not indicated**

Dysmorphic features

Almost all patients have some dysmorphic facial features, which seem to be different between IHPRF1/2 and CLIFAHDD patients. Most common facial features reported for each syndrome are summarized in **TABLES 7** and **9**, but a variety of other features are also described, such as down slanting palpebral fissures, fine hair, palpebral ptosis, retrognathia or a high nasal bridge. Some individuals are just described as having hypotonic facies with mild dysmorphism. Plagiocephaly and dolichocephaly are reported in some cases of IHPRF1 and 2. Interestingly, postnatal microcephaly is common in IHPRF1 and 2, whereas only five cases of CLIFAHDD documented this (248, 253).

Distal arthrogryposis is a distinctive feature of CLIFAHDD syndrome, with camptodactyly, ulnar deviation of wrist and/or fingers and clubfoot also reported in most patients. Also, about half of the authors reported joint contractures in hips, knees or elbows. In contrast, none of the cases of IHPRF1/2 have been diagnosed with arthrogryposis, though there were a few cases of clubfoot and joint contractures in IHPRF2 patients (237).

Developmental delay, intellectual disability and behavioral manifestations

All cases, regardless of the mutation, reported global developmental delay and intellectual disability when this information was available. These are described as severe in almost all cases of IHPRF1 and 2, with most patients being non-verbal and non-ambulatory. Data for CLIFAHDD is more inconsistent in this regard. Nevertheless, a high number of patients did not develop speech, but showed more variability in gross motor milestones.

Behavioral problems are not always described, which constitutes a clear bias. Most cases of CLIFAHDD do not provide sufficient information. Autistic features, irritability and hypersensitivity to stimuli are reported mostly in IHPRF2 patients. Self-injury behaviors are also reported (229, 239, 241), while other patients are described as being sociable and having a happy disposition (93, 240, 241, 243, 246).

TABLE 9: Symptoms for the CLIFAHDD syndrome

System reviewed	Clinical description	Reference
Perinatal problems	- Polyhydramnios - Oligohydramnios - Clubfoot detected before birth - Need for hospitalization at birth - Fetal or newborn death	Karakaya et *al*, 2016 (249) Bend et *al*, 2016 (134) Sivaraman et *al*, 2016 (250) Vivero et *al*, 2017 (253) Pergande et *al,* 2020 (260) Kumaki et *al*, 2022 (252) Winczewska-Wiktor et *al*, 2022 (255) Liao et *al*, 2022 (258) Byrne et *al*, 2023 (259)
Growth, feeding difficulties and gastrointestinal disturbances	- Poor sucking after birth - Feeding difficulties (not characterized) - Failure to thrive - Need for feeding tube - Gastroesophageal reflux disease - Severe constipation	Chong et *al*, 2015 (247) Fukai et *al*, 2016 (248) Bend et *al*, 2016 (134) Lozic et *al*, 2016 (207) Vivero et *al*, 2017 (253) Bramswig et *al*, 2018 (229) Kumaki et *al*, 2022 (252)

		Winczewska-Wiktor et *al*, 2022 (255)
Dysmorphic facial features	- Divergent strabismus - Broad nasal bridge - Anteverted nasal tip, large nares - Short and/or long philtrum - Short columella - Micrognatia - Pursed lips, small mouth - Full cheeks, deep nasolabial folds - H-shaped dimpled chin	All authors reported some dysmorphic facial features. See table 8 for the complete list of references.
Musculoskeletal features	- Distal arthrogryposis - Camptodactyly - Ulnar deviation of wrist and/or fingers - Clubfoot - Calcaneovalgus deformity - Joint contractures (hips, knees, elbows) - Short neck	All authors reported arthrogryposis. See table 8 for the complete list of references.
Developmental milestones, cognitive functioning, psychiatric disturbances	- All authors reported developmental delay and intellectual disability, but data regarding severity is inconsistent; usually severe when reported. - Hyperactivity	All authors. See table 8 for the complete list of references.
Other neurological disturbances	- Seizures - Episodic ataxia - Slurred speech and gait ataxia - Stereotypic movements	Chong et *al*, 2015 (247) Aoyagi et *al*, 2015 (256) Fukai et *al*, 2016 (248) Wang et *al*, 2016 (254) Vivero et *al*, 2017 (253) Bramswig et *al*, 2018 (229)
Respiratory disturbances	- Central sleep apneas - Periodic breathing with frequent central apneas - Respiratory insufficiency	Chong et *al*, 2015 (247) Bend et *al*, 2016 (134) Lozic et *al*, 2016 (207) Stark et *al,* 2016 (261) Vivero et *al*, 2017 (253) Pergande et *al*, 2020 (260) Kumaki et *al*, 2022 (252) Winczewska-Wiktor et *al*, 2022 (255)
Sleep disturbances	- Complete reversion of sleep-wake cycle	Lozic et *al*, 2016 (207)
Other	- Inguinal hernia - Increased tendency to infections - Small ventricular or atrial defect in echocardiography - Patent foramen ovale - Bilateral hydronephrosis - Episodes of severe dysautonomia - Excessive drooling	Chong et *al*, 2015 (247) Aoyagi et *al*, 2015 (256) Karakaya et *al*, 2016 (249) Lozic et *al*, 2016 (207) Bend et *al*, 2016 (134) Vivero et *al*, 2017 (253) Pergande et *al*, 2020 (260) Winczewska-Wiktor et *al*, 2022 (255) Liao et *al*, 2022 (258)
Sensitivity to volatile anesthetics	- Sevoflurane sensitivity caused respiratory depression and cardiac arrest	Lozic et *al*, 2016 (207)

Epilepsy and movement disorders

The NALCN channelosome regulates the RMP of neurons and their excitability, leading to the possibility of excitability disorders in NALCN syndromes, including epilepsy. Almost all authors reported presence/absence of seizures, which are more common in IHPRF1 and 2 syndromes, affecting approximately half of the patients. Age of onset is very variable, ranging from the first months of life up to 13-year-old in IHPRF1, and up to 5-year-old in IHPRF2. Most cases present with bilateral tonic-clonic seizures, but authors also describe behavioral arrest, tonic, atonic and myoclonic seizures. Electroencephalogram (EEG) recordings could be simply reported as abnormal, or as showing generalized slowing, generalized spike and wave epileptiform activity, or, in some cases, multifocal epileptiform discharges.

Only 5 IHPRF patients are reported to have refractory epilepsy, out of a total of 32, although this is highly dependent on the moment of publication and can have changed over time; furthermore, in 10 cases this information is not available. Kelesoglu et *al* 2023 reported a case with only febrile seizures at 7 months (246). Antiseizure medications do not seem to be selected specifically with *NALCN*/*UNC-80* mutations in mind, as they are those commonly used for a broad spectrum of epilepsies: valproic acid, levetiracetam, lamotrigine and phenobarbital, either in monotherapy or in combination. Also, Ope et *al*, 2020, reported good seizure control with carbamazepine in one patient (231), while Gal et *al*, 2016, reported two cases treated with vigabatrin (225), one of whom died after a status epilepticus complicated with sepsis and respiratory failure. Ketogenic diet was successful in one case reported by Bramswig et *al*, 2018, but had no effect in the case of IHPRF2 reported by Hong et *al*, 2018 (229, 242).

Epilepsy is reported in five cases of CLIFAHDD, but there is insufficient data to document the type of seizures or response to treatment (247, 253).

Persistent hypotonia after birth is the main motor manifestation in all cases, and only a few authors report spastic paraparesis or hypertonia in upper or lower limbs (221, 229, 238, 249, 253, 260). NALCN is also expressed in the basal ganglia, which could lead to the appearance of movement disorders (263). In this regard, several patients with IHPRF1 and 2 syndromes present with hyperkinetic disorders, such as choreoathetoid movements of limbs, dyskinesia, dystonia and stereotypes, although a specific description is usually lacking (**TABLE 7**). Magnetic Resonance Imaging (MRI) is reported as normal in approximately half of the patients with IHPRF1 and 2 syndromes, but Bramswig et *al*, 2018, and Pérez et *al*, 2015, reported the finding of a thin corpus callosum in some patients, as did Karayaka et *al*, 2016, and Vivero et *al*, 2017, in three cases with CLIFAHDD (229, 237, 249, 253). As for CLIFAHDD, some authors describe a cerebellar syndrome with gait ataxia and slurred speech, which present as episodic ataxia in a case described by Aoyagi et *al*, 2015, but developed progressively during young adulthood in the patients reported by Wang et *al*, 2016, and Bramswig et *al*, 2018 (229, 254, 256). Interestingly, cerebellar atrophy is observed in the MRI of 11 CLIFAHDD patients (229, 247, 248, 252-254, 256). In addition, Aoyagi et *al*, 2015 and Kumaki et *al*, 2022, also documented a previous normal MRI, further suggesting that cerebellar involvement may develop progressively (252, 256).

Respiratory and sleep disturbances

Chong et *al*, 2015, reported several cases of respiratory insufficiency in their series of 14 patients with CLIFAHDD, but did not characterize the dysfunction (247). Since then, respiratory disturbances are reported more frequently, mostly in IHPRF1 and CLIFAHDD, and are characterized as periodic breathing patterns with frequent central apneas (228, 236, 242, 260, 261). This periodic breathing in human patients is reminiscent to the pattern described in animal models. Indeed, Lu et *al*, 2007 showed pathological breathing patterns characterized by several seconds of apnea followed by short episodes of deep breaths in a knockout model of *Nalcn* in mice, which was predictive of death in the first 24h of life (2). Treatment of the reported cases is based on oxygen supplementation at night, associated or not with positive airway pressure therapy. A tracheostomy is necessary in severe cases (134, 207, 252, 253). Hong et *al*, 2018, documented complete resolution of apneas after instauration of bilevel positive airway pressure (BPAP) in a patient with IHPRF2 (242). Winczewska-Wiktor et *al*, 2022, reported a case of CLIFAHDD with severe central apneas in which a myasthenic syndrome was suspected before the definitive diagnosis, which improved after empirical treatment with pyridostigmine bromide (255). However, continuous positive airway pressure (CPAP) and oxygen supplementation were used at the same time, which could have contributed to the clinical improvement.

In agreement with a role for the NALCN channelosome in regulating sleep, Lozic et *al*, 2016, Stray-Pedersen et *al*, 2016, Takenouchi et *al*, 2018, and Campbell et *al*, 2018, described a complete reversion in sleep-wake cycle in at least one patient for each one of the three syndromes (93, 207, 226, 236). Other authors also reported sleep disturbances, which seem to be common in these syndromes, but most did not characterize them. Maselli et *al*, 2022, noted a high index of periodic limb movements index in a case with IHPRF1 syndrome, in association with iron-deficiency anemia. This index remained high despite dietary treatment and improvement of sleep efficiency after initiation of BPAP, hypothesizing a possible genetic association (234).

Constipation, dysautonomia and other manifestations

NALCN is expressed in the interstitial cells of Cajal in the gastrointestinal tract, mediating the pacemaking of gastrointestinal functions (78). Almost all individuals with IHPRF1 and 2 syndromes are reported to have constipation. This is less frequently described in individuals with CLIFAHDD, but in these patients, there is a larger proportion of gastroesophageal reflux disease, which could lead to frequent vomiting in severe cases. These findings suggest that there may be different patterns of involvement of interstitial cells of Cajal in the upper and lower intestine, depending on whether the mutation results in a loss- or gain-of-function. However, this should be interpreted with caution, as there are authors who do not report the presence of these symptoms, so it could correspond to a reporting bias. In a similar line, some authors reported patients with excessive drooling, mainly in CLIFAHDD syndrome (207, 232, 247, 255). Other authors reported frequent aspiration pneumonias or an inability to clear airway secretions (229, 244, 253), which suggests that excessive drooling might be more common, but it could be easily overlooked and thus underreported. Although sialorrhea could be a consequence of swallowing difficulties. NALCN is expressed in several glands (1, 56), but a possible role in the regulation of salivary secretions is yet to be explored.

NALCN is also expressed in the dorsal motor nucleus of the vagus, linking it to autonomic control (264). However, are not taken into account respiratory, sleep, and gastrointestinal disturbances, only a few authors have reported other forms of dysautonomia. Karayaka et *al*, 2016, and Bend et *al*, 2016, reported two CLIFAHDD patients with severe episodes of apnea, hyperthermia, tachycardia (249), or bradycardia and hypertension (134). Frequent life-threatening episodes led to intubation in the case reported by Bend et *al*, 2016, but the patient worsened over time and life support was eventually withdrawn (134).

Lastly, it is noteworthy that cardiac and endocrine functioning are reported as normal in the majority of cases in which this information is available, however there are no systematic studies addressing the possibility of subclinical cardiac and endocrine involvement, which linked to the inability of these patients to communicate, rises the possibility of overlooking mild or evolving cardiac and endocrine pathology. Possible disturbances in other systems, like kidney or urological functioning, are not significantly reported, so there is insufficient information in this regard.

4- Therapies in the IHPRF and CLIFAHDD syndromes

With the exception of the study mentioned above reporting a beneficial effect of a treatment with pyridostigmine bromide on severe central apneas observed in a CLIFAHDD patient (255), there are no efficient therapies for treating patients identified to date. However, the development of animal and cell models have paved the way for identifying pharmacological and gene therapy approaches. For example, the ability to functionally express the NALCN channelosome in recombinant systems such as *Xenopus* oocytes and HEK-293T cells led to the identification of molecules with inhibitory properties (2, 27, 89). One may hypothesize NALCN blockers could be used to treat patients with the gain-of-function CLIFAHDD syndrome. However, the currently known compounds (*i.e.*, 2-APB, Lamotrigine, Verapamil, and N-benzhydryl quinuclidine compounds) are low-affinity and non-specific NALCN blockers. It remains necessary to identify more specific NALCN channelosome blockers that could be of clinical relevance to treat patients with CLIFAHDD mutations. Both invertebrate (*i.e.*, *C. elegans* and *D. melanogaster*) and vertebrate (*i.e.*, *M. musculus*) animal models are now available (**TABLE 10**). This includes loss- and gain-of-function alleles that may reasonably be considered as relevant to investigate novel therapeutics for the IHPRF and CLIFAHDD syndromes respectively. In keeping with this idea, a targeted drug screening aiming to identify drugs that correct locomotion deficits in a *C. elegans* gain-of-function *nca-1* mutant (*i.e.*, a CLIFAHDD model) (100) identified 2-ABP, nifedipine, nimodipine, flunarizine, and ethoxzolamide as significantly rescuers of abnormal movements in mutant animals. Whether these compounds are able to rescue the altered sleep phenotype observed in the *Dreamless* mouse, a gain-of-function (CLIFAHDD) mouse model (69), remains to be investigated. Conversely, drugs that block K^+ channels (*e.g.*, 4-AP, Quinine, Quinidine, loratadine) and gap junctions (*i.e.*, CBNX) significantly improve movement of *C. elegans* loss-of-function mutants for *nca-1:nca-2*, (*i.e.*, a IHPRF1 model), *unc-80* (*i.e.*, a IHPRF2 model) and *unc-79* (265). The relevance of these compounds to rescue phenotypes observed in loss-of-function (IHPRF1/2) mouse models needs to be explored. Taken together, these data provide proof-of-principle that it is possible to pharmacologically modify NALCN function *in vivo* in order to correct (at least partially) phenotypes induced by functional deficiencies of the channel.

TABLE 10: Animal models to study NALCN channelosome-related diseases

Specie	Genetic change	Functional effect (Disease)	References
M. musculus	Knockout of *Nalcn*	Loss-of-function (IHPRF1)	Lu et *al*, 2007 (2)
M. musculus	Conditional Knockout of *Nalcn*	Loss-of-function	Flourakis et *al*, 2015 (38) Philippart & Khaliq, 2018 (72) Zhang et *al*, 2021 (61) Do et al, 2020 (73)
M. musculus	Knockout of *Unc-79*	Loss-of-function (IHPRF ?)*	Nakayama et *al*, 2006 (137)
M. musculus	Hypomorphic mutation (*Unc-79*)	Loss-of-function (IHPRF ?)*	Speca et *al*, 2010 (47)
M. musculus	Knockout of *Unc-80*	Loss-of-function (IHPRF2)	Wie et *al*, 2020 (49)
M. musculus	p.N315K	Gain-of-function (CLIFAHDD)	Funato et *al*, 2016 (69)
C. elegans	*nca-1;nca-2* (Random mutagenesis)	Loss-of function (IHPRF1)	Jospin et *al*, 2007 (32)
C. elegans	*unc-79*	Loss-of-function (IHPRF ?)*	Sedensky & Meneely, 1987 (129)
C. elegans	*unc-80*	Loss-of-function (IHPRF2)	Sedensky & Meneely, 1987 (129)
C. elegans	p.R403Q (NCA-1) p.A717V (NCA-1) (Random mutagenesis)	Gain-of-function (CLIFAHDD)	Yeh et *al*, 2008 (34)
C. elegans	Transgenesis with p.R1230Q (p.R1181Q in human)	Gain-of-function (CLIFAHDD)	Aoyagi et *al*, 2015 (256)
C. elegans	p.V359G (p.V313G) p.Y625S (p.Y578S) p.E373K (p.E327K) p.T560N (T513N) p.F559V (p.F512V) p.L556S (p.L509S) p.L637F (p.L590F) p.D647E (p.D600E) p.A643V (p.A596V) (knockin with CRISPR/Cas9)	Gain-of-function** Gain-of-function** Gain-of-function** Gain-of-function Gain-of-function Gain-of-function Gain-of-function Gain-of-function Gain-of-function (CLIFAHDD)	Bend et *al*, 2016 (134)
D. melanogaster	*na*	Loss-of function (IHPRF1)	Krishnan & Nash, 1990 (132)
D. melanogaster	*unc-79*	Loss-of function (IHPRF ?)*	Humphrey et *al*, 2007 (33)

***Given the requirement of *UNC-79* in the NALCN channelosome function, loss-of-function animal models may be relevant as IHPRF models. **First described as loss-of-function based on locomotor phenotype.**

Gene therapy approaches may also be relevant to treat patients with the IHPRF1/2 and CLIFAHDD syndromes. In this context, genome editing techniques combined with the use of viral vectors may be used to correct mutations found in patients *in vivo* (266). In the case of the CLIFAHDD syndrome, it is also conceivable to use *in vivo* AAV-based RNA interference strategies to partially reduce *NALCN* expression to restore NALCN current levels toward more physiological ranges. The development of such treatment strategies will require mouse models and other technologies such as brain organoids to provide proof-of-concept. In the context of NALCN loss-of-function, a study suggested that NALCN

and TRPC3 maybe interchangeable in neurons opening possibilities for compensatory therapy by promoting or enhancing TRPC3 function (82). Specifically, midbrain dopaminergic (DA) neurons are slow pacemakers that maintain extracellular DA level, in which both TRPC3 and NALCN contribute equally to slow depolarization. However, in TRPC3 knockout mice, the lack of TRPC3 is compensated by NALCN through a transcription-dependent mechanism that remains uncharacterized. Perhaps, it would be possible to rescue the *in vivo* the loss-of-function of NALCN by expressing TRPC3 under the control of the NALCN promoter using an AAV-based approach.

5- Syndromes linked to heterozygous variants of UNC-79 and NALCN

A recent study reported 6 unrelated patients with heterozygous *de novo* truncating and presumed loss-of-function mutations in *UNC-79* responsible for a panel of severe neurological symptoms with a patient-dependent variability (48). This includes mild developmental delay affecting both motor and verbal skills, hypotonia, autistic features and epileptic seizures. Of note, the phenotypes described for UNC79 variants seem milder than those of IHPRF1 and 2, as all patients are ambulatory, and all but one case could communicate using words or short sentences. Autistic features, attention deficit and irritability are common, and epilepsy is described as one of the main prominent symptoms, but otherwise patients did not exhibit growth failure, gastrointestinal or major dysmorphic features. The seizure-like phenotype is recapitulated in *D. melanogaster* by knocking down *unc-79* expression both globally and specifically in neurons. In addition, *Unc-79* haploinsufficiency in mouse leads to deficiency in hippocampal-dependent learning and memory. In keeping with the idea that haploinsufficiency of the NALCN channelosome components may induce a disease state, another study reported 2 patients, a father and son, presenting with focal epilepsy. One of them exhibits a discrete atrophy of the left temporal lobe including the left hippocampus. A genetic panel performed in both patients showed an heterozygous deletion in *NALCN* that includes the exon #27 (267). This exon encodes for most of the IIIS5 transmembrane segment and its deletion is predicted to result in a loss-of-function phenotype. Curiously, epileptic seizures are not described in relatives of IHPRF1 and IHPRF2 patients with heterozygous predicted loss-of-function mutations in *NALCN* and *UNC-80* respectively. Indeed, these relatives are apparently healthy and are not described as having epilepsy.

6- Other diseases

In addition to rare genetic diseases, the NALCN channelosome components are implicated in other human diseases (**Table 11**). This chapter reviews several other human conditions in which the NALCN channelosome may be involved.

Psychiatric disorders

Psychiatric disorders differ from most of the other medical conditions in their intrinsic multifactorial etiology in which both genetic and experiential factors contribute to their development (268). Considering the crucial role of *NALCN* in regulating neuronal excitability, its association with psychiatric disorders is not surprising. Several association studies highlighted a possible role of *NALCN* in schizophrenia and/or bipolar disorders (269-274). However, a lack of association of *NALCN* with schizophrenia is also reported (275, 276). *NALCN* is also described as a potential susceptibility locus for

alcoholism (277, 278). Supporting a role of the NALCN channelosome in alcoholic addiction, another study revealed a possible association of *UNC-79* with alcohol and nicotine dependence (279). Of note, a region of chromosome 2 that includes *UNC-80* is also found to be involved in alcoholic addition (280, 281). This is consistent with the ethanol hypersensitivity of *C. elegans* specimens bearing null alleles for the NALCN channelosome (47, 150, 157). Furthermore, and as noted above, *Nalcn* in NAc may contribute to the ethanol-induced acute stimulant responses and locomotor sensitization in mouse, given that Lwt/+ (Unc-79 loss-of-function) mice exhibit an increase in both sensitivity to the acute sedative effects of ethanol, and in their appetitive for consumption of ethanol (47, 156).

UNC-79, *UNC-80* and NLF-1/FAM155A have also been implicated in autism (282-284), while other studies have reported a chromosome 2 region that includes *UNC-80* which is involved in autism (285-287). A role of the NALCN channelosome in autism is supported by autistic features seen in patients suffering with CLIFAHDD and IHPRF syndromes (*see above*). Decreased expression of *UNC-80* is reported in the context of the neonatal opioid withdrawal syndrome (288). Children who develop this syndrome are at increased risk of attention-related disorders, lower IQ, and poorer performance in academic testing compared to their unexposed counterparts (289). A correlation between *Nalcn* and depression is reported in a mouse model (63). Indeed, reduced expression of *Nalcn* and subsequent alterations in electrical activity are observed in glutamatergic neurons of the ventral dentate gyrus in an inflammation-induced depression mouse model. Moreover, the overexpression of *Nalcn* in these neurons decreases the susceptibility of mice to inflammation-induced depression. *FAM155A*, *UNC-80* and *NALCN-AS1* are also putative susceptibility loci for anorexia nervosa, anxiety and attention-deficit hyperactivity disorder respectively (290-292), and Lwt/+ mice also exhibit a hyperactive phenotype (47).

TABLE 11: The NALCN channelosome in other diseases

Disease	gene	Study Type	Reference
Schizophrenia/Bipolar disorders			
Bipolar Disorder	*NALCN*	GWAS	Baum et *al*, 2008a,b (269, 270)
Schizophrenia	*NALCN*	PBA/GWAS	Askland et *al*, 2009 (271)
Bipolar Disorder	*NALCN*	GWAS	Ollila et al, 2009 (272)
Bipolar Disorder + Schizophrenia	*NALCN*	GWAS	Wang et *al*, 2010 (273)
Schizophrenia	*NALCN*	CCS	Zhang et *al*, 2018 (274)
Anorexia Nervosa	*NLF-1/FAM155A*	GWAS	Wang et *al*, 2011 (290)
Addiction	*UNC-80 ?**	AS	Schuckit et *al*, 2001 (280)
	*UNC-80 ?**	AS	Nurnberger et *al*, 2001(281)
	UNC-79	GWAS	Lind et *al*, 2010 (279)
	NALCN	GWAS	Wetherill et *al*, 2014 (277)
	NALCN	CCS	Baronas et *al*, 2018 (278)
Attention-Deficit Hyperactivity Disorder	*NLF-1/FAM155A ?**	FBAT	Anney et *al*, 2008 (293)
	NALCN-AS1	CCS	Kweon et *al*, 2018 (291)
Anxiety	*UNC-80*	GWAS	Chu et *al*, 2021 (292)

Autism	*UNC-80 ?**	microdeletion	Brandau et *al*, 2008 (285)
	*UNC-80 ?**	microdeletion	Rosenfeld et *al*, 2010 (286)
	UNC-80	WES (nonsense mut)	Iossifov et *al*, 2012 (282)
	*UNC-80 ?**	Microdeletion	Jang et *al*, 2015 (287)
	UNC-79	WES (DNV)	Krupp et *al*, 2017 (283)
	NLF-1/FAM155A	ELISA from plasma (Down)	Al-Mazidi et *al*, 2023 (284)
Neonatal opioid withdrawal syndrome	*UNC-80*	CNV (Decrease)	Radhakrishna et *al*, 2021 (288)
Depression	*Nalcn*	Mouse model	Wang et *al*, 2023 (63)
Alzheimer Disease	*UNC-80 ?**	LA	Scott et *al*, 2003 (294)
	*UNC-79 ?**	WGAS	Grupe et *al*, 2007 (295)
	*UNC-79 ?**	LA	Lee et *al*, 2008 (296)
	UNC-80	Differential editing level in hippocampus from patients	Khermesh et *al*, 2016 (297)
	NALCN	WGAS	Prokopenko et *al*, 2021 (298)
Ataxia/Dystonia	*UNC-80*	CNV (Decrease)	Canet-Pons et *al*, 2021 (299)
Cervical dystonia	*NALCN*	GWAS	Mok et *al*, 2014 (300)
Parkinson disease	*NALCN*	*AS*	Yang et *al*, 2021 (301)
Epilepsy	*NALCN*	Change in alternative splicing in brain tissues from patients with mTLE	Heinzen et *al,* 2007 (302)
	*UNC-80?**	LA	Ratnapriya et *al*, 2010 (303)
	*UNC-80?**	LA	Epicure Consortium et *al*, 2012 (304)
	UNC-80	WES (point mutation)	Yang et *al*, 2017 (305)
	UNC-80	Microdeletion	Westphal et *al*, 2018 (306)
Restless legs syndrome	*NALCN*, *NALCN-AS1*	AS	Balaban et *al*, 2012 (307)
Polyglutamine disorders	*NLF-1/FAM155A*?	Genome analysis	Whan et *al*, 2010 (308)
Cancer			
Gastric, Instestinal, pancreatic adenocarcinomas	*Nalcn*	Knockout in mouse models	Rahrmann et *al*, 2022 (309)
Prostate cancer	*NALCN*	knockdown/overexpression	Folcher et *al*, 2023 (310)
Tumor-derived endothelial cells	*NLF-1/FAM155A*	Exome Sequencing (Mut)	McGuire et *al*, 2012 (311)
Pancreatic cancer	*NALCN*	CNV (Down)	Biankin et *al*, 2012 (262)
	UNC-80	CNV (Down)	Hu et al, 2017 (312)
Non-Small Cell lung cancer	*NALCN*	GWAS	Lee et *al*, 2013 (313)
Non-Small Cell lung cancer with brain metastasis	*UNC-79*	CNV (Gain)	Kim et *al*, 2023 (102)
Lung adenocarcicoma	*NALCN*	CNV (Down)	He et *al*, 2023 (314)
Lung squamous cell carcinoma	*NALCN*	CNV (Down)	He et *al*, 2023 (314)

Ewing Sarcoma	*UNC-80*	Deep Sequencing (Mut)	Agelopoulos et *al*, 2015 (315)
Hepatocellular Carcinoma	*UNC-79*	WES (Mut)	Zhan et *al*, 2017 (316)
	NALCN	CNV (Down)	Chen et *al*, 2018 (317)
	NALCN	CNV (Down)	He et *al*, 2023 (314)
Neuroblastoma	*NALCN, UNC-79*	WES (Mut)	Esposito et *al*, 2018 (318)
Clear Cell Renal Cell Carcinoma	*NALCN-AS1*	CNV (Gain)	Wang et *al*, 2018 (319)
	NLF-1/FAM155A	GWM (hypermethylated)	Kang et *al*, 2019 (320)
	NALCN	CNV (Down)	He et *al*, 2023 (314)
`Kidney renal papillary cell carcinoma	*NALCN*	CNV (Down)	He et *al*, 2023 (314)
Papillary Thyroid Carcinoma	*NLF-1/FAM155B*	CNV (Down)	Yu et *al*, 2019 (321)
	NLF-1/FAM155B	GWM (hypermethylated)	Li et al, 2022 (322)
Glioma/Glioblastoma	*NLF-1/FAM155A*	CNV (Down)	Fontanillo et *al*, 2012 (323)
	NALCN	CNV (Down)	Wang et *al*, 2015 (324)
	NALCN	CNV (Down)	Zhang et *al*, 2020 (325)
	NALCN	CNV (Down)	He et *al*, 2023 (314)
	circNALCN	CNV (Down)	Liu et *al*, 2021 (326)
Bladder	*NALCN-AS1*	CNV (Down)	Zhong et *al*, 2022 (327)
	NALCN	CNV (Down)	He et *al*, 2023 (314)
Colorectal	*NALCN*	CNV (gain)	Huang et *al*, 2023 (328)
	NALCN	CNV (Down)	He et *al*, 2023 (314)
Rectum adenocarcinoma	*NALCN*	CNV (Down)	He et *al*, 2023 (314)
Breast invasive carcinoma	*NALCN*	CNV (Down)	He et *al*, 2023 (314)
Cervical squamous cell carcinoma & endocervical adenocarcinoma	*NALCN*	CNV (Down)	He et *al*, 2023 (314)
Thyroid carcinoma	*NALCN*	CNV (Down)	He et *al*, 2023 (314)
Uterine corpus endometrial carcinoma	*NALCN*	CNV (Down)	He et *al*, 2023 (314)
Cholangio carcinoma	*NALCN*	CNV (Gain)	He et *al*, 2023 (314)
Pheochromocytoma	*NALCN*	CNV (Gain)	He et *al*, 2023 (314)
Paraganglioma	*NALCN*	CNV (Gain)	He et *al*, 2023 (314)
Stomach adenocarcinoma	*NALCN*	CNV (Gain)	He et *al*, 2023 (314)
Chemotherapy toxicity	*NALCN*	QTL	King et *al*, 2014 (329)
Randall plaques	*NALCN*	CNV (Down)	Taguchi et *al*, 2017 (330)
Coronary Heart disease	*NALCN*	MCA	Yan et *al*, 2018 (331)

Congenital Heart Disease	*NALCN*	CNV (Down)	Audain et *al*, 2021 (332)
Hypertension	*NLF-1/FAM155A*	GWAS	Adeyemo et *al*, 2009 (333)
Obesity	*NLF-1/FAM155A*	GWAS	Wilson et *al*, 2015 (334)
Primary Ovarian Insufficiency	*NLF-1/FAM155A*	CNV (up)	Li et *al*, 2016 (335)
Diverticular disease and diverticulitis	*NLF-1/FAM155A* *NLF-1/FAM155A* *NLF-1/FAM155A* *NLF-1/FAM155A*	GWAS GWAS GWAS GWAS	Sigurdsson et *al*, 2017 (336) Maguire et *al*, 2018 (337) Schafmayer et *al*, 2019 (338) Reichert et *al*, 2020 (339)
Chiari malformation Type I	*NLF-1/FAM155A*	AS	AvSar et *al*, 2020 (340)
Primary biliary cirrhosis	*NLF-1/FAM155A*	GWAS	Hirschfield et *al*, 2009 (341)
13q syndrome	*NALCN* *NLF-1/FAM155A*		Brown et *al*, 1995 (214) Kirchhoff et *al*, 2009 (215) Huang et *al*, 2012 (216) Lalani et *al*, 2013 (217)
Brain anomalies	*UNC-80?*	microdeletion	van Binsbergen et *al*, 2014 (220)
Mental retardation, dysmorphic features	*UNC-80?*	microdeletion	Bisgaard et *al*, 2006 (219)

*** Other genes may be involved in the considered genomic region. Abbreviations: GWAS, genome wide association study; PBA, pathways-based analysis; QTL, quantitative trait loci; CCS, case control study; AS, association study; WES, whole exome sequencing; WGS, whole genome sequencing; CNV, copy number variation; GWM, genome wide methylation; FBAT, family-based association test; MCA, multiple correlation analysis; LA: linkage analysis; DNV, *de novo* variation; IA, integrative analysis; WB, western blotting; mTLE, mesial temporal lobe epilepsy; ELISA: enzyme-linked immunosorbent assay.**

Neurodegenerative disorders

Alzheimer's disease (AD) is a neurodegenerative disorder characterized by gradual deterioration of cognitive function, memory, and inability to perform daily, social, or occupational activities. Its etiology is associated with the accumulation of β-amyloid peptides, phosphorylated tau protein, and neuro-inflammatory and oxidative processes in the brain (342). Rare variants of several genes have been associated with AD (343). This includes genome regions where *UNC-79* and *UNC-80* reside (294-296), however these regions also bear other genes including *MAP2* on chromosome 2 which is associated with AD (344). *UNC-80* also exhibits a change in gene editing levels in the hippocampus from patients with AD (297). More recently, a genome-wide association study (GWAS) identified *NALCN* as a potential susceptibility locus for AD (298). Electrophysiologically, inhibitory interneurons from APdE9 mice, a model for AD, exhibit altered electrical activity (345). Indeed, these neurons exhibit an inability to reliably spike, a higher RMP, an enhanced depolarizability in response to applied stimulus, and smaller mean AP amplitude as compared to those from control mice, all consistent with an increase in a Na^+ background conductance. It is tempting to speculate that NALCN contributes to this Na^+ background conductance although other proteins could be involved including amyloid β which can itself form a cation-permeable pore at the plasma membrane (346-348).

Another association study suggested *NALCN* could be a susceptibility locus for Parkinson's disease (PD)(301). PD is a common neurodegenerative movement disorder for which the etiology in most patients is unknown, but different genetic causes have been identified (349). Notably, *NALCN* was also identified as a susceptibility locus for cervical dystonia (300), and dystonia often precedes other motor symptoms in PD (350, 351).

However, a lack of association between *NALCN* and dystonia is also reported in two studies (352, 353). Nonetheless, an involvement of *NALCN* in PD is supported by the fact that disturbances observed in patients with PD are similar to phenotypes reported in animal models for NALCN channelosome dysfunctions (263). Of note, a decrease in the copy number of *Unc-80* is reported in a mouse model for spinocerebellar ataxia type 2 (299). Some patients with the CLIFAHDD syndrome also exhibited episodic ataxia (*see above* and **TABLE 9**). Since NLF-1/FAM155A contains polyglutamine repeats, it is possible it could be involved in polyglutamine disorders (308).

Epilepsy

Epilepsy is a brain condition characterized by the recurrence of unprovoked seizures and is one of the most common serious brain conditions, affecting over 70 million people worldwide. It is characterized by a lasting predisposition to generate spontaneous epileptic seizures and has numerous neurobiological, cognitive, and psychosocial consequences (354). A study aiming to identify disease-associated alternative splicing patterns in ion channel genes by comprehensively screening affected brain tissue collected from patients with mesial temporal lobe epilepsy revealed an altered alternative splicing pattern for *NALCN* (302). A genomic region on chromosome 2 associated with susceptibility to epilepsy which includes *UNC-80* was also described (303, 304). Point mutations within *UNC-80* in patients with early onset epileptic spasm with unknown reason are also reported (305). More recently, a microdeletion of a chromosomic region including the *UNC-80* gene (but also *LANCL1* and *MAP2*) was detected in a patient with epilepsy (305, 306). Several patients with the IHPRF and CLIFAHDD syndromes as well as with monoallelic predicted loss-of-function variants of *NALCN* and *UNC-79* also exhibit seizures (*see above* and **TABLES 7** & **9**). Taken together, these data strongly point the NALCN channelosome-encoding genes as susceptibility loci for epilepsy.

Movement disorder

An association study suggested is a susceptibility locus for the restless leg syndrome within 13q32.3-33.2, where *NALCN* and *NALCN-AS1* reside (307). This syndrome is a common neurological disorder affecting up to 15% of the general population and is categorized as a sleep-related movement disorder.

Cancer

A recent study demonstrated that *Nalcn* is a key regulator of cancer metastasis in mouse. Indeed, deletion of *Nalcn* from gastric, intestinal, or pancreatic adenocarcinomas in mice models does not alter tumor incidence, but markedly increases the number of circulating tumor cells and metastases (309). Conversely, NALCN is also described as promoting metastasis as a major initiator and regulator of Ca^{2+} oscillations required for invadopodia formation in human prostate cancer cells (310). Several other studies also indicate a possible association of the NALCN channelosome with several types of cancers (**TABLE 11**). This includes the report of somatic mutations within *NALCN*, *UNC-79* and *UNC-80* in pancreatic cancer, hepatocellular carcinoma, and Erwin sarcoma respectively (262, 315, 316). Mutations within *NALCN* and *UNC-79* are also described in neuroblastoma (318). In addition, the COSMIC database that provides a catalogue of somatic mutations in cancer references a large number of mutations for NALCN channelosome-encoding genes in a

large panel of cancer types (https://cancer.sanger.ac.uk/cosmic). Functional consequences of these mutations and a correlation between NALCN function and cancer severity have now to be explored. Copy number variations (CNV) are also reported, where *NALCN* is downregulated in hepatocellular carcinoma and glioma/glioblastoma (317, 324, 325). NALCN expression is also differentially regulated in colorectal cancer cells where it could interact with endomucin to exert a carcinogenic role (328). A recent data mining analysis also revealed that NALCN expression is significantly downregulated in bladder urothelial carcinoma, breast invasive carcinoma, cervical squamous cell carcinoma, endocervical adenocarcinoma, colon adenocarcinoma, glioblastoma multiforme, kidney renal clear cell carcinoma, kidney renal papillary cell carcinoma, liver hepatocellular carcinoma, lung adenocarcinoma, lung squamous cell carcinoma, rectum adenocarcinoma, thyroid carcinoma, uterine corpus endometrial carcinoma, but upregulated in cholangiocarcinoma, pheochromocytoma and paraganglioma, stomach adenocarcinoma (314). Downregulation of *UNC-80*, *NLF-1/FAM155A* and *NLF-1/FAM155B* are described in pancreatic cancer, glioma/glioblastoma and Papillary Thyroid Carcinoma respectively (312, 321-323). Conversely, upregulation of *NALCN-AS1*, *NLF-1/FAM155A,* and *UNC-79* are reported in clear cell renal cell carcinoma, tumor-derived endothelial cells and non-small cell lung cancer with brain metastasis respectively (102, 311, 319). In this context, the NALCN channelosome could be involved in proliferation and migration of lung cancer A549 cells (102). Also, a downregulation of NALCN-AS1 is correlated with survival in patients with bladder cancer (327). Interestingly, a study reported the existence of a circular RNA referred to as *circNALCN* which is derived from exons 2 to 7 of *NALCN* (326). This *CircNALCN* element is downregulated in glioma tissues and acts as a sponge for miR-493-3p, affecting the expression of PTEN to modulate glioma tumorigenesis and progression. In addition to all these findings, a genome-wide association study suggested a possible association between *NALCN* and non-small cell lung cancer and *NLF-1/FAM155A* was found to be hypermethylated in clear cell renal cell carcinoma (313, 320). Overall, these studies indicate a possible role of the NALCN channelosome in cancer. However, whether detected alterations within these genes reflect a cause or a consequence of cancer must be investigated. Of interest for cancer treatment, a study aiming to map quantitative trait loci affecting toxicity to chemotherapy in *D. melanogaster* highlighted *na/Dmα1U* as impacting toxicity to carboplatin (329).

Miscellaneous

In addition to studies mentioned above, the NALCN channelosome is also suspected to be involved in other disorders. Microarray analysis from renal papillary highlighted that a down regulation of *NALCN* is associated with calcium phosphate lesions in the renal papilla known as Randall's plaques (330). *NALCN* is also associated to coronary heart disease (multiple correlation analysis) and found to have a decrease expression level in congenital heart disease (331, 332). Genome-wide association studies also suggest *NLF-1/FAM155A* as a susceptibility locus in hypertension and obesity (333, 334). Indeed, *NLF-1/FAM155A* is associated with several other diseases including primary ovarian insufficiency, diverticular disease and diverticulitis, Chiari malformation of type I and primary biliary cirrhosis (335-341). However, another study did not find any association between *NLF-1/FAM155A* with either diverticular disease or diverticulitis (355).

V- CONCLUDING REMARKS

NALCN channel: from cloning to structure, physiological roles and diseases

While it took more than 8 years from its initial molecular cloning (1) to its first functional description (2), NALCN is now well documented as a channel that critically regulates the resting membrane potential and the electrical activity of neurons and other cell types. Recent studies also established that NALCN channel requires a complex arrangement of 4 subunits (*NALCN, UNC-80*, *UNC-79* and *NLF1/ FAM155*) for its proper activity (31). Several studies in *C. elegans* and *D. melanogaster* mutant animals had previously described phenotypic features linked to NALCN deficiency, even before knowing its channel function (*reviewed in* (356)), but the ground-breaking findings by Lu et *al*, 2007 (2) launched and fostered investigations related to its physiology, functional regulation, and pathophysiology. Molecular characterization of NALCN channelosome has also recently benefited from the elucidation of its 3D Cryo-EM structure. Unfortunately, no selective pharmacological modulator of NALCN, either inhibitor or activator, has been identified to date. Such molecules will undoubtedly be valuable to better decipher the physiological roles of NALCN, and eventually treat NALCN-related pathologies. This review highlights how the use of various and complementary animal models, mainly *M. musculus*, *C. elegans*, and *D. Melanogaster*, revealed the precise involvement of NALCN in key physiological functions including respiratory and circadian rhythms, sleep, nociception, gastrointestinal motility, parturition and locomotion (**TABLE 3**). These animal and cell models led to the identification of pathways that regulate the NALCN channelosome both at the transcriptional and functional levels (**TABLES 2** & **10**). Last but not least, genetic diseases resulting from mutations within the NALCN channelosome-encoding genes have been described as well as possible associations with other human diseases (**TABLES 5-9**; **TABLES 12**), increasing our understanding of NALCN functions.

Overall, an increasing number of studies point to major roles of the NALCN channelosome in physiology, as well as its involvement in human diseases when dysfunctional. Addressing some of the remaining questions in the near future (pictured in **FIGURE 11**) will further increase our knowledge of how NALCN contributes to the fundamental physiological process of cell excitability.

Perspectives offered by some unresolved issues

Most of the recent work identified how *NALCN* is important in many neurophysiological processes. However, NALCN is also expressed in the heart, aorta and endocrine glands where its physiological roles have not yet been described (56). Deciphering the physiological roles of NALCN in non-neuronal tissues requires further investigation, and may ultimately lead to important novel discoveries regarding NALCN functions. The availability of animal models, especially mice in which *Nalcn* expression may be modulated in a Cre-dependent manner now allows research that can fill gaps in our knowledge. Other vertebrate animal models such as zebrafish could also be relevant for the study of physiological function of the NALCN channelosome. Indeed, zebrafish with predicted loss-of-function alleles for *nalcn*, *unc-79*, *unc-80* and *nlf-1/fam155a* (but not *nlf-1/fam155b*) are now available (https://zebrafish.org).

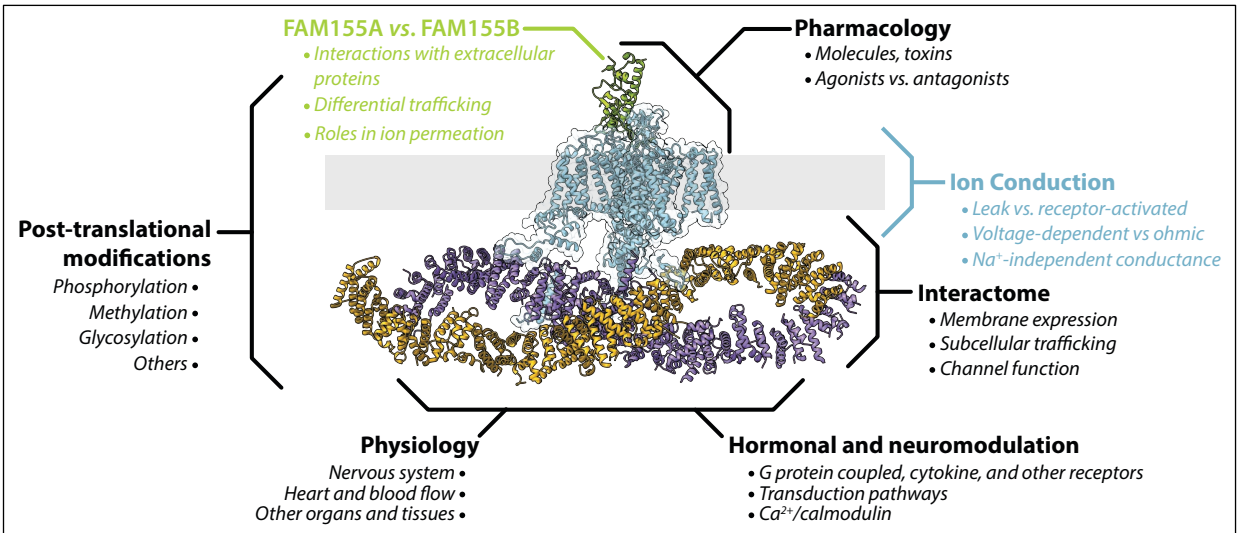

FIGURE 11. Schematic representation of outstanding issues for NALCN. There are major recent findings (*exposed in this review*) that significantly contribute to the current knowledge of the molecular and functional specificities of the NALCN channel. However, many open questions remain regarding how NALCN and its channelosome are regulated by two distinct NLF-1/FAM155 subunits receptors and potential additional protein partners, and/or by post-translational modifications. How hormones and neurotransmitters pathways modulate the NALCN channelosome is essentially unknown. Similarly, how NALCN is coupled to cellular and transduction pathways also remain poorly understood. Deciphering the physiological relevance of the NALCN channelosome activity in various organs and cell types will be a major issue in the coming years. All these considering that identification of a specific/selective pharmacology will be also crucial to characterize in deep the molecular (biophysical) properties NALCN, further explore its physiological roles, and develop potential therapeutics with applications in human diseases.

NALCN regulates cellular excitability in the pituitary somatolactotroph GH3 cell line (76), as well as the β-pancreatic MIN6 cell line (56), and is consequently involved in hormone release. In MIN6 cells, NALCN behaves as an acetylcholine-activated Na^+ current through activation of the M3 muscarinic receptor, without detectable leak channel activity. Similarly, activation of NALCN by leptin, without a background/constitutive Na^+ leak current, is described in leptin receptor-expressing neurons of type 1 in the nucleus of the solitary tract (73). A hypothesis that has been put forward is that the leak activity of NALCN could result from basal activity of src kinase (19). However, pharmacological inhibition of this kinase does not affect the Na^+ leak current generated by NALCN when expressed in *Xenopus* oocytes (30). Why NALCN acts as a leak channel in some cell types and as a receptor-activated channel in others is yet not understood.

Electrophysiological recordings in endocrine pituitary cells also revealed a correlation between a Na^+-independent conductance and the expression level of *NALCN* (76). Whether NALCN conducts this Na^+-independent conductance or impact on other channels' function, as could be the case through allosteric modulation, is currently unknown. NALCN current is also described to be both positively and negatively regulated by few G proteins-coupled receptors (GPCRs). Whether other GPCRs or members of other families of membrane receptors may modulate NALCN current and the underlying mechanisms is a crucial question towards understanding NALCN physiology. The possibility to functionally express NALCN in recombinant systems now allows for a candidate-based approach to identify NALCN-coupled GPCRs.

Several recent studies have identified a voltage-dependent component of the NALCN current (30, 45, 94), contrasting early reports on NALCN current described as a pure 'ohmic' leak current (2). This novel finding is supported by the non-linear current-voltage relationship and the time-dependent decay in NALCN current amplitude, measured during a test-pulse protocol, and attributable to a deactivation process (*see* **FIGURE 6**). These findings should stimulate further studies of the gating mechanism for NALCN. The voltage-dependent mode *versus* the ohmic mode of NALCN gating may possibly depend on cellular environment, or on the complex organization and regulation of the NALCN channelosome. It could also be affected by genetic mutations as reported in Bouasse et *al* 2019 (94). The physiological relevance of a 'voltage-gated' NALCN activity is not yet known but could likely impact NALCN's contributions not only to RMP, but also membrane excitation.

Of note, instead of a "depolarizing" role, the NALCN channelosome is also proposed to have a "hyperpolarizing" function in myometrial cells through functional coupling with SLO2.1, a Na^+-activated K^+ channel (104). In this context, Na^+ ions entering the cell through NALCN act as a second messenger that activate SLO2.1 causing a negative shift in the membrane potential. This raises the possibility that this process also occurs in other cell types including neurons, and possibly involves additional Na^+-activated K^+ channels.

Further characterization of the proteins that belong to the NALCN channelosome and regulate its function is also needed, as well as the identification of post-translational modifications. NALCN associates with at least UNC-79, UNC-80 and NLF-1/FAM155A (or NLF-1/FAM155B) whose properties and roles are still poorly understood. Whether these proteins have NALCN-independent functions and whether additional proteins contribute to the NALCN complex are important questions that need to be addressed. Indeed, CaM and Endomucin were recently proposed to also belong to the NALCN channelosome complex (31, 46, 328). However, such biochemical studies of NALCN are hampered by the lack of specific antibodies to immuno-precipitate NALCN (as well as UNC-79, UNC-80 and NLF-1/FAM155A and NLF-1/FAM155B). Some new commercially available antibodies that recognize native NALCN and the development of a GFP-tagged NALCN mouse model (49) will make it possible to explore its interactome and post-translational modifications in different tissues and cell types. These approaches might also provide clues as to why NALCN behaves as leak channel in some cell types and not in others, why it exhibits a voltage-sensitivity in some conditions and not in others, and whether the NALCN channelosome could interact with other channels and receptors.

With respect to NLF-1/FAM155, the physiological relevance of 2 interchangeable NLF-1/FAM155 (A and B) paralogues is another unresolved question (**FIGURE 11**). Since the 2 corresponding mRNA do not seem to be expressed in the same regions of the body (https://www.gtexportal.org), a comparative proteomics study could indicate whether these 2 proteins interact differently with other proteins. Considering the 3D structure of the NALCN channelosome, it is also conceivable that NLF-1/FAM155A and NLF-1/FAM155B proteins could differentially interact with extracellular matrix proteins similarly to the $\alpha_2\delta$-1 subunit of Ca_v channels (357).

NALCN is critically missing selective pharmacological blockers. Some blockers of NALCN channelosome function have been tentatively described, however these molecules are not specific and exhibit a low affinity for NALCN. The identification of specific

compounds able to activate or inhibit NALCN currents is an important objective not only for providing tools for physiological studies but also as potential therapeutic agents. This is especially true for the CLIFAHDD syndrome, which is induced by gain-of-function mutations in NALCN. Indeed, partial inhibition of gain-of-function pathogenic variants of NALCN in patients with the CLIFAHDD syndrome is predicted to have beneficial effects. The possibility to functionally express NALCN in cell lines such as HEK-293T cells paves the way for setting up of high throughput pharmacological screening assays, for example by using automated patch-clamp devices (358). The Cryo-EM structure of the NALCN channelosome also allows for simulation and machine learning strategies towards drug design (359).

Finally, an important and stimulating question to address is life expectancy of living organisms with NALCN channelosome dysfunction. Remarkably, NALCN channelosome dysfunctions do not affect life expectancy in both *C. elegans* and *D. melanogaster* while *Nalcn* and *Unc-80* knockout mice die within 24h after birth from respiratory defects. There is also a great variability in the severity of the syndromes in patients carrying different loss- and gain-of function mutations of *NALCN,* or loss-of-functions of *UNC-80* (**TABLES 5**,**6**,**8**). This probably reflects the different importance of NALCN channelosome function across species, or the existence of specific compensatory mechanisms in some species/individuals but not in others.

Perspectives

Research on NALCN has progressed significantly, and the importance of this channel in physiology and disease is clear. Though many questions remain unanswered, continued efforts and the development of new tools are set to increase our understanding of how NALCN contributes to cell excitability, a fundamental and finely balanced physiological process, and how its dysregulation and contributions to disease can be mitigated.

ACKNOWLEDGMENTS

The authors would like to thank Tanzim Hoque for conducting the electrophysiological recordings used to generate Figure 5, and Dr Hélène Hirbec and Dr. Stephan A. Pless for critical reading of parts of the manuscript.

GRANTS

This work was supported by grants from ANR (ANR-21-NEU2-0004-01) to A.M. and from AEI (PCI2021-122051-2A) to A.G.-N. in the frame of the ERA-NET Neuron 2021 call on neurodevelopmental disorders (https://www.neuron-eranet.eu/projects/RestoreLeak/) as well as NSERC (Discovery Grant no. RGPIN-2021-03557 and RTI grant no. RTI-2021-00776) to A.S.

This work was also supported by Labex 'Ion Channel Science and Therapeutics' (ANR-11-LABX-0015), Fondation Maladies Rares (FMR), Association Française contre les Myopathies (AFM) and Fondation pour la Recherche Médicale (FRM) and a CNRS-University of Toronto PRC grant.

DISCLOSURES

The authors have no conflicts of interest, financial or otherwise, to disclose.

REFERENCES

1. **Lee J-H, Cribbs LL, and Perez-Reyes E**. Cloning of a novel four repeat protein related to voltage-gated sodium and calcium channels. *FEBS letters* 445: 231-236, 1999.
2. **Lu B, Su Y, Das S, Liu J, Xia J, and Ren D**. The neuronal channel NALCN contributes resting sodium permeability and is required for normal respiratory rhythm. *Cell* 129: 371-383, 2007.
3. **Hodgkin AL, and Katz B**. The effect of sodium ions on the electrical activity of giant axon of the squid. *J Physiol* 108: 37-77, 1949.
4. **Llinás RR**. The intrinsic electrophysiological properties of mammalian neurons: insights into central nervous system function. *Science* 242: 1654-1664, 1988.
5. **Abdul Kadir L, Stacey M, and Barrett-Jolley R**. Emerging roles of the membrane potential: action beyond the action potential. *Frontiers in physiology* 1661, 2018.
6. **Khaliq ZM, and Bean BP**. Pacemaking in dopaminergic ventral tegmental area neurons: depolarizing drive from background and voltage-dependent sodium conductances. *Journal of Neuroscience* 30: 7401-7413, 2010.
7. **Enyedi P, and Czirják G**. Molecular background of leak K+ currents: two-pore domain potassium channels. *Physiological reviews* 90: 559-605, 2010.
8. **Thomas D, and Goldstein SAN**. Two-P-Domain (K2P) Potassium Channels: Leak Conductance Regulators of Excitability. In: *Encyclopedia of Neuroscience*, edited by Squire LR. Oxford: Academic Press, 2009, p. 1207-1220.
9. **Conn PJ, and Kaczmarek LK**. The bag cell neurons ofAplysia. *Molecular neurobiology* 3: 237-273, 1989.
10. **Wilson GF, Richardson FC, Fisher TE, Olivera BM, and Kaczmarek LK**. Identification and characterization of a Ca2+-sensitive nonspecific cation channel underlying prolonged repetitive firing in Aplysia neurons. *Journal of Neuroscience* 16: 3661-3671, 1996.
11. **Hatcher NG, and Sweedler JV**. Aplysia bag cells function as a distributed neurosecretory network. *Journal of neurophysiology* 99: 333-343, 2008.
12. **Guérineau NC, Monteil A, and Lory P**. Sodium background currents in endocrine/neuroendocrine cells: Towards unraveling channel identity and contribution in hormone secretion. *Frontiers in neuroendocrinology* 63: 100947, 2021.
13. **Ren D**. Sodium leak channels in neuronal excitability and rhythmic behaviors. *Neuron* 72: 899-911, 2011.
14. **Favero M, Varghese G, and Castro-Alamancos MA**. The state of somatosensory cortex during neuromodulation. *Journal of neurophysiology* 108: 1010-1024, 2012.
15. **Crill WE**. Persistent sodium current in mammalian central neurons. *Annual review of physiology* 58: 349-362, 1996.
16. **Lewis AH, and Raman IM**. Resurgent current of voltage-gated Na(+) channels. *J Physiol* 592: 4825-4838, 2014.
17. **Biel M, Wahl-Schott C, Michalakis S, and Zong X**. Hyperpolarization-activated cation channels: from genes to function. *Physiol Rev* 89: 847-885, 2009.
18. **Boscardin E, Alijevic O, Hummler E, Frateschi S, and Kellenberger S**. The function and regulation of acid-sensing ion channels (ASICs) and the epithelial Na(+) channel (ENaC): IUPHAR Review 19. *Br J Pharmacol* 173: 2671-2701, 2016.
19. **Cochet-Bissuel M, Lory P, and Monteil A**. The sodium leak channel, NALCN, in health and disease. *Front Cell Neurosci* 8: 132, 2014.

20. **Lu TZ, and Feng ZP**. NALCN: a regulator of pacemaker activity. *Mol Neurobiol* 45: 415-423, 2012.
21. **Zhang MQ**. Computational prediction of eukaryotic protein-coding genes. *Nat Rev Genet* 3: 698-709, 2002.
22. **Perez-Reyes E**. Molecular characterization of a novel family of low voltage-activated, T-type, calcium channels. *J Bioenerg Biomembr* 30: 313-318, 1998.
23. **Santoro B, Grant SG, Bartsch D, and Kandel ER**. Interactive cloning with the SH3 domain of N-src identifies a new brain specific ion channel protein, with homology to eag and cyclic nucleotide-gated channels. *Proc Natl Acad Sci U S A* 94: 14815-14820, 1997.
24. **Santoro B, Liu DT, Yao H, Bartsch D, Kandel ER, Siegelbaum SA, and Tibbs GR**. Identification of a gene encoding a hyperpolarization-activated pacemaker channel of brain. *Cell* 93: 717-729, 1998.
25. **Altschul SF, Gish W, Miller W, Myers EW, and Lipman DJ**. Basic local alignment search tool. *J Mol Biol* 215: 403-410, 1990.
26. **Yu FH, and Catterall WA**. The VGL-chanome: a protein superfamily specialized for electrical signaling and ionic homeostasis. *Sci STKE* 2004: re15, 2004.
27. **Kschonsak M, Chua HC, Noland CL, Weidling C, Clairfeuille T, Bahlke OØ, Ameen AO, Li ZR, Arthur CP, and Ciferri C**. Structure of the human sodium leak channel NALCN. *Nature* 587: 313-318, 2020.
28. **Xie J, Ke M, Xu L, Lin S, Huang J, Zhang J, Yang F, Wu J, and Yan Z**. Structure of the human sodium leak channel NALCN in complex with FAM155A. *Nature communications* 11: 1-13, 2020.
29. **Kang Y, Wu J-X, and Chen L**. Structure of voltage-modulated sodium-selective NALCN-FAM155A channel complex. *Nature communications* 11: 1-10, 2020.
30. **Chua H, Wulf M, Weidling C, Rasmussen L, and Pless S**. The NALCN channel complex is voltage sensitive and directly modulated by extracellular calcium. *Science advances* 6: eaaz3154, 2020.
31. **Kschonsak M, Chua HC, Weidling C, Chakouri N, Noland CL, Schott K, Chang T, Tam C, Patel N, Arthur CP, Leitner A, Ben-Johny M, Ciferri C, Pless SA, and Payandeh J**. Structural architecture of the human NALCN channelosome. *Nature* 603: 180-186, 2022.
32. **Jospin M, Watanabe S, Joshi D, Young S, Hamming K, Thacker C, Snutch TP, Jorgensen EM, and Schuske K**. UNC-80 and the NCA ion channels contribute to endocytosis defects in synaptojanin mutants. *Curr Biol* 17: 1595-1600, 2007.
33. **Humphrey JA, Hamming KS, Thacker CM, Scott RL, Sedensky MM, Snutch TP, Morgan PG, and Nash HA**. A putative cation channel and its novel regulator: cross-species conservation of effects on general anesthesia. *Current Biology* 17: 624-629, 2007.
34. **Yeh E, Ng S, Zhang M, Bouhours M, Wang Y, Wang M, Hung W, Aoyagi K, Melnik-Martinez K, Li M, Liu F, Schafer WR, and Zhen M**. A putative cation channel, NCA-1, and a novel protein, UNC-80, transmit neuronal activity in C. elegans. *PLoS Biol* 6: e55, 2008.
35. **Xie L, Gao S, Alcaire SM, Aoyagi K, Wang Y, Griffin JK, Stagljar I, Nagamatsu S, and Zhen M**. NLF-1 delivers a sodium leak channel to regulate neuronal excitability and modulate rhythmic locomotion. *Neuron* 77: 1069-1082, 2013.
36. **Lear BC, Darrah EJ, Aldrich BT, Gebre S, Scott RL, Nash HA, and Allada R**. UNC79 and UNC80, putative auxiliary subunits of the NARROW ABDOMEN ion channel, are indispensable for robust circadian locomotor rhythms in Drosophila. *PLoS One* 8: e78147, 2013.

37. **Topalidou I, Chen P-A, Cooper K, Watanabe S, Jorgensen EM, and Ailion M**. The NCA-1 and NCA-2 ion channels function downstream of Gq and Rho to regulate locomotion in Caenorhabditis elegans. *Genetics* 206: 265-282, 2017.
38. **Flourakis M, Kula-Eversole E, Hutchison AL, Han TH, Aranda K, Moose DL, White KP, Dinner AR, Lear BC, Ren D, Diekman CO, Raman IM, and Allada R**. A Conserved Bicycle Model for Circadian Clock Control of Membrane Excitability. *Cell* 162: 836-848, 2015.
39. **Edgar RC**. MUSCLE: multiple sequence alignment with high accuracy and high throughput. *Nucleic acids research* 32: 1792-1797, 2004.
40. **Capella-Gutiérrez S, Silla-Martínez JM, and Gabaldón T**. trimAl: a tool for automated alignment trimming in large-scale phylogenetic analyses. *Bioinformatics* 25: 1972-1973, 2009.
41. **Kalyaanamoorthy S, Minh BQ, Wong TK, Von Haeseler A, and Jermiin LS**. ModelFinder: fast model selection for accurate phylogenetic estimates. *Nature methods* 14: 587-589, 2017.
42. **Minh BQ, Schmidt HA, Chernomor O, Schrempf D, Woodhams MD, Von Haeseler A, and Lanfear R**. IQ-TREE 2: new models and efficient methods for phylogenetic inference in the genomic era. *Molecular biology and evolution* 37: 1530-1534, 2020.
43. **Lu B, Su Y, Das S, Wang H, Wang Y, Liu J, and Ren D**. Peptide neurotransmitters activate a cation channel complex of NALCN and UNC-80. *Nature* 457: 741-744, 2009.
44. **Lu B, Zhang Q, Wang H, Wang Y, Nakayama M, and Ren D**. Extracellular calcium controls background current and neuronal excitability via an UNC79-UNC80-NALCN cation channel complex. *Neuron* 68: 488-499, 2010.
45. **Kang Y, and Chen L**. Structure and mechanism of NALCN-FAM155A-UNC79-UNC80 channel complex. *Nat Commun* 13: 2639, 2022.
46. **Zhou L, Liu H, Zhao Q, Wu J, and Yan Z**. Architecture of the human NALCN channelosome. *Cell Discovery* 8: 1-11, 2022.
47. **Speca DJ, Chihara D, Ashique AM, Bowers MS, Pierce-Shimomura JT, Lee J, Rabbee N, Speed TP, Gularte RJ, Chitwood J, Medrano JF, Liao M, Sonner JM, Eger EI, 2nd, Peterson AS, and McIntire SL**. Conserved role of unc-79 in ethanol responses in lightweight mutant mice. *PLoS Genet* 6: 2010.
48. **Bayat A, Liu Z, Luo S, Fenger CD, Hojte AF, Isidor B, Cogne B, Larson A, Zanus C, Flavio F, Keren B, Musante L, Gourfinkel-An I, Perrine C, Demily C, Lesca G, Liao W, and Ren D**. A new neurodevelopmental disorder linked to heterozygous variants in UNC79. *Genet Med* 100894, 2023.
49. **Wie J, Bharthur A, Wolfgang M, Narayanan V, Ramsey K, Group CRR, Aranda K, Zhang Q, Zhou Y, and Ren D**. Intellectual disability-associated UNC80 mutations reveal inter-subunit interaction and dendritic function of the NALCN channel complex. *Nat Commun* 11: 3351, 2020.
50. **Pei J, and Grishin NV**. Cysteine-rich domains related to Frizzled receptors and Hedgehog-interacting proteins. *Protein Sci* 21: 1172-1184, 2012.
51. **Senatore A, Monteil A, van Minnen J, Smit AB, and Spafford JD**. NALCN ion channels have alternative selectivity filters resembling calcium channels or sodium channels. *PLoS One* 8: e55088, 2013.
52. **Liebeskind BJ, Hillis DM, and Zakon HH**. Phylogeny unites animal sodium leak channels with fungal calcium channels in an ancient, voltage-insensitive clade. *Molecular biology and evolution* 29: 3613-3616, 2012.
53. **Zimmermann B, Robb SM, Genikhovich G, Fropf WJ, Weilguny L, He S, Chen S, Lovegrove-Walsh J, Hill EM, and Ragkousi K**. Sea anemone genomes reveal ancestral metazoan chromosomal macrosynteny. *BioRxiv* 2020.

54. **Kapli P, and Telford MJ**. Topology-dependent asymmetry in systematic errors affects phylogenetic placement of Ctenophora and Xenacoelomorpha. *Science advances* 6: eabc5162, 2020.
55. **Whelan NV, Kocot KM, Moroz LL, and Halanych KM**. Error, signal, and the placement of Ctenophora sister to all other animals. *Proceedings of the National Academy of Sciences* 112: 5773-5778, 2015.
56. **Swayne LA, Mezghrani A, Varrault A, Chemin J, Bertrand G, Dalle S, Bourinet E, Lory P, Miller RJ, and Nargeot J**. The NALCN ion channel is activated by M3 muscarinic receptors in a pancreatic β-cell line. *EMBO reports* 10: 873-880, 2009.
57. **Zeisel A, Hochgerner H, Lonnerberg P, Johnsson A, Memic F, van der Zwan J, Haring M, Braun E, Borm LE, La Manno G, Codeluppi S, Furlan A, Lee K, Skene N, Harris KD, Hjerling-Leffler J, Arenas E, Ernfors P, Marklund U, and Linnarsson S**. Molecular Architecture of the Mouse Nervous System. *Cell* 174: 999-1014 e1022, 2018.
58. **Kang HJ, Kawasawa YI, Cheng F, Zhu Y, Xu X, Li M, Sousa AM, Pletikos M, Meyer KA, Sedmak G, Guennel T, Shin Y, Johnson MB, Krsnik Z, Mayer S, Fertuzinhos S, Umlauf S, Lisgo SN, Vortmeyer A, Weinberger DR, Mane S, Hyde TM, Huttner A, Reimers M, Kleinman JE, and Sestan N**. Spatio-temporal transcriptome of the human brain. *Nature* 478: 483-489, 2011.
59. **Hahn S, Um KB, Kim SW, Kim HJ, and Park MK**. Proximal dendritic localization of NALCN channels underlies tonic and burst firing in nigral dopaminergic neurons. *J Physiol* 601: 171-193, 2023.
60. **Amazu C, Ma X, Henkes C, Ferreira JJ, Santi CM, and England SK**. Progesterone and estrogen regulate NALCN expression in human myometrial smooth muscle cells. *Am J Physiol Endocrinol Metab* 318: E441-E452, 2020.
61. **Zhang D, Zhao W, Liu J, Ou M, Liang P, Li J, Chen Y, Liao D, Bai S, Shen J, Chen X, Huang H, and Zhou C**. Sodium leak channel contributes to neuronal sensitization in neuropathic pain. *Prog Neurobiol* 202: 102041, 2021.
62. **Li J, Chen Y, Liu J, Zhang D, Liang P, Lu P, Shen J, Miao C, Zuo Y, and Zhou C**. Elevated Expression and Activity of Sodium Leak Channel Contributes to Neuronal Sensitization of Inflammatory Pain in Rats. *Front Mol Neurosci* 14: 723395, 2021.
63. **Wang J, Yang Y, Liu J, Qiu J, Zhang D, Ou M, Kang Y, Zhu T, and Zhou C**. Loss of sodium leak channel (NALCN) in the ventral dentate gyrus impairs neuronal activity of the glutamatergic neurons for inflammation-induced depression in male mice. *Brain Behav Immun* 110: 13-29, 2023.
64. **Nash HA, Scott RL, Lear BC, and Allada R**. An unusual cation channel mediates photic control of locomotion in Drosophila. *Curr Biol* 12: 2152-2158, 2002.
65. **Lear BC, Lin JM, Keath JR, McGill JJ, Raman IM, and Allada R**. The ion channel narrow abdomen is critical for neural output of the Drosophila circadian pacemaker. *Neuron* 48: 965-976, 2005.
66. **Simakov O, Kawashima T, Marlétaz F, Jenkins J, Koyanagi R, Mitros T, Hisata K, Bredeson J, Shoguchi E, and Gyoja F**. Hemichordate genomes and deuterostome origins. *Nature* 527: 459-465, 2015.
67. **Wong ED, Skrzypek MS, Weng S, Binkley G, Meldal BHM, Perfetto L, Orchard SE, Engel SR, Cherry JM, and Project SGD**. Integration of macromolecular complex data into the Saccharomyces Genome Database. *Database (Oxford)* 2019: 2019.
68. **Lutas A, Lahmann C, Soumillon M, and Yellen G**. The leak channel NALCN controls tonic firing and glycolytic sensitivity of substantia nigra pars reticulata neurons. *Elife* 5: 2016.
69. **Funato H, Miyoshi C, Fujiyama T, Kanda T, Sato M, Wang Z, Ma J, Nakane S, Tomita J, Ikkyu A, Kakizaki M, Hotta-Hirashima N, Kanno S, Komiya H, Asano F,**

Honda T, Kim SJ, Harano K, Muramoto H, Yonezawa T, Mizuno S, Miyazaki S, Connor L, Kumar V, Miura I, Suzuki T, Watanabe A, Abe M, Sugiyama F, Takahashi S, Sakimura K, Hayashi Y, Liu Q, Kume K, Wakana S, Takahashi JS, and Yanagisawa M. Forward-genetics analysis of sleep in randomly mutagenized mice. *Nature* 539: 378-383, 2016.

70. **Shi Y, Abe C, Holloway BB, Shu S, Kumar NN, Weaver JL, Sen J, Perez-Reyes E, Stornetta RL, Guyenet PG, and Bayliss DA**. Nalcn Is a "Leak" Sodium Channel That Regulates Excitability of Brainstem Chemosensory Neurons and Breathing. *J Neurosci* 36: 8174-8187, 2016.

71. **Ford NC, Ren D, and Baccei ML**. NALCN channels enhance the intrinsic excitability of spinal projection neurons. *Pain* 159: 1719-1730, 2018.

72. **Philippart F, and Khaliq ZM**. Gi/o protein-coupled receptors in dopamine neurons inhibit the sodium leak channel NALCN. *Elife* 7: e40984, 2018.

73. **Do J, Chang Z, Sekerková G, McCrimmon DR, and Martina M**. A leptin-mediated neural mechanism linking breathing to metabolism. *Cell reports* 33: 108358, 2020.

74. **Lu TZ, and Feng ZP**. A sodium leak current regulates pacemaker activity of adult central pattern generator neurons in Lymnaea stagnalis. *PLoS One* 6: e18745, 2011.

75. **Gao S, Xie L, Kawano T, Po MD, Guan S, Zhen M, Pirri JK, and Alkema MJ**. The NCA sodium leak channel is required for persistent motor circuit activity that sustains locomotion. *Nat Commun* 6: 6323, 2015.

76. **Impheng H, Lemmers C, Bouasse M, Legros C, Pakaprot N, Guerineau NC, Lory P, and Monteil A**. The sodium leak channel NALCN regulates cell excitability of pituitary endocrine cells. *FASEB J* 35: e21400, 2021.

77. **Ou M, Zhao W, Liu J, Liang P, Huang H, Yu H, Zhu T, and Zhou C**. The General Anesthetic Isoflurane Bilaterally Modulates Neuronal Excitability. *iScience* 23: 100760, 2020.

78. **Kim BJ, Chang IY, Choi S, Jun JY, Jeon JH, Xu WX, Kwon YK, Ren D, and So I**. Involvement of Na(+)-leak channel in substance P-induced depolarization of pacemaking activity in interstitial cells of Cajal. *Cell Physiol Biochem* 29: 501-510, 2012.

79. **Reinl EL, Cabeza R, Gregory IA, Cahill AG, and England SK**. Sodium leak channel, non-selective contributes to the leak current in human myometrial smooth muscle cells from pregnant women. *Mol Hum Reprod* 21: 816-824, 2015.

80. **Yeh SY, Huang WH, Wang W, Ward CS, Chao ES, Wu Z, Tang B, Tang J, Sun JJ, Esther van der Heijden M, Gray PA, Xue M, Ray RS, Ren D, and Zoghbi HY**. Respiratory Network Stability and Modulatory Response to Substance P Require Nalcn. *Neuron* 94: 294-303 e294, 2017.

81. **Yang Y, Ou M, Liu J, Zhao W, Zhuoma L, Liang Y, Zhu T, Mulkey DK, and Zhou C**. Volatile Anesthetics Activate a Leak Sodium Conductance in Retrotrapezoid Nucleus Neurons to Maintain Breathing during Anesthesia in Mice. *Anesthesiology* 133: 824-838, 2020.

82. **Um KB, Hahn S, Kim SW, Lee YJ, Birnbaumer L, Kim HJ, and Park MK**. TRPC3 and NALCN channels drive pacemaking in substantia nigra dopaminergic neurons. *Elife* 10: 2021.

83. **Gonzalez JC, Lee H, Vincent AM, Hill AL, Goode LK, King GD, Gamble KL, Wadiche JI, and Overstreet-Wadiche L**. Circadian regulation of dentate gyrus excitability mediated by G-protein signaling. *Cell Rep* 42: 112039, 2023.

84. **Yang L, Pierce S, Gould TW, Craviso GL, and Leblanc N**. Ultrashort nanosecond electric pulses activate a conductance in bovine adrenal chromaffin cells that involves cation entry through TRPC and NALCN channels. *Arch Biochem Biophys* 109252, 2022.

85. **Hu J, Han J, Li H, Zhang X, Liu LL, Chen F, and Zeng B**. Human Embryonic Kidney 293 Cells: A Vehicle for Biopharmaceutical Manufacturing, Structural Biology, and Electrophysiology. *Cells Tissues Organs* 205: 1-8, 2018.

86. **Ooi A, Wong A, Esau L, Lemtiri-Chlieh F, and Gehring C**. A Guide to Transient Expression of Membrane Proteins in HEK-293 Cells for Functional Characterization. *Front Physiol* 7: 300, 2016.
87. **Thomas P, and Smart TG**. HEK293 cell line: a vehicle for the expression of recombinant proteins. *J Pharmacol Toxicol Methods* 51: 187-200, 2005.
88. **Eigenbrod O, Debus KY, Reznick J, Bennett NC, Sanchez-Carranza O, Omerbasic D, Hart DW, Barker AJ, Zhong W, Lutermann H, Katandukila JV, Mgode G, Park TJ, and Lewin GR**. Rapid molecular evolution of pain insensitivity in multiple African rodents. *Science* 364: 852-859, 2019.
89. **Hahn S, Kim SW, Um KB, Kim HJ, and Park MK**. N-benzhydryl quinuclidine (NBQN) compounds are a potent and Src kinase-independent inhibitor of NALCN channels. *Br J Pharmacol* 2020.
90. **Boone AN, Senatore A, Chemin J, Monteil A, and Spafford JD**. Gd3+ and calcium sensitive, sodium leak currents are features of weak membrane-glass seals in patch clamp recordings. *PLoS One* 9: e98808, 2014.
91. **Egan JM, Peterson CA, and Fry WM**. Lack of current observed in HEK293 cells expressing NALCN channels. *Biochim Open* 6: 24-28, 2018.
92. **Lee SY, Vuong TA, Wen X, Jeong HJ, So HK, Kwon I, Kang JS, and Cho H**. Methylation determines the extracellular calcium sensitivity of the leak channel NALCN in hippocampal dentate granule cells. *Exp Mol Med* 51: 1-14, 2019.
93. **Stray-Pedersen A, Cobben JM, Prescott TE, Lee S, Cang C, Aranda K, Ahmed S, Alders M, Gerstner T, Aslaksen K, Tetreault M, Qin W, Hartley T, Jhangiani SN, Muzny DM, Tarailo-Graovac M, van Karnebeek CD, Care4Rare Canada C, Baylor-Hopkins Center for Mendelian G, Lupski JR, Ren D, and Yoon G**. Biallelic Mutations in UNC80 Cause Persistent Hypotonia, Encephalopathy, Growth Retardation, and Severe Intellectual Disability. *Am J Hum Genet* 98: 202-209, 2016.
94. **Bouasse M, Impheng H, Servant Z, Lory P, and Monteil A**. Functional expression of CLIFAHDD and IHPRF pathogenic variants of the NALCN channel in neuronal cells reveals both gain- and loss-of-function properties. *Sci Rep* 9: 11791, 2019.
95. **Dolezal V, Castell X, Tomasi M, and Diebler MF**. Stimuli that induce a cholinergic neuronal phenotype of NG108-15 cells upregulate ChAT and VAChT mRNAs but fail to increase VAChT protein. *Brain Res Bull* 54: 363-373, 2001.
96. **Dolezal V, Lisa V, Diebler MF, Kasparova J, and Tucek S**. Differentiation of NG108-15 cells induced by the combined presence of dbcAMP and dexamethasone brings about the expression of N and P/Q types of calcium channels and the inhibitory influence of muscarinic receptors on calcium influx. *Brain Res* 910: 134-141, 2001.
97. **Rambeck B, and Wolf P**. Lamotrigine clinical pharmacokinetics. *Clin Pharmacokinet* 25: 433-443, 1993.
98. **Billups SJ, and Carter BL**. Mibefradil: a new class of calcium-channel antagonists. *Ann Pharmacother* 32: 659-671, 1998.
99. **Triggle DJ**. L-type calcium channels. *Curr Pharm Des* 12: 443-457, 2006.
100. **Kasap M, Aamodt EJ, Sagrera CE, and Dwyer DS**. Novel pharmacological modulation of dystonic phenotypes caused by a gain-of-function mutation in the Na+ leak-current channel. *Behav Pharmacol* 2019.
101. **Guinamard R, Simard C, and Del Negro C**. Flufenamic acid as an ion channel modulator. *Pharmacol Ther* 138: 272-284, 2013.
102. **Kim K, Lee J, Lee JY, Yong SH, Kim EY, Jung JY, Kang YA, Park MS, Kim YS, Oh CM, and Lee SH**. Clinical features and molecular genetics associated with brain metastasis in suspected early-stage non-small cell lung cancer. *Front Oncol* 13: 1148475, 2023.

103. **Zhang XW, Li L, Hu WQ, Hu MN, Tao Y, Hu H, Miao XK, Yang WL, Zhu Q, and Mou LY**. Neurokinin-1 receptor promotes non-small cell lung cancer progression through transactivation of EGFR. *Cell Death Dis* 13: 41, 2022.
104. **Ferreira JJ, Amazu C, Puga-Molina LC, Ma X, England SK, and Santi CM**. SLO2.1/NALCN a sodium signaling complex that regulates uterine activity. *iScience* 24: 103210, 2021.
105. **Wang H, and Ren D**. UNC80 functions as a scaffold for Src kinases in NALCN channel function. *Channels (Austin)* 3: 161-163, 2009.
106. **Guerineau NC, Bossu JL, Gahwiler BH, and Gerber U**. Activation of a nonselective cationic conductance by metabotropic glutamatergic and muscarinic agonists in CA3 pyramidal neurons of the rat hippocampus. *J Neurosci* 15: 4395-4407, 1995.
107. **Shirayama T, Matsumoto K, and Pappano AJ**. Carbachol-induced sodium current in guinea pig ventricular myocytes is not regulated by guanine nucleotides. *J Pharmacol Exp Ther* 265: 641-648, 1993.
108. **Topalidou I, Cooper K, Pereira L, and Ailion M**. Dopamine negatively modulates the NCA ion channels in C. elegans. *PLoS genetics* 13: e1007032, 2017.
109. **Hoyt JM, Wilson SK, Kasa M, Rise JS, Topalidou I, and Ailion M**. The SEK-1 p38 MAP kinase pathway modulates Gq signaling in Caenorhabditis elegans. *G3: Genes, Genomes, Genetics* 7: 2979-2989, 2017.
110. **Wittmack EK, Rush AM, Hudmon A, Waxman SG, and Dib-Hajj SD**. Voltage-gated sodium channel Nav1.6 is modulated by p38 mitogen-activated protein kinase. *J Neurosci* 25: 6621-6630, 2005.
111. **Hudmon A, Choi JS, Tyrrell L, Black JA, Rush AM, Waxman SG, and Dib-Hajj SD**. Phosphorylation of sodium channel Na(v)1.8 by p38 mitogen-activated protein kinase increases current density in dorsal root ganglion neurons. *J Neurosci* 28: 3190-3201, 2008.
112. **Hablitz JJ, Heinemann U, and Lux HD**. Step reductions in extracellular Ca2+ activate a transient inward current in chick dorsal root ganglion cells. *Biophys J* 50: 753-757, 1986.
113. **Xiong Z, Lu W, and MacDonald JF**. Extracellular calcium sensed by a novel cation channel in hippocampal neurons. *Proc Natl Acad Sci U S A* 94: 7012-7017, 1997.
114. **Formenti A, De Simoni A, Arrigoni E, and Martina M**. Changes in extracellular Ca2+ can affect the pattern of discharge in rat thalamic neurons. *J Physiol* 535: 33-45, 2001.
115. **Burgo A, Carmignoto G, Pizzo P, Pozzan T, and Fasolato C**. Paradoxical Ca2+ rises induced by low external Ca2+ in rat hippocampal neurones. *J Physiol* 549: 537-552, 2003.
116. **Smith SM, Bergsman JB, Harata NC, Scheller RH, and Tsien RW**. Recordings from single neocortical nerve terminals reveal a nonselective cation channel activated by decreases in extracellular calcium. *Neuron* 41: 243-256, 2004.
117. **Chinopoulos C, Connor JA, and Shuttleworth CW**. Emergence of a spermine-sensitive, non-inactivating conductance in mature hippocampal CA1 pyramidal neurons upon reduction of extracellular Ca2+: dependence on intracellular Mg2+ and ATP. *Neurochem Int* 50: 148-158, 2007.
118. **Hille B**. Ionic channels of excitable membranes, 3rd ed. *Sinauer Associates, Sunderland, MA*
, 2001.
119. **Nicholls JG, Martin AR, Wallace BG, and Fuchs PA**. From Neuron to Brain, 4th. ed. 2001.
120. **Sanderson P, Mavoungou R, and Albe-Fessard D**. Changes in substantia nigra pars reticulata activity following lesions of the substantia nigra pars compacta. *Neurosci Lett* 67: 25-30, 1986.

121. **Gulley JM, Kuwajima M, Mayhill E, and Rebec GV**. Behavior-related changes in the activity of substantia nigra pars reticulata neurons in freely moving rats. *Brain Res* 845: 68-76, 1999.
122. **Maurice N, Thierry AM, Glowinski J, and Deniau JM**. Spontaneous and evoked activity of substantia nigra pars reticulata neurons during high-frequency stimulation of the subthalamic nucleus. *J Neurosci* 23: 9929-9936, 2003.
123. **Deransart C, Hellwig B, Heupel-Reuter M, Leger JF, Heck D, and Lucking CH**. Single-unit analysis of substantia nigra pars reticulata neurons in freely behaving rats with genetic absence epilepsy. *Epilepsia* 44: 1513-1520, 2003.
124. **Berger C, and Kloting N**. Leptin Receptor Compound Heterozygosity in Humans and Animal Models. *Int J Mol Sci* 22: 2021.
125. **Hansen SB**. Lipid agonism: The PIP2 paradigm of ligand-gated ion channels. *Biochim Biophys Acta* 1851: 620-628, 2015.
126. **Ben-Johny M, Dick IE, Sang L, Limpitikul WB, Kang PW, Niu J, Banerjee R, Yang W, Babich JS, Issa JB, Lee SR, Namkung H, Li J, Zhang M, Yang PS, Bazzazi H, Adams PJ, Joshi-Mukherjee R, Yue DN, and Yue DT**. Towards a Unified Theory of Calmodulin Regulation (Calmodulation) of Voltage-Gated Calcium and Sodium Channels. *Curr Mol Pharmacol* 8: 188-205, 2015.
127. **Zhen M, and Samuel AD**. C. elegans locomotion: small circuits, complex functions. *Curr Opin Neurobiol* 33: 117-126, 2015.
128. **Wen Q, Gao S, and Zhen M**. Caenorhabditis elegans excitatory ventral cord motor neurons derive rhythm for body undulation. *Philos Trans R Soc Lond B Biol Sci* 373: 2018.
129. **Sedensky MM, and Meneely PM**. Genetic analysis of halothane sensitivity in Caenorhabditis elegans. *Science* 236: 952-954, 1987.
130. **Pierce-Shimomura JT, Chen BL, Mun JJ, Ho R, Sarkis R, and McIntire SL**. Genetic analysis of crawling and swimming locomotory patterns in C. elegans. *Proc Natl Acad Sci U S A* 105: 20982-20987, 2008.
131. **Zhou C, Luo J, He X, Zhou Q, He Y, Wang X, and Ma L**. The NALCN Channel Regulator UNC-80 Functions in a Subset of Interneurons To Regulate Caenorhabditis elegans Reversal Behavior. *G3 (Bethesda)* 10: 199-210, 2020.
132. **Krishnan KS, and Nash HA**. A genetic study of the anesthetic response: mutants of Drosophila melanogaster altered in sensitivity to halothane. *Proc Natl Acad Sci U S A* 87: 8632-8636, 1990.
133. **Guan Z, Scott RL, and Nash HA**. A new assay for the genetic study of general anesthesia in Drosophila melanogaster: use in analysis of mutations in the X-chromosomal 12E region. *J Neurogenet* 14: 25-42, 2000.
134. **Bend EG, Si Y, Stevenson DA, Bayrak-Toydemir P, Newcomb TM, Jorgensen EM, and Swoboda KJ**. NALCN channelopathies: Distinguishing gain-of-function and loss-of-function mutations. *Neurology* 87: 1131-1139, 2016.
135. **Bouhours M, Po MD, Gao S, Hung W, Li H, Georgiou J, Roder JC, and Zhen M**. A co-operative regulation of neuronal excitability by UNC-7 innexin and NCA/NALCN leak channel. *Mol Brain* 4: 16, 2011.
136. **Speca DJ, Rabbee N, Chihara D, Speed TP, and Peterson AS**. A genetic screen for behavioral mutations that perturb dopaminergic homeostasis in mice. *Genes Brain Behav* 5: 19-28, 2006.
137. **Nakayama M, Iida M, Koseki H, and Ohara O**. A gene-targeting approach for functional characterization of KIAA genes encoding extremely large proteins. *FASEB J* 20: 1718-1720, 2006.

138. **Reinl EL, Zhao P, Wu W, Ma X, Amazu C, Bok R, Hurt KJ, Wang Y, and England SK**. Na+-Leak Channel, Non-Selective (NALCN) Regulates Myometrial Excitability and Facilitates Successful Parturition. *Cell Physiol Biochem* 48: 503-515, 2018.
139. **Mir B, Iyer S, Ramaswami M, and Krishnan KS**. A genetic and mosaic analysis of a locus involved in the anesthesia response of Drosophila melanogaster. *Genetics* 147: 701-712, 1997.
140. **Lu TZ, Kostelecki W, Sun CL, Dong N, Perez Velazquez JL, and Feng ZP**. High sensitivity of spontaneous spike frequency to sodium leak current in a Lymnaea pacemaker neuron. *Eur J Neurosci* 44: 3011-3022, 2016.
141. **Ghezzi A, Liebeskind BJ, Thompson A, Atkinson NS, and Zakon HH**. Ancient association between cation leak channels and Mid1 proteins is conserved in fungi and animals. *Frontiers in molecular neuroscience* 7: 15, 2014.
142. **Murakami K, Palermo J, Stanhope BA, Gibbs AG, and Keene AC**. A screen for sleep and starvation resistance identifies a wake-promoting role for the auxiliary channel unc79. *G3 (Bethesda)* 11: 2021.
143. **Joiner WJ, Friedman EB, Hung HT, Koh K, Sowcik M, Sehgal A, and Kelz MB**. Genetic and anatomical basis of the barrier separating wakefulness and anesthetic-induced unresponsiveness. *PLoS Genet* 9: e1003605, 2013.
144. **Huang H, Hayden DJ, Zhu CT, Bennett HL, Venkatachalam V, Skuja LL, and Hart AC**. Gap Junctions and NCA Cation Channels Are Critical for Developmentally Timed Sleep and Arousal in Caenorhabditis elegans. *Genetics* 210: 1369-1381, 2018.
145. **Saro G, Lia AS, Thapliyal S, Marques F, Busch KE, and Glauser DA**. Specific Ion Channels Control Sensory Gain, Sensitivity, and Kinetics in a Tonic Thermonociceptor. *Cell Rep* 30: 397-408 e394, 2020.
146. **Sinke AP, Caputo C, Tsaih SW, Yuan R, Ren D, Deen PM, and Korstanje R**. Genetic analysis of mouse strains with variable serum sodium concentrations identifies the Nalcn sodium channel as a novel player in osmoregulation. *Physiol Genomics* 43: 265-270, 2011.
147. **Morgan PG, and Cascorbi HF**. Effect of anesthetics and a convulsant on normal and mutant Caenorhabditis elegans. *Anesthesiology* 62: 738-744, 1985.
148. **Morgan PG, Sedensky MM, Meneely PM, and Cascorbi HF**. The effect of two genes on anesthetic response in the nematode Caenorhabditis elegans. *Anesthesiology* 69: 246-251, 1988.
149. **Morgan PG, Sedensky M, and Meneely PM**. Multiple sites of action of volatile anesthetics in Caenorhabditis elegans. *Proc Natl Acad Sci U S A* 87: 2965-2969, 1990.
150. **Morgan PG, and Sedensky MM**. Mutations affecting sensitivity to ethanol in the nematode, Caenorhabditis elegans. *Alcohol Clin Exp Res* 19: 1423-1429, 1995.
151. **Nash HA, Campbell DB, and Krishnan KS**. New mutants of Drosophila that are resistant to the anesthetic effects of halothane. *Ann N Y Acad Sci* 625: 540-544, 1991.
152. **Campbell DB, and Nash HA**. Use of Drosophila mutants to distinguish among volatile general anesthetics. *Proc Natl Acad Sci U S A* 91: 2135-2139, 1994.
153. **Leibovitch BA, Campbell DB, Krishnan KS, and Nash HA**. Mutations that affect ion channels change the sensitivity of Drosophila melanogaster to volatile anesthetics. *J Neurogenet* 10: 1-13, 1995.
154. **Nishikawa K, and Kidokoro Y**. Halothane presynaptically depresses synaptic transmission in wild-type Drosophila larvae but not in halothane-resistant (har) mutants. *Anesthesiology* 90: 1691-1697, 1999.
155. **van Swinderen B**. A succession of anesthetic endpoints in the Drosophila brain. *J Neurobiol* 66: 1195-1211, 2006.

156. **Wu Y, Zhang D, Liu J, Yang Y, Ou M, Liu B, and Zhou C**. Sodium Leak Channel in the Nucleus Accumbens Modulates Ethanol-Induced Acute Stimulant Responses and Locomotor Sensitization in Mice: A Brief Research Report. *Front Neurosci* 15: 687470, 2021.
157. **Davies AG, Friedberg RI, Gupta H, Chan CL, Shelton KL, and Bettinger JC**. Different genes influence toluene- and ethanol-induced locomotor impairment in C. elegans. *Drug Alcohol Depend* 122: 47-54, 2012.
158. **Burg ED, Langan ST, and Nash HA**. Drosophila social clustering is disrupted by anesthetics and in narrow abdomen ion channel mutants. *Genes Brain Behav* 12: 338-347, 2013.
159. **Li X, Yang L, Zhang S, and Shen J**. The molecular mechanism of the transcriptional activator SWI regulating gene ARID1B affecting swallowing dysfunction after stroke in rats. *Pharmazie* 76: 494-498, 2021.
160. **Lu X, Liu SF, Wang HH, Yu F, Liu JJ, Zhao YM, and Zhao SL**. A biological study of supernumerary teeth derived dental pulp stem cells based on RNA-seq analysis. *Int Endod J* 52: 819-828, 2019.
161. **Gu J, Liang Q, Liu C, and Li S**. Genomic Analyses Reveal Adaptation to Hot Arid and Harsh Environments in Native Chickens of China. *Front Genet* 11: 582355, 2020.
162. **Kolosov A, Getmantseva L, Kolosova M, Romanets T, Bakoev N, Romanets E, Bakoeva I, Kostyunina O, Prytkov Y, Tretiakova O, and Bakoev S**. Investigation of the Genetic Architecture of Pigs Subjected to Breeding Intensification. *Genes (Basel)* 13: 2022.
163. **Yang Y, Li X, Ye S, Chen X, Wang L, Qian Y, Xin Q, Li L, and Gong P**. Identification of genes related to sexual differentiation and sterility in embryonic gonads of Mule ducks by transcriptome analysis. *Front Genet* 13: 1037810, 2022.
164. **Ramirez JM, and Baertsch N**. Defining the Rhythmogenic Elements of Mammalian Breathing. *Physiology (Bethesda)* 33: 302-316, 2018.
165. **Ramirez JM, and Baertsch NA**. The Dynamic Basis of Respiratory Rhythm Generation: One Breath at a Time. *Annu Rev Neurosci* 41: 475-499, 2018.
166. **Ghali MGZ**. Respiratory rhythm generation and pattern formation: oscillators and network mechanisms. *J Integr Neurosci* 18: 481-517, 2019.
167. **Gauda EB, Conde S, Bassi M, Zoccal DB, Almeida Colombari DS, Colombari E, and Despotovic N**. Leptin: Master Regulator of Biological Functions that Affects Breathing. *Compr Physiol* 10: 1047-1083, 2020.
168. **Taylor BE, and Lukowiak K**. The respiratory central pattern generator of Lymnaea: a model, measured and malleable. *Respir Physiol* 122: 197-207, 2000.
169. **Lin Y, Han M, Shimada B, Wang L, Gibler TM, Amarakone A, Awad TA, Stormo GD, Van Gelder RN, and Taghert PH**. Influence of the period-dependent circadian clock on diurnal, circadian, and aperiodic gene expression in Drosophila melanogaster. *Proc Natl Acad Sci U S A* 99: 9562-9567, 2002.
170. **Helfrich-Forster C**. Neurobiology of the fruit fly's circadian clock. *Genes Brain Behav* 4: 65-76, 2005.
171. **Abruzzi KC, Rodriguez J, Menet JS, Desrochers J, Zadina A, Luo W, Tkachev S, and Rosbash M**. Drosophila CLOCK target gene characterization: implications for circadian tissue-specific gene expression. *Genes Dev* 25: 2374-2386, 2011.
172. **Moose DL, Haase SJ, Aldrich BT, and Lear BC**. The Narrow Abdomen Ion Channel Complex Is Highly Stable and Persists from Development into Adult Stages to Promote Behavioral Rhythmicity. *Front Cell Neurosci* 11: 159, 2017.
173. **Yang ND, Mellor RL, Hermanstyne TO, and Nerbonne JM**. Effects of NALCN-encoded Na(+) leak currents on the repetitive firing properties of SCN neurons depend on K(+)-driven rhythmic changes in input resistance. *J Neurosci* 2023.
174. **Weber F, and Dan Y**. Circuit-based interrogation of sleep control. *Nature* 538: 51-59, 2016.

175. **Scammell TE, Arrigoni E, and Lipton JO**. Neural Circuitry of Wakefulness and Sleep. *Neuron* 93: 747-765, 2017.
176. **Parkington HC, Tonta MA, Brennecke SP, and Coleman HA**. Contractile activity, membrane potential, and cytoplasmic calcium in human uterine smooth muscle in the third trimester of pregnancy and during labor. *Am J Obstet Gynecol* 181: 1445-1451, 1999.
177. **Parkington HC, and Coleman HA**. Excitability in uterine smooth muscle. *Front Horm Res* 27: 179-200, 2001.
178. **Chan YW, van den Berg HA, Moore JD, Quenby S, and Blanks AM**. Assessment of myometrial transcriptome changes associated with spontaneous human labour by high-throughput RNA-seq. *Exp Physiol* 99: 510-524, 2014.
179. **Soloff MS, Jeng YJ, Izban MG, Sinha M, Luxon BA, Stamnes SJ, and England SK**. Effects of progesterone treatment on expression of genes involved in uterine quiescence. *Reprod Sci* 18: 781-797, 2011.
180. **Miyoshi H, Yamaoka K, Garfield RE, and Ohama K**. Identification of a non-selective cation channel current in myometrial cells isolated from pregnant rats. *Pflugers Arch* 447: 457-464, 2004.
181. **Kitazawa T, Hirama R, Masunaga K, Nakamura T, Asakawa K, Cao J, Teraoka H, Unno T, Komori S, Yamada M, Wess J, and Taneike T**. Muscarinic receptor subtypes involved in carbachol-induced contraction of mouse uterine smooth muscle. *Naunyn Schmiedebergs Arch Pharmacol* 377: 503-513, 2008.
182. **Kitazawa T, Uchiyama F, Hirose K, and Taneike T**. Characterization of the muscarinic receptor subtype that mediates the contractile response of acetylcholine in the swine myometrium. *Eur J Pharmacol* 367: 325-334, 1999.
183. **Hage TA, and Salkoff L**. Sodium-activated potassium channels are functionally coupled to persistent sodium currents. *J Neurosci* 32: 2714-2721, 2012.
184. **Takahashi I, and Yoshino M**. Functional coupling between sodium-activated potassium channels and voltage-dependent persistent sodium currents in cricket Kenyon cells. *J Neurophysiol* 114: 2450-2459, 2015.
185. **Sanders KM, Koh SD, and Ward SM**. Interstitial cells of cajal as pacemakers in the gastrointestinal tract. *Annu Rev Physiol* 68: 307-343, 2006.
186. **Jun JY, Choi S, Yeum CH, Chang IY, You HJ, Park CK, Kim MY, Kong ID, Kim MJ, Lee KP, So I, and Kim KW**. Substance P induces inward current and regulates pacemaker currents through tachykinin NK1 receptor in cultured interstitial cells of Cajal of murine small intestine. *Eur J Pharmacol* 495: 35-42, 2004.
187. **d'antonio C, Wang B, McKay C, and Huizinga JD**. Substance P activates a non-selective cation channel in murine pacemaker ICC. *Neurogastroenterol Motil* 21: 985-e979, 2009.
188. **Klein S, Seidler B, Kettenberger A, Sibaev A, Rohn M, Feil R, Allescher HD, Vanderwinden JM, Hofmann F, Schemann M, Rad R, Storr MA, Schmid RM, Schneider G, and Saur D**. Interstitial cells of Cajal integrate excitatory and inhibitory neurotransmission with intestinal slow-wave activity. *Nat Commun* 4: 1630, 2013.
189. **Piras IS, Perdigones N, Zismann V, Briones N, Facista S, Rivera JL, Rozanski E, London CA, and Hendricks WPD**. Identification of Genetic Susceptibility Factors Associated with Canine Gastric Dilatation-Volvulus. *Genes (Basel)* 11: 2020.
190. **Gazzola KM, and Nelson LL**. The relationship between gastrointestinal motility and gastric dilatation-volvulus in dogs. *Top Companion Anim Med* 29: 64-66, 2014.
191. **Sun H, Xu J, Della Penna KB, Benz RJ, Kinose F, Holder DJ, Koblan KS, Gerhold DL, and Wang H**. Dorsal horn-enriched genes identified by DNA microarray, in situ hybridization and immunohistochemistry. *BMC Neurosci* 3: 11, 2002.

192. **Chiang MC, Bowen A, Schier LA, Tupone D, Uddin O, and Heinricher MM**. Parabrachial Complex: A Hub for Pain and Aversion. *J Neurosci* 39: 8225-8230, 2019.
193. **Gilron I, Baron R, and Jensen T**. Neuropathic pain: principles of diagnosis and treatment. *Mayo Clin Proc* 90: 532-545, 2015.
194. **Colloca L, Ludman T, Bouhassira D, Baron R, Dickenson AH, Yarnitsky D, Freeman R, Truini A, Attal N, Finnerup NB, Eccleston C, Kalso E, Bennett DL, Dworkin RH, and Raja SN**. Neuropathic pain. *Nat Rev Dis Primers* 3: 17002, 2017.
195. **Aoki I, and Mori I**. Molecular biology of thermosensory transduction in C. elegans. *Curr Opin Neurobiol* 34: 117-124, 2015.
196. **Albeg A, Smith CJ, Chatzigeorgiou M, Feitelson DG, Hall DH, Schafer WR, Miller DM, 3rd, and Treinin M**. C. elegans multi-dendritic sensory neurons: morphology and function. *Mol Cell Neurosci* 46: 308-317, 2011.
197. **Chuang GT, Liu PH, Chyan TW, Huang CH, Huang YY, Lin CH, Lin JW, Hsu CN, Tsai RY, Hsieh ML, Lee HL, Yang WS, Robinson-Cohen C, Hsiung CN, Shen CY, and Chang YC**. Genome-wide association study for circulating fibroblast growth factor 21 and 23. *Sci Rep* 10: 14578, 2020.
198. **She QY, Bao JF, Wang HZ, Liang H, Huang W, Wu J, Zhong Y, Ling H, Li A, and Qin SL**. Fibroblast growth factor 21: A "rheostat" for metabolic regulation? *Metabolism* 130: 155166, 2022.
199. **Milman A, Venteo S, Bossu JL, Fontanaud P, Monteil A, Lory P, and Guerineau NC**. A sodium background conductance controls the spiking pattern of mouse adrenal chromaffin cells in situ. *J Physiol* 599: 1855-1883, 2021.
200. **Kho M, Smith JA, Verweij N, Shang L, Ryan KA, Zhao W, Ware EB, Gansevoort RT, Irvin MR, Lee JE, Turner ST, Sung J, van der Harst P, Arnett DK, Baylin A, Park SK, Seo YA, Kelly KM, Chang YPC, Zhou X, Lieske JC, and Kardia SLR**. Genome-Wide Association Meta-Analysis of Individuals of European Ancestry Identifies Suggestive Loci for Sodium Intake, Potassium Intake, and Their Ratio Measured from 24-Hour or Half-Day Urine Samples. *J Nutr* 150: 2635-2645, 2020.
201. **Hemmings HC, Jr., Akabas MH, Goldstein PA, Trudell JR, Orser BA, and Harrison NL**. Emerging molecular mechanisms of general anesthetic action. *Trends Pharmacol Sci* 26: 503-510, 2005.
202. **Sonner JM, Antognini JF, Dutton RC, Flood P, Gray AT, Harris RA, Homanics GE, Kendig J, Orser B, Raines DE, Trudell J, Vissel B, and Eger EI, 2nd**. Inhaled anesthetics and immobility: mechanisms, mysteries, and minimum alveolar anesthetic concentration. *Anesth Analg* 97: 718-740, 2003.
203. **Hemmings HC, Jr.** Sodium channels and the synaptic mechanisms of inhaled anaesthetics. *Br J Anaesth* 103: 61-69, 2009.
204. **Herold KF, Andersen OS, and Hemmings HC, Jr.** Divergent effects of anesthetics on lipid bilayer properties and sodium channel function. *Eur Biophys J* 46: 617-626, 2017.
205. **Covarrubias M, Barber AF, Carnevale V, Treptow W, and Eckenhoff RG**. Mechanistic Insights into the Modulation of Voltage-Gated Ion Channels by Inhalational Anesthetics. *Biophys J* 109: 2003-2011, 2015.
206. **Riegelhaupt PM, Tibbs GR, and Goldstein PA**. HCN and K(2P) Channels in Anesthetic Mechanisms Research. *Methods Enzymol* 602: 391-416, 2018.
207. **Lozic B, Johansson S, Lovric Kojundzic S, Markic J, Knappskog PM, Hahn AF, and Boman H**. Novel NALCN variant: altered respiratory and circadian rhythm, anesthetic sensitivity. *Ann Clin Transl Neurol* 3: 876-883, 2016.
208. **Weiss F, Lorang MT, Bloom FE, and Koob GF**. Oral alcohol self-administration stimulates dopamine release in the rat nucleus accumbens: genetic and motivational determinants. *J Pharmacol Exp Ther* 267: 250-258, 1993.

209. **Rose JH, Calipari ES, Mathews TA, and Jones SR**. Greater ethanol-induced locomotor activation in DBA/2J versus C57BL/6J mice is not predicted by presynaptic striatal dopamine dynamics. *PLoS One* 8: e83852, 2013.
210. **Su H, Zhu L, Li J, Wang R, Liu D, Han W, Cadet JL, and Chen T**. Regulation of microRNA-29c in the nucleus accumbens modulates methamphetamine -induced locomotor sensitization in mice. *Neuropharmacology* 148: 160-168, 2019.
211. **Ferreira S, Soares LM, Lira CR, Yokoyama TS, Engi SA, Cruz FC, and Leao RM**. Ethanol-induced locomotor sensitization: Neuronal activation in the nucleus accumbens and medial prefrontal cortex. *Neurosci Lett* 749: 135745, 2021.
212. **Porru S, Lopez-Cruz L, Carratala-Ros C, Salamone JD, Acquas E, and Correa M**. Impact of Caffeine on Ethanol-Induced Stimulation and Sensitization: Changes in ERK and DARPP-32 Phosphorylation in Nucleus Accumbens. *Alcohol Clin Exp Res* 45: 608-619, 2021.
213. **Oo JA, Brandes RP, and Leisegang MS**. Long non-coding RNAs: novel regulators of cellular physiology and function. *Pflugers Arch* 474: 191-204, 2022.
214. **Brown S, Russo J, Chitayat D, and Warburton D**. The 13q- syndrome: the molecular definition of a critical deletion region in band 13q32. *Am J Hum Genet* 57: 859-866, 1995.
215. **Kirchhoff M, Bisgaard AM, Stoeva R, Dimitrov B, Gillessen-Kaesbach G, Fryns JP, Rose H, Grozdanova L, Ivanov I, Keymolen K, Fagerberg C, Tranebjaerg L, Skovby F, and Stefanova M**. Phenotype and 244k array-CGH characterization of chromosome 13q deletions: an update of the phenotypic map of 13q21.1-qter. *Am J Med Genet A* 149A: 894-905, 2009.
216. **Huang C, Yang YF, Yin N, Chen JL, Wang J, Zhang H, and Tan ZP**. Congenital heart defect and mental retardation in a patient with a 13q33.1-34 deletion. *Gene* 498: 308-310, 2012.
217. **Lalani SR, Shaw C, Wang X, Patel A, Patterson LW, Kolodziejska K, Szafranski P, Ou Z, Tian Q, Kang SH, Jinnah A, Ali S, Malik A, Hixson P, Potocki L, Lupski JR, Stankiewicz P, Bacino CA, Dawson B, Beaudet AL, Boricha FM, Whittaker R, Li C, Ware SM, Cheung SW, Penny DJ, Jefferies JL, and Belmont JW**. Rare DNA copy number variants in cardiovascular malformations with extracardiac abnormalities. *Eur J Hum Genet* 21: 173-181, 2013.
218. **Brown S, Gersen S, Anyane-Yeboa K, and Warburton D**. Preliminary definition of a "critical region" of chromosome 13 in q32: report of 14 cases with 13q deletions and review of the literature. *Am J Med Genet* 45: 52-59, 1993.
219. **Bisgaard AM, Kirchhoff M, Tumer Z, Jepsen B, Brondum-Nielsen K, Cohen M, Hamborg-Petersen B, Bryndorf T, Tommerup N, and Skovby F**. Additional chromosomal abnormalities in patients with a previously detected abnormal karyotype, mental retardation, and dysmorphic features. *Am J Med Genet A* 140: 2180-2187, 2006.
220. **van Binsbergen E, Ellis RJ, Abdelmalik N, Jarvis J, Randhawa K, Wyatt-Ashmead J, Canham N, Thorpe-Beeston JG, Mancini GM, and Van Haelst MM**. A fetus with de novo 2q33.2q35 deletion including MAP2 with brain anomalies, esophageal atresia, and laryngeal stenosis. *Am J Med Genet A* 164A: 194-198, 2014.
221. **Koroglu C, Seven M, and Tolun A**. Recessive truncating NALCN mutation in infantile neuroaxonal dystrophy with facial dysmorphism. *J Med Genet* 50: 515-520, 2013.
222. **Seven M, Ozkilic A, and Yuksel A**. Dysmorphic face in two siblings with infantile neuroaxonal dystrophy. *Genet Couns* 13: 465-473, 2002.
223. **Al-Sayed MD, Al-Zaidan H, Albakheet A, Hakami H, Kenana R, Al-Yafee Y, Al-Dosary M, Qari A, Al-Sheddi T, Al-Muheiza M, Al-Qubbaj W, Lakmache Y, Al-Hindi H, Ghaziuddin M, Colak D, and Kaya N**. Mutations in NALCN cause an autosomal-recessive syndrome with severe hypotonia, speech impairment, and cognitive delay. *Am J Hum Genet* 93: 721-726, 2013.

224. **Farwell KD, Shahmirzadi L, El-Khechen D, Powis Z, Chao EC, Tippin Davis B, Baxter RM, Zeng W, Mroske C, Parra MC, Gandomi SK, Lu I, Li X, Lu H, Lu HM, Salvador D, Ruble D, Lao M, Fischbach S, Wen J, Lee S, Elliott A, Dunlop CL, and Tang S**. Enhanced utility of family-centered diagnostic exome sequencing with inheritance model-based analysis: results from 500 unselected families with undiagnosed genetic conditions. *Genet Med* 17: 578-586, 2015.

225. **Gal M, Magen D, Zahran Y, Ravid S, Eran A, Khayat M, Gafni C, Levanon EY, and Mandel H**. A novel homozygous splice site mutation in NALCN identified in siblings with cachexia, strabismus, severe intellectual disability, epilepsy and abnormal respiratory rhythm. *Eur J Med Genet* 59: 204-209, 2016.

226. **Takenouchi T, Inaba M, Uehara T, Takahashi T, Kosaki K, and Mizuno S**. Biallelic mutations in NALCN: Expanding the genotypic and phenotypic spectra of IHPRF1. *Am J Med Genet A* 176: 431-437, 2018.

227. **Angius A, Cossu S, Uva P, Oppo M, Onano S, Persico I, Fotia G, Atzeni R, Cuccuru G, Asunis M, Cucca F, Pruna D, and Crisponi L**. Novel NALCN biallelic truncating mutations in siblings with IHPRF1 syndrome. *Clin Genet* 93: 1245-1247, 2018.

228. **Bourque DK, Dyment DA, MacLusky I, Kernohan KD, Care4Rare Canada C, and McMillan HJ**. Periodic breathing in patients with NALCN mutations. *J Hum Genet* 63: 1093-1096, 2018.

229. **Bramswig NC, Bertoli-Avella AM, Albrecht B, Al Aqeel AI, Alhashem A, Al-Sannaa N, Bah M, Brohl K, Depienne C, Dorison N, Doummar D, Ehmke N, Elbendary HM, Gorokhova S, Heron D, Horn D, James K, Keren B, Kuechler A, Ismail S, Issa MY, Marey I, Mayer M, McEvoy-Venneri J, Megarbane A, Mignot C, Mohamed S, Nava C, Philip N, Ravix C, Rolfs A, Sadek AA, Segebrecht L, Stanley V, Trautman C, Valence S, Villard L, Wieland T, Engels H, Strom TM, Zaki MS, Gleeson JG, Ludecke HJ, Bauer P, and Wieczorek D**. Genetic variants in components of the NALCN-UNC80-UNC79 ion channel complex cause a broad clinical phenotype (NALCN channelopathies). *Hum Genet* 137: 753-768, 2018.

230. **Carneiro TN, Krepischi AC, Costa SS, Tojal da Silva I, Vianna-Morgante AM, Valieris R, Ezquina SA, Bertola DR, Otto PA, and Rosenberg C**. Utility of trio-based exome sequencing in the elucidation of the genetic basis of isolated syndromic intellectual disability: illustrative cases. *Appl Clin Genet* 11: 93-98, 2018.

231. **Ope O, Bhoj EJ, Nelson B, Li D, Hakonarson H, and Sobering AK**. A homozygous truncating NALCN variant in two Afro-Caribbean siblings with hypotonia and dolichocephaly. *Am J Med Genet A* 182: 1877-1880, 2020.

232. **Karimi AH, Karimi MR, Farnia P, Parvini F, and Foroutan M**. A Homozygous Truncating Mutation in NALCN Causing IHPRF1: Detailed Clinical Manifestations and a Review of Literature. *Appl Clin Genet* 13: 151-157, 2020.

233. **Khan A, Tian S, Tariq M, Khan S, Safeer M, Ullah N, Akbar N, Javed I, Asif M, Ahmad I, Ullah S, Satti HS, Khan R, Naeem M, Ali M, Rendu J, Faure J, Dieterich K, Latypova X, Baig SM, Malik NA, Zhang F, Khan TN, and Liu C**. NGS-driven molecular diagnosis of heterogeneous hereditary neurological disorders reveals novel and known variants in disease-causing genes. *Mol Genet Genomics* 297: 1601-1613, 2022.

234. **Maselli K, Park H, Breilyn MS, and Arens R**. Severe central sleep apnea in a child with biallelic variants in NALCN. *J Clin Sleep Med* 18: 2507-2513, 2022.

235. **Abul-Husn NS, Marathe PN, Kelly NR, Bonini KE, Sebastin M, Odgis JA, Abhyankar A, Brown K, Di Biase M, Gallagher KM, Guha S, Ioele N, Okur V, Ramos MA, Rodriguez JE, Rehman AU, Thomas-Wilson A, Edelmann L, Zinberg RE, Diaz GA, Greally JM, Jobanputra V, Suckiel SA, Horowitz CR, Wasserstein MP, Kenny EE, and**

Gelb BD. Molecular diagnostic yield of genome sequencing versus targeted gene panel testing in racially and ethnically diverse pediatric patients. *medRxiv* 2023.
236. **Campbell J, FitzPatrick DR, Azam T, Gibson NA, Somerville L, Joss SK, and Urquhart DS**. NALCN dysfunction as a cause of disordered respiratory rhythm with central apnea. *Pediatrics* 141: S485-S490, 2018.
237. **Perez Y, Kadir R, Volodarsky M, Noyman I, Flusser H, Shorer Z, Gradstein L, Birnbaum RY, and Birk OS**. UNC80 mutation causes a syndrome of hypotonia, severe intellectual disability, dyskinesia and dysmorphism, similar to that caused by mutations in its interacting cation channel NALCN. *J Med Genet* 53: 397-402, 2016.
238. **Shamseldin HE, Faqeih E, Alasmari A, Zaki MS, Gleeson JG, and Alkuraya FS**. Mutations in UNC80, Encoding Part of the UNC79-UNC80-NALCN Channel Complex, Cause Autosomal-Recessive Severe Infantile Encephalopathy. *Am J Hum Genet* 98: 210-215, 2016.
239. **Valkanas E, Schaffer K, Dunham C, Maduro V, du Souich C, Rupps R, Adams DR, Baradaran-Heravi A, Flynn E, Malicdan MC, Gahl WA, Toro C, and Boerkoel CF**. Phenotypic evolution of UNC80 loss of function. *Am J Med Genet A* 170: 3106-3114, 2016.
240. **Obeid T, Hamzeh AR, Saif F, Nair P, Mohamed M, Al-Ali MT, and Bastaki F**. Identification of a novel homozygous UNC80 variant in a child with infantile hypotonia with psychomotor retardation and characteristic facies-2 (IHPRF2). *Metab Brain Dis* 33: 869-873, 2018.
241. **He Y, Ji X, Yan H, Ye X, Liu Y, Wei W, Xiao B, and Sun Y**. Biallelic UNC80 mutations caused infantile hypotonia with psychomotor retardation and characteristic facies 2 in two Chinese patients with variable phenotypes. *Gene* 660: 13-17, 2018.
242. **Hong H, Kamerman-Kretzmer R, Kato R, Rosser T, VanHirtum-Das M, and Davidson Ward SL**. Case Report of Pediatric Channelopathies With UNC80 and KCNJ11 Mutations Having Abnormal Respiratory Control Treated With Positive Airway Pressure Therapy. *J Clin Sleep Med* 14: 1419-1425, 2018.
243. **Kuptanon C, Srichomthong C, Ittiwut C, Wechapinan T, Sri-Udomkajorn S, Iamopas O, Phokaew C, Suphapeetiporn K, and Shotelersuk V**. Whole exome sequencing revealed mutations in FBXL4, UNC80, and ADK in Thai patients with severe intellectual disabilities. *Gene* 696: 21-27, 2019.
244. **Stenehjem KK, Schweigert J, and Kumar P**. Atypical Presentation of Viral Gastroenteritis in a Three-year-old Child Due to a UNC80 Mutation. *Cureus* 11: e4395, 2019.
245. **Tao Y, Han D, Wei Y, Wang L, Song W, and Li X**. Case Report: Complete Maternal Uniparental Disomy of Chromosome 2 With a Novel UNC80 Splicing Variant c.5609-4G> A in a Chinese Patient With Infantile Hypotonia With Psychomotor Retardation and Characteristic Facies 2. *Front Genet* 12: 747422, 2021.
246. **Kelesoglu FM, Kaya M, and Sayili ET**. Novel nonsense mutation in UNC80 in a Turkish patient further validates the sociable skill and severe gastrointestinal problems as part of disease spectrum. *Am J Med Genet A* 2023.
247. **Chong JX, McMillin MJ, Shively KM, Beck AE, Marvin CT, Armenteros JR, Buckingham KJ, Nkinsi NT, Boyle EA, Berry MN, Bocian M, Foulds N, Uzielli ML, Haldeman-Englert C, Hennekam RC, Kaplan P, Kline AD, Mercer CL, Nowaczyk MJ, Klein Wassink-Ruiter JS, McPherson EW, Moreno RA, Scheuerle AE, Shashi V, Stevens CA, Carey JC, Monteil A, Lory P, Tabor HK, Smith JD, Shendure J, Nickerson DA, University of Washington Center for Mendelian G, and Bamshad MJ**. De novo mutations in NALCN cause a syndrome characterized by congenital contractures of the limbs and face, hypotonia, and developmental delay. *Am J Hum Genet* 96: 462-473, 2015.
248. **Fukai R, Saitsu H, Okamoto N, Sakai Y, Fattal-Valevski A, Masaaki S, Kitai Y, Torio M, Kojima-Ishii K, Ihara K, Chernuha V, Nakashima M, Miyatake S, Tanaka F,**

Miyake N, and Matsumoto N. De novo missense mutations in NALCN cause developmental and intellectual impairment with hypotonia. *J Hum Genet* 61: 451-455, 2016.
249. **Karakaya M, Heller R, Kunde V, Zimmer KP, Chao CM, Nurnberg P, and Cirak S**. Novel Mutations in the Nonselective Sodium Leak Channel (NALCN) Lead to Distal Arthrogryposis with Increased Muscle Tone. *Neuropediatrics* 47: 273-277, 2016.
250. **Sivaraman I, Friedman NR, and Prayson RA**. Muscle biopsy findings in a child with NALCN gene mutation. *J Clin Neurosci* 34: 222-223, 2016.
251. **Angius A, Uva P, Oppo M, Buers I, Persico I, Onano S, Cuccuru G, Van Allen MI, Hulait G, Aubertin G, Muntoni F, Fry AE, Anneren G, Stattin EL, Palomares-Bralo M, Santos-Simarro F, Cucca F, Crisponi G, Rutsch F, and Crisponi L**. Exome sequencing in Crisponi/cold-induced sweating syndrome-like individuals reveals unpredicted alternative diagnoses. *Clin Genet* 95: 607-614, 2019.
252. **Kumaki T, Enomoto Y, Aida N, Goto T, and Kurosawa K**. Progression of cerebral and cerebellar atrophy in congenital contractures of limbs and face, hypotonia, and developmental delay. *Pediatr Int* 64: e14734, 2022.
253. **Vivero M, Cho MT, Begtrup A, Wentzensen IM, Walsh L, Payne K, Zarate YA, Bosanko K, Schaefer GB, DeBrosse S, Pollack L, Mason K, Retterer K, DeWard S, Juusola J, and Chung WK**. Additional de novo missense genetic variants in NALCN associated with CLIFAHDD syndrome. *Clin Genet* 91: 929-931, 2017.
254. **Wang Y, Koh K, Ichinose Y, Yasumura M, Ohtsuka T, and Takiyama Y**. A de novo mutation in the NALCN gene in an adult patient with cerebellar ataxia associated with intellectual disability and arthrogryposis. *Clin Genet* 90: 556-557, 2016.
255. **Winczewska-Wiktor A, Hirschfeld AS, Badura-Stronka M, Wojsyk-Banaszak I, Sobkowiak P, Bartkowska-Sniatkowska A, Babak V, and Steinborn B**. Central Apneas Due to the CLIFAHDD Syndrome Successfully Treated with Pyridostigmine. *Int J Environ Res Public Health* 19: 2022.
256. **Aoyagi K, Rossignol E, Hamdan FF, Mulcahy B, Xie L, Nagamatsu S, Rouleau GA, Zhen M, and Michaud JL**. A Gain-of-Function Mutation in NALCN in a Child with Intellectual Disability, Ataxia, and Arthrogryposis. *Hum Mutat* 36: 753-757, 2015.
257. **Vissers L, van Nimwegen KJM, Schieving JH, Kamsteeg EJ, Kleefstra T, Yntema HG, Pfundt R, van der Wilt GJ, Krabbenborg L, Brunner HG, van der Burg S, Grutters J, Veltman JA, and Willemsen M**. A clinical utility study of exome sequencing versus conventional genetic testing in pediatric neurology. *Genet Med* 19: 1055-1063, 2017.
258. **Liao Z, Liu Y, Wang Y, Lu Q, Peng Y, and Liu Q**. Case Report: A de novo Variant in NALCN Associated With CLIFAHDD Syndrome in a Chinese Infant. *Front Pediatr* 10: 927392, 2022.
259. **Byrne AB, Arts P, Ha TT, Kassahn KS, Pais LS, O'Donnell-Luria A, Broad Institute Center for Mendelian G, Babic M, Frank MSB, Feng J, Wang P, Lawrence DM, Eshraghi L, Arriola L, Toubia J, Nguyen H, Genomic Autopsy Study Research N, McGillivray G, Pinner J, McKenzie F, Morrow R, Lipsett J, Manton N, Khong TY, Moore L, Liebelt JE, Schreiber AW, King-Smith SL, Hardy TSE, Jackson MR, Barnett CP, and Scott HS**. Genomic autopsy to identify underlying causes of pregnancy loss and perinatal death. *Nat Med* 29: 180-189, 2023.
260. **Pergande M, Motameny S, Ozdemir O, Kreutzer M, Wang H, Daimaguler HS, Becker K, Karakaya M, Ehrhardt H, Elcioglu N, Ostojic S, Chao CM, Kawalia A, Duman O, Koy A, Hahn A, Reimann J, Schoner K, Schanzer A, Westhoff JH, Schwaibold EMC, Cossee M, Imbert-Bouteille M, von Pein H, Haliloglu G, Topaloglu H, Altmuller J, Nurnberg P, Thiele H, Heller R, and Cirak S**. The genomic and clinical landscape of fetal akinesia. *Genet Med* 22: 511-523, 2020.

261. **Stark Z, Tan TY, Chong B, Brett GR, Yap P, Walsh M, Yeung A, Peters H, Mordaunt D, Cowie S, Amor DJ, Savarirayan R, McGillivray G, Downie L, Ekert PG, Theda C, James PA, Yaplito-Lee J, Ryan MM, Leventer RJ, Creed E, Macciocca I, Bell KM, Oshlack A, Sadedin S, Georgeson P, Anderson C, Thorne N, Melbourne Genomics Health A, Gaff C, and White SM**. A prospective evaluation of whole-exome sequencing as a first-tier molecular test in infants with suspected monogenic disorders. *Genet Med* 18: 1090-1096, 2016.

262. **Biankin AV, Waddell N, Kassahn KS, Gingras MC, Muthuswamy LB, Johns AL, Miller DK, Wilson PJ, Patch AM, Wu J, Chang DK, Cowley MJ, Gardiner BB, Song S, Harliwong I, Idrisoglu S, Nourse C, Nourbakhsh E, Manning S, Wani S, Gongora M, Pajic M, Scarlett CJ, Gill AJ, Pinho AV, Rooman I, Anderson M, Holmes O, Leonard C, Taylor D, Wood S, Xu Q, Nones K, Fink JL, Christ A, Bruxner T, Cloonan N, Kolle G, Newell F, Pinese M, Mead RS, Humphris JL, Kaplan W, Jones MD, Colvin EK, Nagrial AM, Humphrey ES, Chou A, Chin VT, Chantrill LA, Mawson A, Samra JS, Kench JG, Lovell JA, Daly RJ, Merrett ND, Toon C, Epari K, Nguyen NQ, Barbour A, Zeps N, Australian Pancreatic Cancer Genome I, Kakkar N, Zhao F, Wu YQ, Wang M, Muzny DM, Fisher WE, Brunicardi FC, Hodges SE, Reid JG, Drummond J, Chang K, Han Y, Lewis LR, Dinh H, Buhay CJ, Beck T, Timms L, Sam M, Begley K, Brown A, Pai D, Panchal A, Buchner N, De Borja R, Denroche RE, Yung CK, Serra S, Onetto N, Mukhopadhyay D, Tsao MS, Shaw PA, Petersen GM, Gallinger S, Hruban RH, Maitra A, Iacobuzio-Donahue CA, Schulick RD, Wolfgang CL, Morgan RA, Lawlor RT, Capelli P, Corbo V, Scardoni M, Tortora G, Tempero MA, Mann KM, Jenkins NA, Perez-Mancera PA, Adams DJ, Largaespada DA, Wessels LF, Rust AG, Stein LD, Tuveson DA, Copeland NG, Musgrove EA, Scarpa A, Eshleman JR, Hudson TJ, Sutherland RL, Wheeler DA, Pearson JV, McPherson JD, Gibbs RA, and Grimmond SM**. Pancreatic cancer genomes reveal aberrations in axon guidance pathway genes. *Nature* 491: 399-405, 2012.

263. **Kasap M, and Dwyer DS**. Na(+) leak-current channel (NALCN) at the junction of motor and neuropsychiatric symptoms in Parkinson's disease. *J Neural Transm (Vienna)* 128: 749-762, 2021.

264. **Goldberg JA, Guzman JN, Estep CM, Ilijic E, Kondapalli J, Sanchez-Padilla J, and Surmeier DJ**. Calcium entry induces mitochondrial oxidant stress in vagal neurons at risk in Parkinson's disease. *Nat Neurosci* 15: 1414-1421, 2012.

265. **Kasap M, Bonnett K, Aamodt EJ, and Dwyer DS**. Akinesia and freezing caused by Na(+) leak-current channel (NALCN) deficiency corrected by pharmacological inhibition of K(+) channels and gap junctions. *J Comp Neurol* 525: 1109-1121, 2017.

266. **Cring MR, and Sheffield VC**. Gene therapy and gene correction: targets, progress, and challenges for treating human diseases. *Gene Ther* 29: 3-12, 2022.

267. **Nguyen E, Tetreault M, Toffa DH, Cossette P, Samarut E, and Nguyen DK**. Novel NALCN variant linked to temporal lobe epilepsy. *Am J Med Genet A* 2023.

268. **Assary E, Vincent JP, Keers R, and Pluess M**. Gene-environment interaction and psychiatric disorders: Review and future directions. *Semin Cell Dev Biol* 77: 133-143, 2018.

269. **Baum AE, Akula N, Cabanero M, Cardona I, Corona W, Klemens B, Schulze TG, Cichon S, Rietschel M, Nothen MM, Georgi A, Schumacher J, Schwarz M, Abou Jamra R, Hofels S, Propping P, Satagopan J, Detera-Wadleigh SD, Hardy J, and McMahon FJ**. A genome-wide association study implicates diacylglycerol kinase eta (DGKH) and several other genes in the etiology of bipolar disorder. *Mol Psychiatry* 13: 197-207, 2008.

270. **Baum AE, Hamshere M, Green E, Cichon S, Rietschel M, Noethen MM, Craddock N, and McMahon FJ**. Meta-analysis of two genome-wide association studies of bipolar disorder reveals important points of agreement. *Mol Psychiatry* 13: 466-467, 2008.

271. **Askland K, Read C, and Moore J**. Pathways-based analyses of whole-genome association study data in bipolar disorder reveal genes mediating ion channel activity and synaptic neurotransmission. *Hum Genet* 125: 63-79, 2009.
272. **Ollila HM, Soronen P, Silander K, Palo OM, Kieseppa T, Kaunisto MA, Lonnqvist J, Peltonen L, Partonen T, and Paunio T**. Findings from bipolar disorder genome-wide association studies replicate in a Finnish bipolar family-cohort. *Mol Psychiatry* 14: 351-353, 2009.
273. **Wang KS, Liu XF, and Aragam N**. A genome-wide meta-analysis identifies novel loci associated with schizophrenia and bipolar disorder. *Schizophr Res* 124: 192-199, 2010.
274. **Zhang T, Zhu L, Ni T, Liu D, Chen G, Yan Z, Lin H, Guan F, and Rice JP**. Voltage-gated calcium channel activity and complex related genes and schizophrenia: A systematic investigation based on Han Chinese population. *J Psychiatr Res* 106: 99-105, 2018.
275. **Souza RP, Rosa DV, Romano-Silva MA, Zhen M, Meltzer HY, Lieberman JA, Remington G, Kennedy JL, and Wong AH**. Lack of association of NALCN genetic variants with schizophrenia. *Psychiatry Res* 185: 450-452, 2011.
276. **Teo C, Zai C, Borlido C, Tomasetti C, Strauss J, Shinkai T, Le Foll B, Wong A, Kennedy JL, and De Luca V**. Analysis of treatment-resistant schizophrenia and 384 markers from candidate genes. *Pharmacogenet Genomics* 22: 807-811, 2012.
277. **Wetherill L, Kapoor M, Agrawal A, Bucholz K, Koller D, Bertelsen SE, Le N, Wang JC, Almasy L, Hesselbrock V, Kramer J, Nurnberger JI, Jr., Schuckit M, Tischfield JA, Xuei X, Porjesz B, Edenberg HJ, Goate AM, and Foroud T**. Family-based association analysis of alcohol dependence criteria and severity. *Alcohol Clin Exp Res* 38: 354-366, 2014.
278. **Baronas K, Rancelis T, Pranculis A, Domarkiene I, Ambrozaityte L, and Kucinskas V**. Novel human genome variants associated with alcohol use disorders identified in a Lithuanian cohort. *Acta Med Litu* 25: 7-13, 2018.
279. **Lind PA, Macgregor S, Vink JM, Pergadia ML, Hansell NK, de Moor MH, Smit AB, Hottenga JJ, Richter MM, Heath AC, Martin NG, Willemsen G, de Geus EJ, Vogelzangs N, Penninx BW, Whitfield JB, Montgomery GW, Boomsma DI, and Madden PA**. A genomewide association study of nicotine and alcohol dependence in Australian and Dutch populations. *Twin Res Hum Genet* 13: 10-29, 2010.
280. **Schuckit MA, Edenberg HJ, Kalmijn J, Flury L, Smith TL, Reich T, Bierut L, Goate A, and Foroud T**. A genome-wide search for genes that relate to a low level of response to alcohol. *Alcohol Clin Exp Res* 25: 323-329, 2001.
281. **Nurnberger JI, Jr., Foroud T, Flury L, Su J, Meyer ET, Hu K, Crowe R, Edenberg H, Goate A, Bierut L, Reich T, Schuckit M, and Reich W**. Evidence for a locus on chromosome 1 that influences vulnerability to alcoholism and affective disorder. *Am J Psychiatry* 158: 718-724, 2001.
282. **Iossifov I, Ronemus M, Levy D, Wang Z, Hakker I, Rosenbaum J, Yamrom B, Lee YH, Narzisi G, Leotta A, Kendall J, Grabowska E, Ma B, Marks S, Rodgers L, Stepansky A, Troge J, Andrews P, Bekritsky M, Pradhan K, Ghiban E, Kramer M, Parla J, Demeter R, Fulton LL, Fulton RS, Magrini VJ, Ye K, Darnell JC, Darnell RB, Mardis ER, Wilson RK, Schatz MC, McCombie WR, and Wigler M**. De novo gene disruptions in children on the autistic spectrum. *Neuron* 74: 285-299, 2012.
283. **Krupp DR, Barnard RA, Duffourd Y, Evans SA, Mulqueen RM, Bernier R, Riviere JB, Fombonne E, and O'Roak BJ**. Exonic Mosaic Mutations Contribute Risk for Autism Spectrum Disorder. *Am J Hum Genet* 101: 369-390, 2017.
284. **Al-Mazidi S, Al-Ayadhi L, Alqahtany F, Abualnaja A, Alzarroug A, Alharbi T, Farhat K, AlMnaizel A, and El-Ansary A**. The possible role of sodium leakage channel

localization factor-1 in the pathophysiology and severity of autism spectrum disorders. *Sci Rep* 13: 9747, 2023.

285. **Brandau DT, Lund M, Cooley LD, Sanger WG, and Butler MG**. Autistic and dysmorphic features associated with a submicroscopic 2q33.3-q34 interstitial deletion detected by array comparative genomic hybridization. *Am J Med Genet A* 146A: 521-524, 2008.

286. **Rosenfeld JA, Ballif BC, Torchia BS, Sahoo T, Ravnan JB, Schultz R, Lamb A, Bejjani BA, and Shaffer LG**. Copy number variations associated with autism spectrum disorders contribute to a spectrum of neurodevelopmental disorders. *Genet Med* 12: 694-702, 2010.

287. **Jang DH, Chae H, and Kim M**. Autistic and Rett-like features associated with 2q33.3-q34 interstitial deletion. *Am J Med Genet A* 167A: 2213-2218, 2015.

288. **Radhakrishna U, Nath SK, Vishweswaraiah S, Uppala LV, Forray A, Muvvala SB, Mishra NK, Southekal S, Guda C, Govindamangalam H, Vargas D, Gardella WG, Crist RC, Berrettini WH, Metpally RP, and Bahado-Singh RO**. Maternal opioid use disorder: Placental transcriptome analysis for neonatal opioid withdrawal syndrome. *Genomics* 113: 3610-3617, 2021.

289. **Jones HE, and Kraft WK**. Analgesia, Opioids, and Other Drug Use During Pregnancy and Neonatal Abstinence Syndrome. *Clin Perinatol* 46: 349-366, 2019.

290. **Wang K, Zhang H, Bloss CS, Duvvuri V, Kaye W, Schork NJ, Berrettini W, Hakonarson H, and Price Foundation Collaborative G**. A genome-wide association study on common SNPs and rare CNVs in anorexia nervosa. *Mol Psychiatry* 16: 949-959, 2011.

291. **Kweon K, Shin ES, Park KJ, Lee JK, Joo Y, and Kim HW**. Genome-Wide Analysis Reveals Four Novel Loci for Attention-Deficit Hyperactivity Disorder in Korean Youths. *Soa Chongsonyon Chongsin Uihak* 29: 62-72, 2018.

292. **Chu X, Ye J, Wen Y, Li P, Cheng B, Cheng S, Zhang L, Liu L, Qi X, Ma M, Liang C, Kafle OP, Wu C, Wang S, Wang X, Ning Y, and Zhang F**. Maternal smoking during pregnancy and risks to depression and anxiety in offspring: An observational study and genome-wide gene-environment interaction analysis in UK biobank cohort. *J Psychiatr Res* 140: 149-158, 2021.

293. **Anney RJ, Lasky-Su J, O'Dushlaine C, Kenny E, Neale BM, Mulligan A, Franke B, Zhou K, Chen W, Christiansen H, Arias-Vasquez A, Banaschewski T, Buitelaar J, Ebstein R, Miranda A, Mulas F, Oades RD, Roeyers H, Rothenberger A, Sergeant J, Sonuga-Barke E, Steinhausen H, Asherson P, Faraone SV, and Gill M**. Conduct disorder and ADHD: evaluation of conduct problems as a categorical and quantitative trait in the international multicentre ADHD genetics study. *Am J Med Genet B Neuropsychiatr Genet* 147B: 1369-1378, 2008.

294. **Scott WK, Hauser ER, Schmechel DE, Welsh-Bohmer KA, Small GW, Roses AD, Saunders AM, Gilbert JR, Vance JM, Haines JL, and Pericak-Vance MA**. Ordered-subsets linkage analysis detects novel Alzheimer disease loci on chromosomes 2q34 and 15q22. *Am J Hum Genet* 73: 1041-1051, 2003.

295. **Grupe A, Abraham R, Li Y, Rowland C, Hollingworth P, Morgan A, Jehu L, Segurado R, Stone D, Schadt E, Karnoub M, Nowotny P, Tacey K, Catanese J, Sninsky J, Brayne C, Rubinsztein D, Gill M, Lawlor B, Lovestone S, Holmans P, O'Donovan M, Morris JC, Thal L, Goate A, Owen MJ, and Williams J**. Evidence for novel susceptibility genes for late-onset Alzheimer's disease from a genome-wide association study of putative functional variants. *Hum Mol Genet* 16: 865-873, 2007.

296. **Lee JH, Barral S, Cheng R, Chacon I, Santana V, Williamson J, Lantigua R, Medrano M, Jimenez-Velazquez IZ, Stern Y, Tycko B, Rogaeva E, Wakutani Y, Kawarai T, St George-Hyslop P, and Mayeux R**. Age-at-onset linkage analysis in Caribbean Hispanics with familial late-onset Alzheimer's disease. *Neurogenetics* 9: 51-60, 2008.

297. **Khermesh K, D'Erchia AM, Barak M, Annese A, Wachtel C, Levanon EY, Picardi E, and Eisenberg E**. Reduced levels of protein recoding by A-to-I RNA editing in Alzheimer's disease. *RNA* 22: 290-302, 2016.
298. **Prokopenko D, Morgan SL, Mullin K, Hofmann O, Chapman B, Kirchner R, Alzheimer's Disease Neuroimaging I, Amberkar S, Wohlers I, Lange C, Hide W, Bertram L, and Tanzi RE**. Whole-genome sequencing reveals new Alzheimer's disease-associated rare variants in loci related to synaptic function and neuronal development. *Alzheimers Dement* 17: 1509-1527, 2021.
299. **Canet-Pons J, Sen NE, Arsovic A, Almaguer-Mederos LE, Halbach MV, Key J, Doring C, Kerksiek A, Picchiarelli G, Cassel R, Rene F, Dieterle S, Fuchs NV, Konig R, Dupuis L, Lutjohann D, Gispert S, and Auburger G**. Atxn2-CAG100-KnockIn mouse spinal cord shows progressive TDP43 pathology associated with cholesterol biosynthesis suppression. *Neurobiol Dis* 152: 105289, 2021.
300. **Mok KY, Schneider SA, Trabzuni D, Stamelou M, Edwards M, Kasperaviciute D, Pickering-Brown S, Silverdale M, Hardy J, and Bhatia KP**. Genomewide association study in cervical dystonia demonstrates possible association with sodium leak channel. *Mov Disord* 29: 245-251, 2014.
301. **Yang WY, Jiang SS, Pu JL, Jin CY, Gao T, Zheng R, Tian J, and Zhang BR**. Association Between Dystonia-Related Genetic Loci and Parkinson's Disease in Eastern China. *Front Neurol* 12: 711050, 2021.
302. **Heinzen EL, Yoon W, Weale ME, Sen A, Wood NW, Burke JR, Welsh-Bohmer KA, Hulette CM, Sisodiya SM, and Goldstein DB**. Alternative ion channel splicing in mesial temporal lobe epilepsy and Alzheimer's disease. *Genome Biol* 8: R32, 2007.
303. **Ratnapriya R, Vijai J, Kadandale JS, Iyer RS, Radhakrishnan K, and Anand A**. A locus for juvenile myoclonic epilepsy maps to 2q33-q36. *Hum Genet* 128: 123-130, 2010.
304. **Consortium E, Leu C, de Kovel CG, Zara F, Striano P, Pezzella M, Robbiano A, Bianchi A, Bisulli F, Coppola A, Giallonardo AT, Beccaria F, Trenite DK, Lindhout D, Gaus V, Schmitz B, Janz D, Weber YG, Becker F, Lerche H, Kleefuss-Lie AA, Hallman K, Kunz WS, Elger CE, Muhle H, Stephani U, Moller RS, Hjalgrim H, Mullen S, Scheffer IE, Berkovic SF, Everett KV, Gardiner MR, Marini C, Guerrini R, Lehesjoki AE, Siren A, Nabbout R, Baulac S, Leguern E, Serratosa JM, Rosenow F, Feucht M, Unterberger I, Covanis A, Suls A, Weckhuysen S, Kaneva R, Caglayan H, Turkdogan D, Baykan B, Bebek N, Ozbek U, Hempelmann A, Schulz H, Ruschendorf F, Trucks H, Nurnberg P, Avanzini G, Koeleman BP, and Sander T**. Genome-wide linkage meta-analysis identifies susceptibility loci at 2q34 and 13q31.3 for genetic generalized epilepsies. *Epilepsia* 53: 308-318, 2012.
305. **Yang X, Pan G, Li WH, Zhang LM, Wu BB, Wang HJ, Zhang P, and Zhou SZ**. [Analysis of gene mutation of early onset epileptic spasm with unknown reason]. *Zhonghua Er Ke Za Zhi* 55: 813-817, 2017.
306. **Westphal DS, Andres S, Makowski C, Meitinger T, and Hoefele J**. MAP2 - A Candidate Gene for Epilepsy, Developmental Delay and Behavioral Abnormalities in a Patient With Microdeletion 2q34. *Front Genet* 9: 99, 2018.
307. **Balaban H, Bayrakli F, Kartal U, Pinarbasi E, Topaktas S, and Kars HZ**. A novel locus for restless legs syndrome on chromosome 13q. *Eur Neurol* 68: 111-116, 2012.
308. **Whan V, Hobbs M, McWilliam S, Lynn DJ, Lutzow YS, Khatkar M, Barendse W, Raadsma H, and Tellam RL**. Bovine proteins containing poly-glutamine repeats are often polymorphic and enriched for components of transcriptional regulatory complexes. *BMC Genomics* 11: 654, 2010.
309. **Rahrmann EP, Shorthouse D, Jassim A, Hu LP, Ortiz M, Mahler-Araujo B, Vogel P, Paez-Ribes M, Fatemi A, Hannon GJ, Iyer R, Blundon JA, Lourenco FC, Kay J,**

Nazarian RM, Hall BA, Zakharenko SS, Winton DJ, Zhu L, and Gilbertson RJ. The NALCN channel regulates metastasis and nonmalignant cell dissemination. *Nat Genet* 54: 1827-1838, 2022.

310. **Folcher A, Gordienko D, Iamshanova O, Bokhobza A, Shapovalov G, Kannancheri-Puthooru D, Mariot P, Allart L, Desruelles E, Spriet C, Diez R, Oullier T, Marionneau-Lambot S, Brisson L, Geraci S, Impheng H, Lehen'kyi V, Haustrate A, Mihalache A, Gosset P, Chadet S, Retif S, Laube M, Sobilo J, Lerondel S, Villari G, Serini G, Pla AF, Roger S, Fromont-Hankard G, Djamgoz M, Clezardin P, Monteil A, and Prevarskaya N**. NALCN-mediated sodium influx confers metastatic prostate cancer cell invasiveness. *EMBO J* e112198, 2023.

311. **McGuire TF, Sajithlal GB, Lu J, Nicholls RD, and Prochownik EV**. In vivo evolution of tumor-derived endothelial cells. *PLoS One* 7: e37138, 2012.

312. **Hu B, Shi C, Jiang HX, and Qin SY**. Identification of novel therapeutic target genes and pathway in pancreatic cancer by integrative analysis. *Medicine (Baltimore)* 96: e8261, 2017.

313. **Lee Y, Yoon KA, Joo J, Lee D, Bae K, Han JY, and Lee JS**. Prognostic implications of genetic variants in advanced non-small cell lung cancer: a genome-wide association study. *Carcinogenesis* 34: 307-313, 2013.

314. **He J, Xu J, Chang Z, Yan J, Zhang L, and Qin Y**. NALCN is a potential biomarker and therapeutic target in human cancers. *Front Genet* 14: 1164707, 2023.

315. **Agelopoulos K, Richter GH, Schmidt E, Dirksen U, von Heyking K, Moser B, Klein HU, Kontny U, Dugas M, Poos K, Korsching E, Buch T, Weckesser M, Schulze I, Besoke R, Witten A, Stoll M, Kohler G, Hartmann W, Wardelmann E, Rossig C, Baumhoer D, Jurgens H, Burdach S, Berdel WE, and Muller-Tidow C**. Deep Sequencing in Conjunction with Expression and Functional Analyses Reveals Activation of FGFR1 in Ewing Sarcoma. *Clin Cancer Res* 21: 4935-4946, 2015.

316. **Zhan H, Jiang J, Sun Q, Ke A, Hu J, Hu Z, Zhu K, Luo C, Ren N, Fan J, Zhou J, and Huang X**. Whole-Exome Sequencing-Based Mutational Profiling of Hepatitis B Virus-Related Early-Stage Hepatocellular Carcinoma. *Gastroenterol Res Pract* 2017: 2029315, 2017.

317. **Chen HQ, Zhao J, Li Y, He LX, Huang YJ, Shu WQ, Cao J, Liu WB, and Liu JY**. Gene expression network regulated by DNA methylation and microRNA during microcystin-leucine arginine induced malignant transformation in human hepatocyte L02 cells. *Toxicol Lett* 289: 42-53, 2018.

318. **Esposito MR, Binatti A, Pantile M, Coppe A, Mazzocco K, Longo L, Capasso M, Lasorsa VA, Luksch R, Bortoluzzi S, and Tonini GP**. Somatic mutations in specific and connected subpathways are associated with short neuroblastoma patients' survival and indicate proteins targetable at onset of disease. *Int J Cancer* 143: 2525-2536, 2018.

319. **Wang J, Zhang C, He W, and Gou X**. Construction and comprehensive analysis of dysregulated long non-coding RNA-associated competing endogenous RNA network in clear cell renal cell carcinoma. *J Cell Biochem* 2018.

320. **Kang HW, Park H, Seo SP, Byun YJ, Piao XM, Kim SM, Kim WT, Yun SJ, Jang W, Shon HS, Ryu KH, Lee SC, Kim WJ, and Kim YJ**. Methylation Signature for Prediction of Progression Free Survival in Surgically Treated Clear Cell Renal Cell Carcinoma. *J Korean Med Sci* 34: e144, 2019.

321. **Yu X, Zhong P, Han Y, Huang Q, Wang J, Jia C, and Lv Z**. Key candidate genes associated with BRAF(V600E) in papillary thyroid carcinoma on microarray analysis. *J Cell Physiol* 234: 23369-23378, 2019.

322. **Li Q, Li Y, Sun X, Zhang X, and Zhang M**. Genomic Analysis of Abnormal DNAM Methylation in Parathyroid Tumors. *Int J Endocrinol* 2022: 4995196, 2022.

323. **Fontanillo C, Aibar S, Sanchez-Santos JM, and De Las Rivas J**. Combined analysis of genome-wide expression and copy number profiles to identify key altered genomic regions in cancer. *BMC Genomics* 13 Suppl 5: S5, 2012.
324. **Wang R, Gurguis CI, Gu W, Ko EA, Lim I, Bang H, Zhou T, and Ko JH**. Ion channel gene expression predicts survival in glioma patients. *Sci Rep* 5: 11593, 2015.
325. **Zhang D, Zhao J, Han C, Liu X, Liu J, and Yang H**. Identification of hub genes related to prognosis in glioma. *Biosci Rep* 40: 2020.
326. **Liu Y, Chen S, Peng G, Liao Y, Fan X, Zhang Z, and Shen C**. CircRNA NALCN acts as an miR-493-3p sponge to regulate PTEN expression and inhibit glioma progression. *Cancer Cell Int* 21: 307, 2021.
327. **Zhong W, Qu H, Yao B, Wang D, and Qiu J**. Analysis of a Long Non-coding RNA associated Signature to Predict Survival in Patients with Bladder Cancer. *Cureus* 14: e24818, 2022.
328. **Huang Q, Li XM, Sun JP, and Zhou Y**. Tumor-derived endomucin promotes colorectal cancer proliferation and metastasis. *Cancer Med* 12: 3222-3236, 2023.
329. **King EG, Kislukhin G, Walters KN, and Long AD**. Using Drosophila melanogaster to identify chemotherapy toxicity genes. *Genetics* 198: 31-43, 2014.
330. **Taguchi K, Hamamoto S, Okada A, Unno R, Kamisawa H, Naiki T, Ando R, Mizuno K, Kawai N, Tozawa K, Kohri K, and Yasui T**. Genome-Wide Gene Expression Profiling of Randall's Plaques in Calcium Oxalate Stone Formers. *J Am Soc Nephrol* 28: 333-347, 2017.
331. **Yan X, Huang Y, and Wu J**. Identify Cross Talk Between Circadian Rhythm and Coronary Heart Disease by Multiple Correlation Analysis. *J Comput Biol* 25: 1312-1327, 2018.
332. **Audain E, Wilsdon A, Breckpot J, Izarzugaza JMG, Fitzgerald TW, Kahlert AK, Sifrim A, Wunnemann F, Perez-Riverol Y, Abdul-Khaliq H, Bak M, Bassett AS, Benson DW, Berger F, Daehnert I, Devriendt K, Dittrich S, Daubeney PE, Garg V, Hackmann K, Hoff K, Hofmann P, Dombrowsky G, Pickardt T, Bauer U, Keavney BD, Klaassen S, Kramer HH, Marshall CR, Milewicz DM, Lemaire S, Coselli JS, Mitchell ME, Tomita-Mitchell A, Prakash SK, Stamm K, Stewart AFR, Silversides CK, Siebert R, Stiller B, Rosenfeld JA, Vater I, Postma AV, Caliebe A, Brook JD, Andelfinger G, Hurles ME, Thienpont B, Larsen LA, and Hitz MP**. Integrative analysis of genomic variants reveals new associations of candidate haploinsufficient genes with congenital heart disease. *PLoS Genet* 17: e1009679, 2021.
333. **Adeyemo A, Gerry N, Chen G, Herbert A, Doumatey A, Huang H, Zhou J, Lashley K, Chen Y, Christman M, and Rotimi C**. A genome-wide association study of hypertension and blood pressure in African Americans. *PLoS Genet* 5: e1000564, 2009.
334. **Wilson CL, Liu W, Yang JJ, Kang G, Ojha RP, Neale GA, Srivastava DK, Gurney JG, Hudson MM, Robison LL, and Ness KK**. Genetic and clinical factors associated with obesity among adult survivors of childhood cancer: A report from the St. Jude Lifetime Cohort. *Cancer* 121: 2262-2270, 2015.
335. **Li L, Zhou X, Wang X, Wang J, Zhang W, Wang B, Cao Y, and Kee K**. A dominant negative mutation at the ATP binding domain of AMHR2 is associated with a defective anti-Mullerian hormone signaling pathway. *Mol Hum Reprod* 22: 669-678, 2016.
336. **Sigurdsson S, Alexandersson KF, Sulem P, Feenstra B, Gudmundsdottir S, Halldorsson GH, Olafsson S, Sigurdsson A, Rafnar T, Thorgeirsson T, Sorensen E, Nordholm-Carstensen A, Burcharth J, Andersen J, Jorgensen HS, Possfelt-Moller E, Ullum H, Thorleifsson G, Masson G, Thorsteinsdottir U, Melbye M, Gudbjartsson DF, Stefansson T, Jonsdottir I, and Stefansson K**. Sequence variants in ARHGAP15, COLQ and FAM155A associate with diverticular disease and diverticulitis. *Nat Commun* 8: 15789, 2017.

337. **Maguire LH, Handelman SK, Du X, Chen Y, Pers TH, and Speliotes EK**. Genome-wide association analyses identify 39 new susceptibility loci for diverticular disease. *Nat Genet* 50: 1359-1365, 2018.
338. **Schafmayer C, Harrison JW, Buch S, Lange C, Reichert MC, Hofer P, Cossais F, Kupcinskas J, von Schonfels W, Schniewind B, Kruis W, Tepel J, Zobel M, Rosendahl J, Jacobi T, Walther-Berends A, Schroeder M, Vogel I, Sergeev P, Boedeker H, Hinrichsen H, Volk A, Erk JU, Burmeister G, Hendricks A, Hinz S, Wolff S, Bottner M, Wood AR, Tyrrell J, Beaumont RN, Langheinrich M, Kucharzik T, Brezina S, Huber-Schonauer U, Pietsch L, Noack LS, Brosch M, Herrmann A, Thangapandi RV, Schimming HW, Zeissig S, Palm S, Focke G, Andreasson A, Schmidt PT, Weitz J, Krawczak M, Volzke H, Leeb G, Michl P, Lieb W, Grutzmann R, Franke A, Lammert F, Becker T, Kupcinskas L, D'Amato M, Wedel T, Datz C, Gsur A, Weedon MN, and Hampe J**. Genome-wide association analysis of diverticular disease points towards neuromuscular, connective tissue and epithelial pathomechanisms. *Gut* 68: 854-865, 2019.
339. **Reichert MC, Kupcinskas J, Schulz A, Schramm C, Weber SN, Krawczyk M, Jungst C, Casper M, Grunhage F, Appenrodt B, Zimmer V, Tamelis A, Lukosiene JI, Pauziene N, Kiudelis G, Jonaitis L, Goeser T, Malinowski M, Glanemann M, Kupcinskas L, and Lammert F**. Common variation in FAM155A is associated with diverticulitis but not diverticulosis. *Sci Rep* 10: 1658, 2020.
340. **AvSar T, Cali SS, Yilmaz B, DemIrc IOG, HolyavkIn C, and Kili CT**. Genome-wide identification of Chiari malformation type I associated candidate genes and chromosomal variations. *Turk J Biol* 44: 449-456, 2020.
341. **Hirschfield GM, Liu X, Xu C, Lu Y, Xie G, Lu Y, Gu X, Walker EJ, Jing K, Juran BD, Mason AL, Myers RP, Peltekian KM, Ghent CN, Coltescu C, Atkinson EJ, Heathcote EJ, Lazaridis KN, Amos CI, and Siminovitch KA**. Primary biliary cirrhosis associated with HLA, IL12A, and IL12RB2 variants. *N Engl J Med* 360: 2544-2555, 2009.
342. **Soria Lopez JA, Gonzalez HM, and Leger GC**. Alzheimer's disease. *Handb Clin Neurol* 167: 231-255, 2019.
343. **Khani M, Gibbons E, Bras J, and Guerreiro R**. Challenge accepted: uncovering the role of rare genetic variants in Alzheimer's disease. *Mol Neurodegener* 17: 3, 2022.
344. **Gutierrez-Vargas JA, Castro-Alvarez JF, Zapata-Berruecos JF, Abdul-Rahim K, and Arteaga-Noriega A**. Neurodegeneration and convergent factors contributing to the deterioration of the cytoskeleton in Alzheimer's disease, cerebral ischemia and multiple sclerosis (Review). *Biomed Rep* 16: 27, 2022.
345. **Perez C, Ziburkus J, and Ullah G**. Analyzing and Modeling the Dysfunction of Inhibitory Neurons in Alzheimer's Disease. *PLoS One* 11: e0168800, 2016.
346. **Arispe N, Pollard HB, and Rojas E**. Giant multilevel cation channels formed by Alzheimer disease amyloid beta-protein [A beta P-(1-40)] in bilayer membranes. *Proc Natl Acad Sci U S A* 90: 10573-10577, 1993.
347. **Pollard HB, Rojas E, and Arispe N**. A new hypothesis for the mechanism of amyloid toxicity, based on the calcium channel activity of amyloid beta protein (A beta P) in phospholipid bilayer membranes. *Ann N Y Acad Sci* 695: 165-168, 1993.
348. **Lin H, Bhatia R, and Lal R**. Amyloid beta protein forms ion channels: implications for Alzheimer's disease pathophysiology. *FASEB J* 15: 2433-2444, 2001.
349. **Balestrino R, and Schapira AHV**. Parkinson disease. *Eur J Neurol* 27: 27-42, 2020.
350. **Katchen M, and Duvoisin RC**. Parkinsonism following dystonia in three patients. *Mov Disord* 1: 151-157, 1986.
351. **Klawans HL, and Paleologos N**. Dystonia-Parkinson syndrome: differential effects of levodopa and dopamine agonists. *Clin Neuropharmacol* 9: 298-302, 1986.

352. **Gomez-Garre P, Huertas-Fernandez I, Caceres-Redondo MT, Alonso-Canovas A, Bernal-Bernal I, Blanco-Ollero A, Bonilla-Toribio M, Burguera JA, Carballo M, Carrillo F, Jose Catalan-Alonso M, Escamilla-Sevilla F, Espinosa-Rosso R, Carmen Fernandez-Moreno M, Garcia-Caldentey J, Garcia-Moreno JM, Giacometti-Silveira S, Gutierrez-Garcia J, Jesus-Maestre S, Lopez-Valdes E, Martinez-Castrillo JC, Medialdea-Natera MP, Mendez-Lucena C, Minguez-Castellanos A, Angel Moya M, Ochoa-Sepulveda JJ, Ojea T, Rodriguez N, Rubio-Agusti I, Sillero-Sanchez M, Del Val J, Vargas-Gonzalez L, and Mir P**. Lack of validation of variants associated with cervical dystonia risk: a GWAS replication study. *Mov Disord* 29: 1825-1828, 2014.

353. **Zhou Q, Yang J, Cao B, Chen Y, Wei Q, Ou R, Song W, Zhao B, Wu Y, and Shang H**. Association Analysis of NALCN Polymorphisms rs1338041 and rs61973742 in a Chinese Population with Isolated Cervical Dystonia. *Parkinsons Dis* 2016: 9281790, 2016.

354. **Fisher RS, Acevedo C, Arzimanoglou A, Bogacz A, Cross JH, Elger CE, Engel J, Jr., Forsgren L, French JA, Glynn M, Hesdorffer DC, Lee BI, Mathern GW, Moshe SL, Perucca E, Scheffer IE, Tomson T, Watanabe M, and Wiebe S**. ILAE official report: a practical clinical definition of epilepsy. *Epilepsia* 55: 475-482, 2014.

355. **Kline BP, Yochum GS, Brinton DL, Schieffer KM, Weaver T, Harris L, Deiling S, Berg AS, and Koltun WA**. COLQ and ARHGAP15 are Associated with Diverticular Disease and are Expressed in the Colon. *J Surg Res* 267: 397-403, 2021.

356. **Snutch TP, and Monteil A**. The sodium "leak" has finally been plugged. *Neuron* 54: 505-507, 2007.

357. **Eroglu C, Allen NJ, Susman MW, O'Rourke NA, Park CY, Ozkan E, Chakraborty C, Mulinyawe SB, Annis DS, Huberman AD, Green EM, Lawler J, Dolmetsch R, Garcia KC, Smith SJ, Luo ZD, Rosenthal A, Mosher DF, and Barres BA**. Gabapentin receptor alpha2delta-1 is a neuronal thrombospondin receptor responsible for excitatory CNS synaptogenesis. *Cell* 139: 380-392, 2009.

358. **Obergrussberger A, Goetze TA, Brinkwirth N, Becker N, Friis S, Rapedius M, Haarmann C, Rinke-Weiss I, Stolzle-Feix S, Bruggemann A, George M, and Fertig N**. An update on the advancing high-throughput screening techniques for patch clamp-based ion channel screens: implications for drug discovery. *Expert Opin Drug Discov* 13: 269-277, 2018.

359. **Zhu Z, Deng Z, Wang Q, Wang Y, Zhang D, Xu R, Guo L, and Wen H**. Simulation and Machine Learning Methods for Ion-Channel Structure Determination, Mechanistic Studies and Drug Design. *Front Pharmacol* 13: 939555, 2022.